

Shuttle Second Stage with a Flexible Payload Mounted on Coulomb Dampers

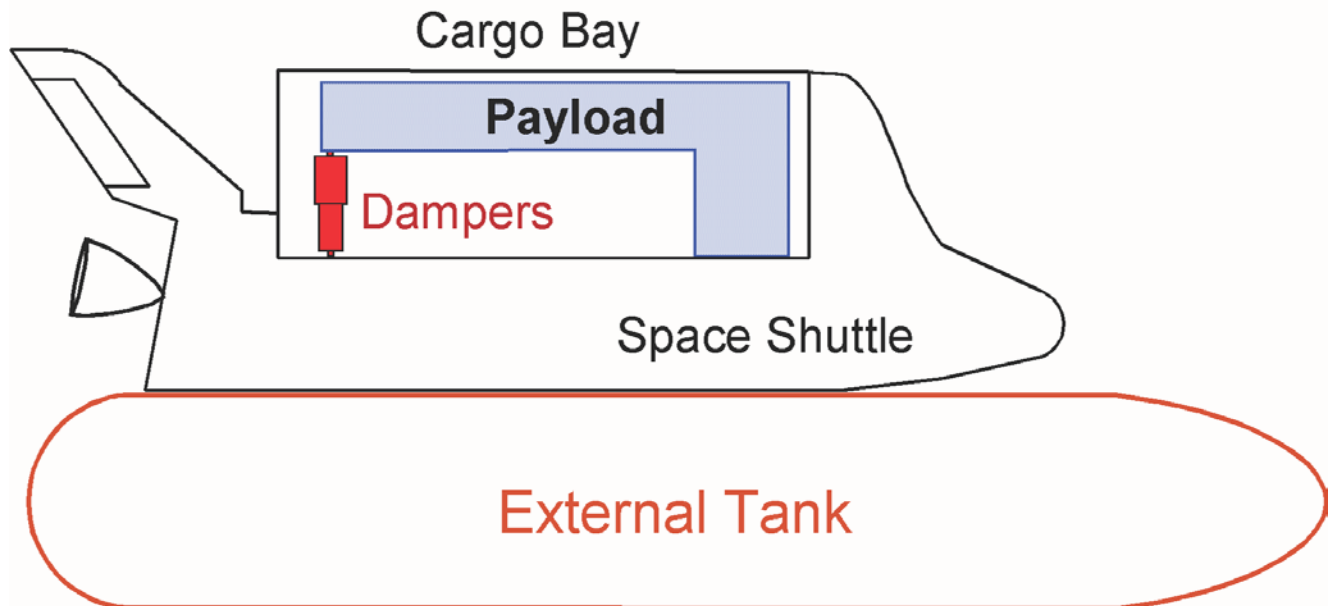


Figure 1 Payload is rigidly attached in one side to the bottom of the Shuttle cargo bay and on the other side it is attached to the cargo bay by means of two Coulomb Dampers.

Control engineers are often challenged with vibration problems that can occur due to dynamics and control system interactions. They often require smart control design solutions that include flexibility compensation filters. In some cases, however, the only practical and robust solution to structural vibrations is a mechanical fix. The following example presents such a design challenge that requires non-linear control analysis and the use of the Describing Function (DF) method because it involves non-linearities that produce structural oscillations (limit-cycles). This flex mode instability problem was predicted on the Space Shuttle ascent 2nd stage in a mission that was carrying a heavy and flexible payload shortly after separating from the solid rocket boosters. Linear analysis shows that this payload has the potential of causing flex mode instability. A software fix using a notch filter was not practical because the flex mode was very strong and at low frequency. Filtering would deteriorate the rigid-body phase margin and degrade robustness. A hardware solution was implemented instead by mounting a pair of non-linear coulomb dampers to attenuate the structural vibrations to acceptably small oscillation amplitudes.

Figure 1 shows the attachment of the flexible payload inside the Shuttle cargo bay. The payload is rigidly attached to the Shuttle on the forward side and on the other side it is attached to the Shuttle by means of two coulomb dampers. The coulomb dampers are non-linear energy dissipating devices (shock absorbers) connected between the payload and the cargo bay. Figure 2 shows the Shuttle payload mounting mechanism inside the cargo bay. The partially shown payload is mounted inside a cradle. The front side of the cradle is directly attached to the Shuttle cargo bay and the rear side of the cradle is attached to the cargo bay by means of the two dampers. One damper is on the left side of the cradle and the other is on the right side. The purpose of the coulomb dampers is to attenuate structural vibrations which otherwise would have been divergent if the payload was directly attached to the vehicle structure on both sides.

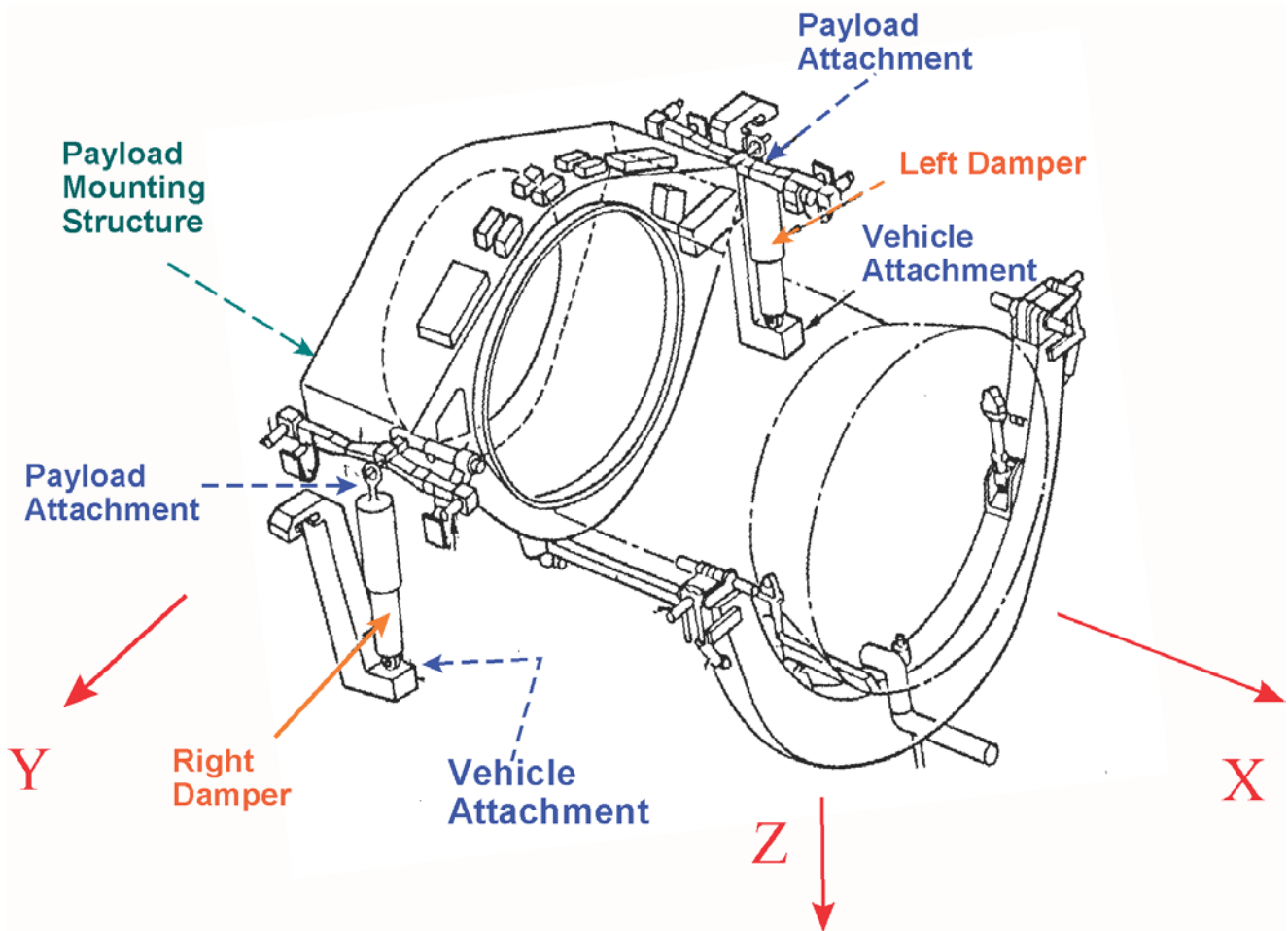


Figure 2 The Payload Cradle is attached on the aft side of the Payload Bay by means of two Coulomb Dampers.

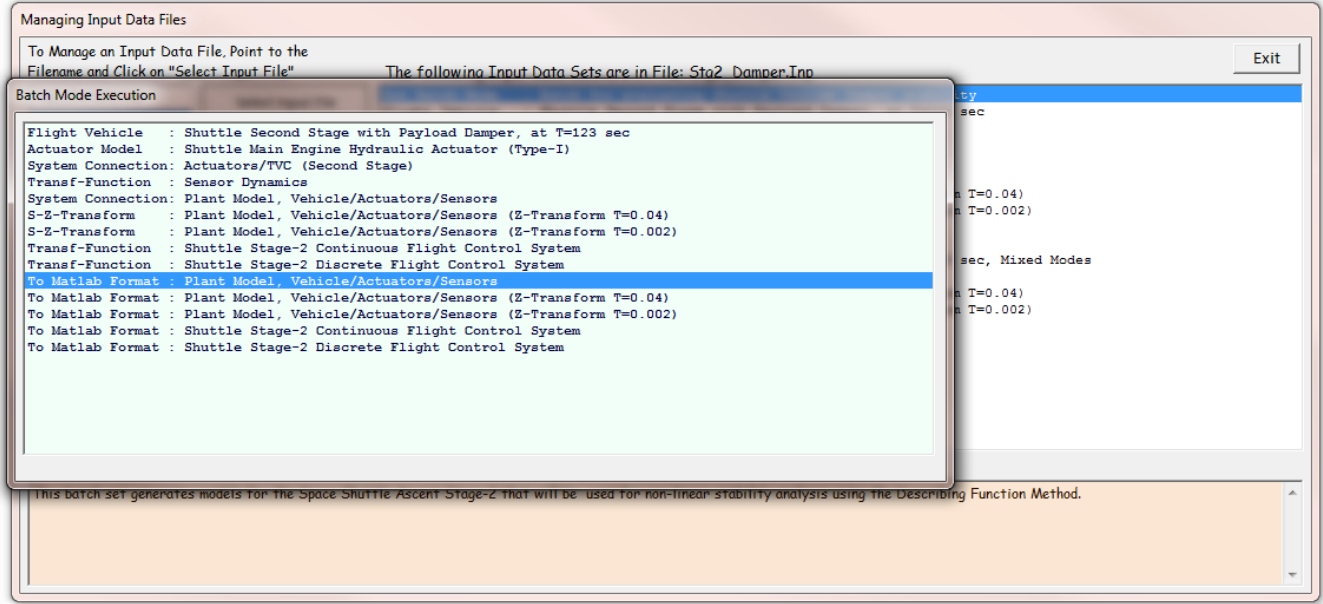
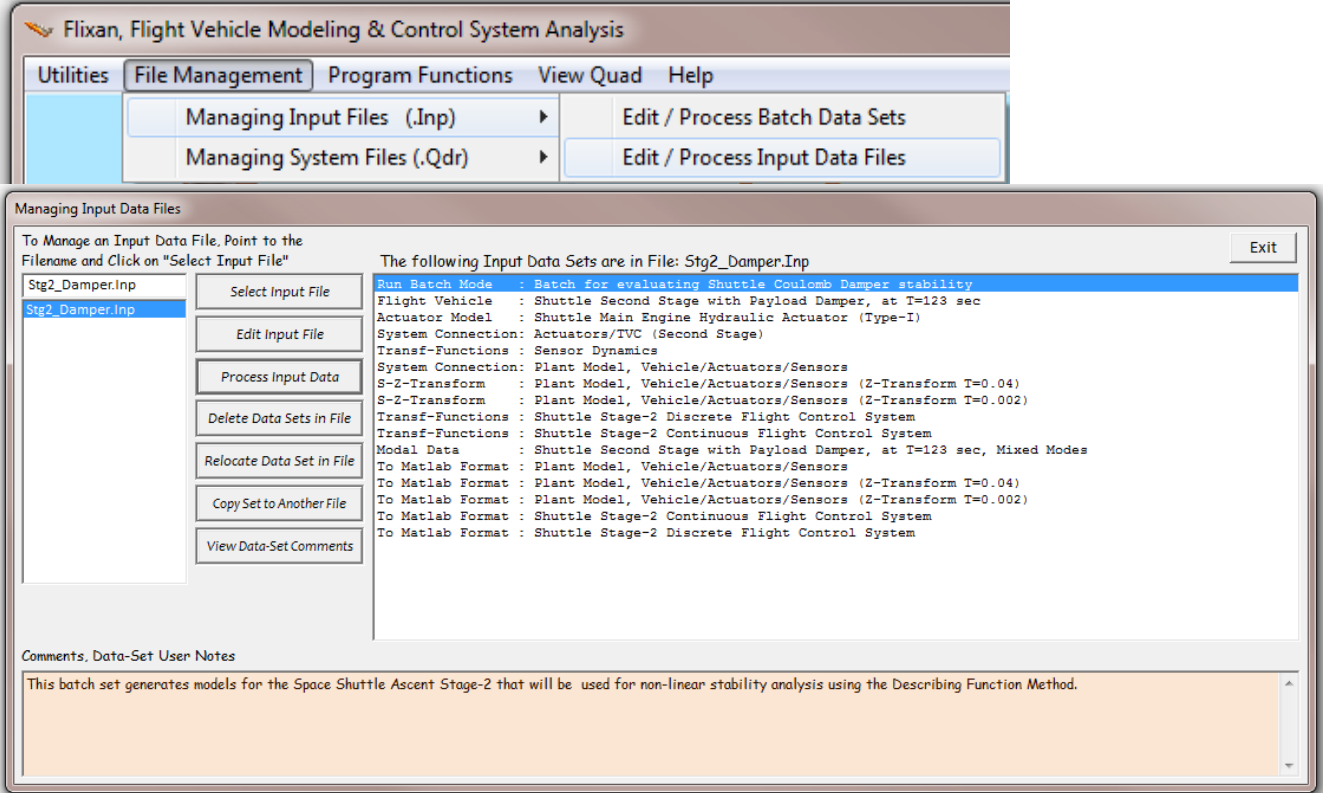
Analysis Overview

In the analysis that follows we will demonstrate the structural instability of the payload and introduce the mechanical dampers that will attenuate it. The purpose of this example is to analyze the dynamic interaction between the flexible structure and the non-linear Coulomb dampers. We will use the Describing Function method to estimate the size and frequency of the limit-cycles caused by the non-linear devices, and simulations to validate the stability analysis. The files for this Shuttle second stage analysis example are located in directory “*Flixan\Examples\Payload Damper*”. The input data file is already prepared in file “*Stg2_Damper.Inp*”. The title of the vehicle data-set is “*Shuttle Second Stage with Payload Damper, at T=123 sec*”. The Matlab analysis files are located in subdirectory “*Payload Damper\Matan*”. The input data file “*Stg2_Damper.Inp*” can be processed quickly by running the batch set located on the top of the file “*Batch for evaluating Shuttle Coulomb Damper stability*”, as shown below. However, for tutorial purposes we will demonstrate the execution of each data-set separately. The following analysis we will be performed in the upcoming sections:

- Extract a set of structural modes and develop linear dynamic models with flexibility for the Shuttle vehicle during second stage.
- Generate state-space models for the engine actuators, sensors, TVC, and the flight control system.

- Combine the continuous vehicle, actuators, TVC, and sensors into a plant system and discretize it using a sampling rate of 40 msec.
- Convert the vehicle and the flight control systems to Matlab format and perform classical stability analysis in Matlab/ Simulink.
- Create a dynamic model for the Coulomb damper and derive its Describing Function (DF)
- Use the Describing Function methodology in the frequency domain using Nichols charts to analyze limit-cycle stability of the flight control system.
- Create time-domain simulations to validate the limit-cycle predictions from the DF analysis.

Batch processing of the input file “Stg2_Damper.Inp”.



1 Selecting the Dominant Structural Modes

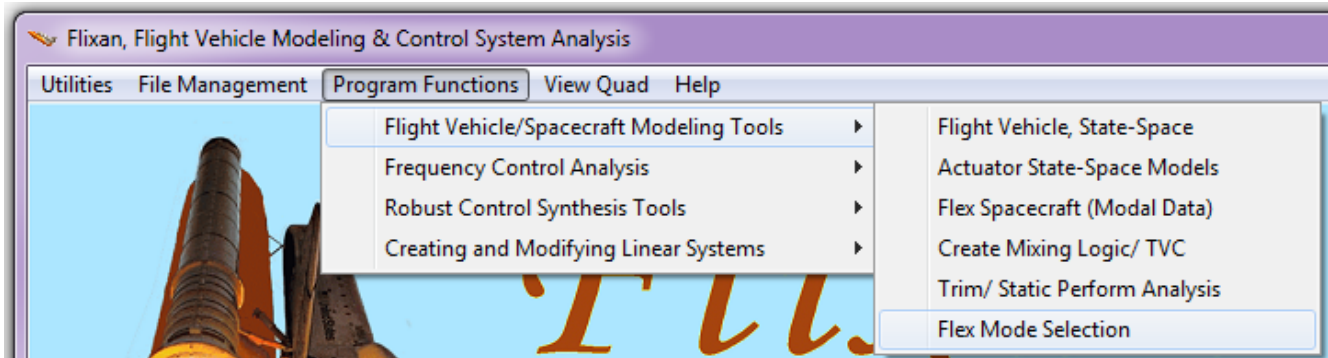
The first step in generating the flexible vehicle model is to prepare a set of structural modes that will be combined with the rigid vehicle data. The modal data file “*Shuttle-Stg2.Mod*” contains the modes for the Shuttle vehicle during second stage. It was generated from a bigger Nastran model and reformatted to be compatible with Flixan. The flex model includes the cradle with flexible payload shown in Figure 2. It is attached to the cargo bay only at the front end. The rear end of the cradle is not connected to the vehicle. The dampers are not included and the payload is cantilevered and free to oscillate at the two ends where the dampers are supposed to connect. The modal data file contains the first 90 modes (including the 6 rigid-body modes) at 14 vehicle locations (nodes) which are relevant for flight control analysis. The file includes the mode frequencies, damping coefficient, and the mode shapes (3 translations and 3 rotations) for each mode at the 14 locations which are important for stability and control analysis. The nodes map file “*Shuttle-Stg2.Nod*” is located in the same folder and it includes descriptions of the 14 structural locations (the nodes). The vehicle locations required for control analysis are the engine gimbals, sensors, the slosh mass locations, and the four attachments for the two coulomb dampers, two attachments on the vehicle side and two attachments on the payload side of the dampers. The nodes file also contains the node ID (a large number generated by Nastran), and the x, y, z coordinates at each location.

The mode selection is a process by which we select a smaller set of dominant structural modes. In this case we will select 27 modes, and we must not include the first 6 because they are rigid-body modes. The selected modes will be combined with the rigid-body vehicle data and generate the flexible vehicle state-space model using the Flixan flight vehicle modeling program. The mode selection process operates by calculating the strength of each mode between actuator and sensor locations and allows the analyst to select a number of modes that have a strong contribution between the two sets of points. The weak modes are ignored. The mode strength comparison can be calculated between any number of actuators and any number of sensors which are included in the modal data and nodes files. The inputs are forces or torques at one or more nodes and in specified directions. The outputs are displacement or rotational measurements at one or more nodes in specified directions. Care must be taken when selecting nodes, either as actuators or as sensors, to make sure that the mode shapes (either translations or rotations) are non-zero in the directions specified. Otherwise, the mode-selection process will not work when the transmissions between actuators and sensors are zero.

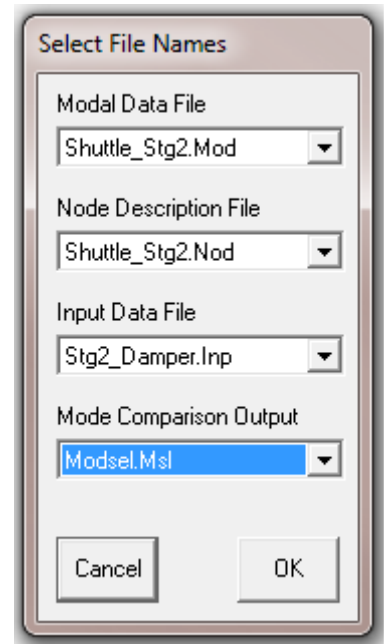
In this particular example we are interested to select a mixed set of modes which are excitable and observable from multiple locations. To begin, we would like to select a set of modes that have strong contributions between the TVC engines and the rate gyros, not only in pitch, which is the most sensitive axis, but also in roll and yaw directions. We would also like to include modes that have strong contributions at the Coulomb damper attachments, mainly in the z-direction since the displacements are along $\pm Z$, both symmetrically (for pitch) and anti-symmetrically (for roll). This requires the mode selection process to be performed several times between different input and output points (actuators and sensors), and in different forcing and measurements directions. The final set of chosen modes consists of a compilation of dominant modes from different mode selection runs and criteria. That is, using different excitation and measurement points, such as, between forces at the gimbals to gyro measurements, and also between forces at the damper attachments on the vehicle side to position measurements at the other end of the damper which is on the payload side. The directions of the application forces depend on the analysis axis. When selecting modes for the pitch axis the

forces are applied symmetrically on both sides along +Z, whereas when we excite the roll axis, the forces are applied anti-symmetrically along $\pm Z$.

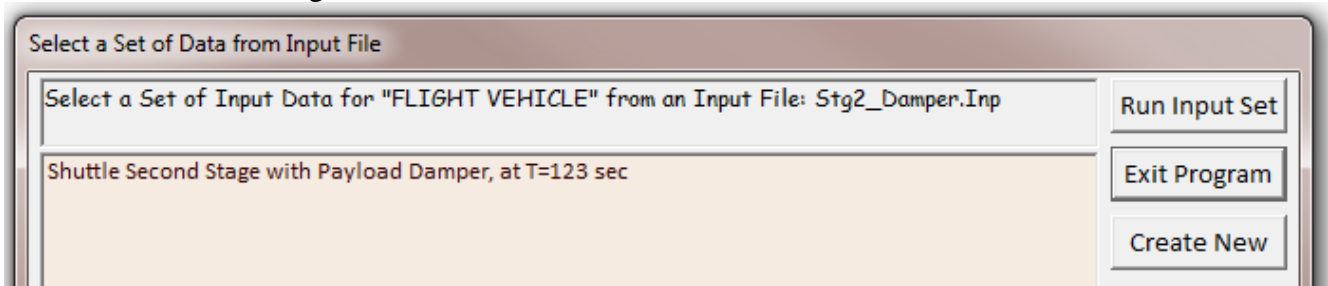
We begin the mode selection process by starting the Flixan program, select the project directory “*Examples \Payload Damper*”, where the vehicle data and the modal data files are located, and from the main menu go to “*Program Functions*”, “*Flight Vehicle/ Spacecraft Modeling Tools*”, and then “*Flex Mode Selection*”.



Click “*Continue*” in the introduction dialog, and use the filename selection menus on the right to select the modal data file “*Shuttle_Stg2.Mod*”, the nodes map file “*Shuttle_Stg2.Nod*”, the vehicle input data file “*Stg2_Damper.Inp*”, and the default output file “*Modsel.Msl*” to save the modal strength results.

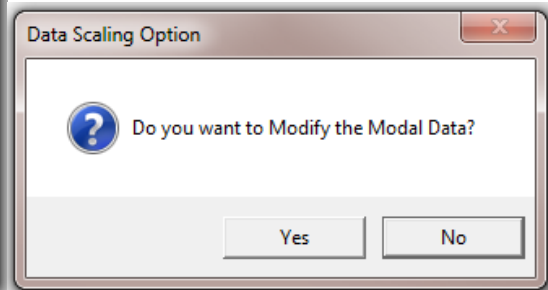
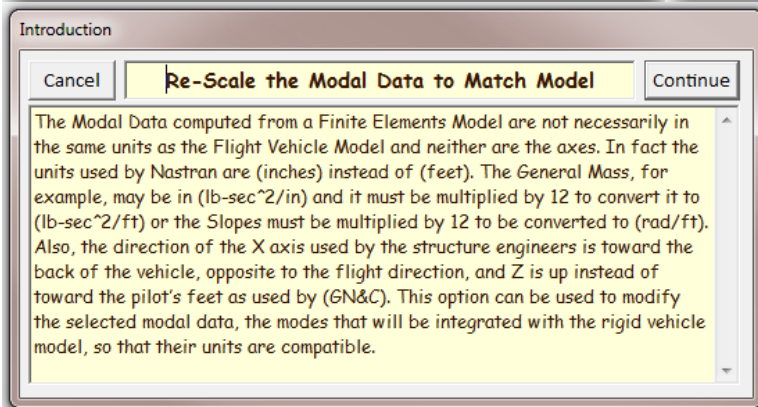
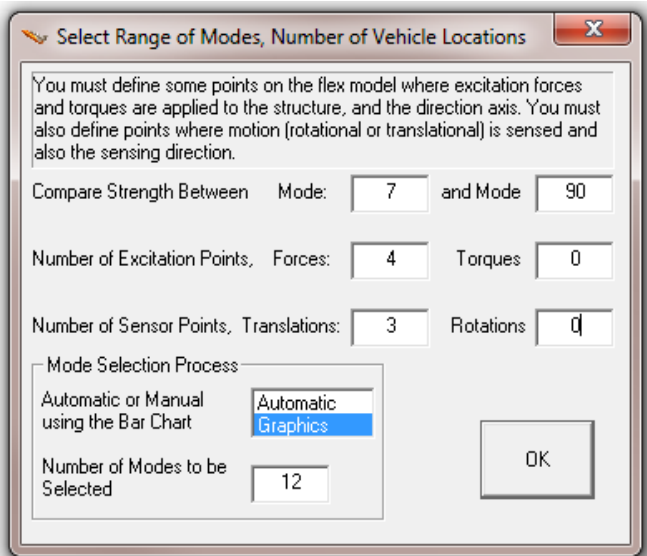
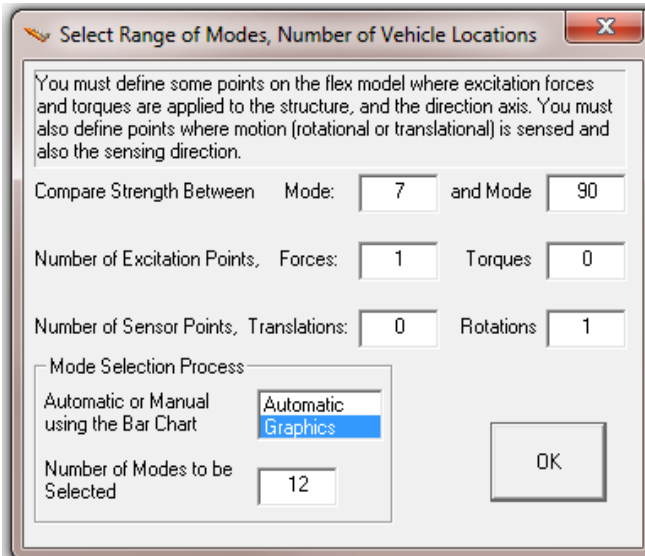


The next step is to locate the flight vehicle data-set in file “*Stg2-Damper.Inp*”. It is used by the mode selection program to identify structural nodes at important vehicle locations, such as the 3 engine gimbals, the gyros and accelerometers, the 2 slosh masses, and the 4 damper attachments where the forces will be applied. The menu below shows the titles of vehicle sets which are already saved in the input file. Select the only vehicle title “*Shuttle Second Stage with Payload Damper, at T=123 sec*” and click on “*Run Input Set*”. Only the selected modes and the mode shapes that correspond to the actuator and sensor locations which are specified in the vehicle data will be transferred and saved as a selected set of flex modes in file “*Stg2_Damper.Inp*” to be used in vehicle modeling.

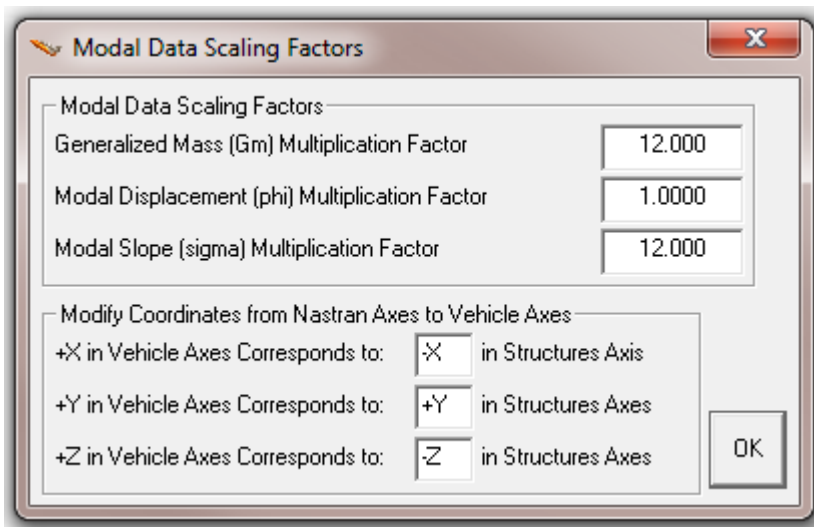


Use the following dialog to define the following parameters:

1. The range of modes to be compared in the mode selection. In this case we exclude the first six rigid-body modes and we compare modes from 7 to 90.
2. The number of excitation force and torque points and the number of translational and rotational sensors used in mode selection. They do not necessarily correspond to vehicle actuator and sensor locations but they are only used for mode strength comparison. Several combinations were attempted. Two possible choices are shown below. In the case on the left the user chooses one force (most likely the engine #1 gimbal in the z direction to excite in pitch) and one rotation measurement (the pitch gyro) in order to select a set of pitch modes. Another choice on the right would be to apply 4 forces (possibly at the 4 damper attachments) and 3 translational measurements (possibly 2 z-translations at the dampers and one z-translation at the accelerometer) to select also a set of pitch modes which are sensitive at the dampers.
3. Use the graphical option to manually select the modes from the bar plot. Ignore the option “Number of modes to be selected”.



Click “OK” to continue, and say “Yes” that you want to modify the modal data. The dialog below is used for scaling and modifying the modal data in order to be compatible with the vehicle data. The directions of the coordinate axes are different between the two models. The x and z directions must be reversed in the Nastran models because +x is defined towards the back of the vehicle and +z is up. The modal data must, therefore, be scaled during mode selection. The generalized mass is in “snails” (lb-sec²/inch) and it must be multiplied by 12 to be converted to “slugs” (lb-sec²/foot). Similarly, the modal slopes are in (rad/inch) in the Nastran model and they must be multiplied by 12 in order to be converted to (rad/foot). The modal displacements are not modified. The mode selection process provides the following dialog which enables us to convert the modal data in order to match the vehicle data. It includes initially the default conversion values described. The scaling values, signs, and axes directions can be over-written by the user to perform the necessary conversions between Nastran and vehicle data, in both, units and in directions.



The next step is to identify the excitation and sensor points on the structure that will be used to calculate and to compare the mode strengths in the mode selection process. It is the locations that correspond to the number of actuator and sensor points that were specified in the previous dialog. We use the following dialogs to select the nodes for those excitation and sensor points. In the case shown below we must select the four points for the four excitation forces at the damper attachments and also the corresponding force direction (along +Z). They will be used for mode selection purposes. The actual vehicle effectors and sensor nodes will be defined later.

The mode selection program provides interactive menus that are used to define the locations of the excitation and sensor points. It displays the nodes map in a menu/ dialog form which allows the user to select the excitation and sensor locations in the structure model, and also the directions of the excitation and measurement. In this mode comparison example we drive the structure at the two attachments of the left damper, along the $\pm z$ direction, with equal and opposite force to excite flexibility. We also excite the structure symmetrically at the right damper attachments with equal and opposite forces to excite flexibility symmetrically from both sides. Note, that if we are interested to excite the structure anti-symmetrically in roll, we should excite the left and right sides in the opposite directions.

Equal and opposite force is applied at the two ends of the left Coulomb damper along $\pm Z$, representing an extension of the device.

Table of Vehicle Structure FEM Nodes

In mode selection, in order to calculate the relative mode strength of a number of modes in a specified direction you must define some node points in the Nastran model where the excitation forces or torques will be applied and also the forcing directions.

Similarly, you must also define the sensor points (translations or rotations) and the sensing directions.

Select a Location (Node) for Force Excitation : 1

LOX SLOSH MASS	1	227	-64.672	0.0
LH2 SLOSH MASS	2	228	-125.338	0.0
Shuttle Main Engine # 1	3	2077	-182.16	0.0
Shuttle Main Engine # 2	4	2243	-184.1	-4.41
Shuttle Main Engine # 3	5	2080	-184.1	4.41
Right Coulomb Damper (payload side)	6	294	-166.08	6.99
Left Coulomb Damper (payload side)	7	3103	-166.08	-6.99
Orbiter IMU/Accelerom (right)	8	2311	-93.62	0.66
Orbiter IMU/Accelerom (left)	9	2308	-93.62	-0.66
Aft Payload Gyro (left)	10	2168	-108.55	-1.08
Aft Payload Gyro (right)	11	2172	-108.55	1.08
Right Coulomb Damper (vehicle side)	12	3101	-166.08	7.29
Left Coulomb Damper (vehicle side)	13	3102	-166.08	-7.29
Forward Payload Gyro	14	1491	-57.75	-3.33

OK
Cancel

Axis
Along-X
Along-Y
Along-Z

Direction
+ (positive)
- (negative)

Table of Vehicle Structure FEM Nodes

In mode selection, in order to calculate the relative mode strength of a number of modes in a specified direction you must define some node points in the Nastran model where the excitation forces or torques will be applied and also the forcing directions.

Similarly, you must also define the sensor points (translations or rotations) and the sensing directions.

Select a Location (Node) for Force Excitation : 2

LOX SLOSH MASS	1	227	-64.672	0.0
LH2 SLOSH MASS	2	228	-125.338	0.0
Shuttle Main Engine # 1	3	2077	-182.16	0.0
Shuttle Main Engine # 2	4	2243	-184.1	-4.41
Shuttle Main Engine # 3	5	2080	-184.1	4.41
Right Coulomb Damper (payload side)	6	294	-166.08	6.99
Left Coulomb Damper (payload side)	7	3103	-166.08	-6.99
Orbiter IMU/Accelerom (right)	8	2311	-93.62	0.66
Orbiter IMU/Accelerom (left)	9	2308	-93.62	-0.66
Aft Payload Gyro (left)	10	2168	-108.55	-1.08
Aft Payload Gyro (right)	11	2172	-108.55	1.08
Right Coulomb Damper (vehicle side)	12	3101	-166.08	7.29
Left Coulomb Damper (vehicle side)	13	3102	-166.08	-7.29
Forward Payload Gyro	14	1491	-57.75	-3.33

OK
Cancel

Axis
Along-X
Along-Y
Along-Z

Direction
+ (positive)
- (negative)

Equal and opposite force is also applied at the two ends of the right Coulomb damper along $\pm Z$, representing an extension of the device. The left and right sides are symmetrically excited for mode selection.

Table of Vehicle Structure FEM Nodes

In mode selection, in order to calculate the relative mode strength of a number of modes in a specified direction you must define some node points in the Nastran model where the excitation forces or torques will be applied and also the forcing directions.

Similarly, you must also define the sensor points (translations or rotations) and the sensing directions.

Select a Location (Node) for Force Excitation : 3

LOX SLOSH MASS	1	227	-64.672	0.0
LH2 SLOSH MASS	2	228	-125.338	0.0
Shuttle Main Engine # 1	3	2077	-182.16	0.0
Shuttle Main Engine # 2	4	2243	-184.1	-4.41
Shuttle Main Engine # 3	5	2080	-184.1	4.41
Right Coulomb Damper (payload side)	6	294	-166.08	6.99
Left Coulomb Damper (payload side)	7	3103	-166.08	-6.99
Orbiter IMU/Accelerom (right)	8	2311	-93.62	0.66
Orbiter IMU/Accelerom (left)	9	2308	-93.62	-0.66
Aft Payload Gyro (left)	10	2168	-108.55	-1.08
Aft Payload Gyro (right)	11	2172	-108.55	1.08
Right Coulomb Damper (vehicle side)	12	3101	-166.08	7.29
Left Coulomb Damper (vehicle side)	13	3102	-166.08	-7.29
Forward Payload Gyro	14	1491	-57.75	-3.33

OK
Cancel

Axis
Along-X
Along-Y
Along-Z

Direction
+ (positive)
- (negative)

Table of Vehicle Structure FEM Nodes

In mode selection, in order to calculate the relative mode strength of a number of modes in a specified direction you must define some node points in the Nastran model where the excitation forces or torques will be applied and also the forcing directions.

Similarly, you must also define the sensor points (translations or rotations) and the sensing directions.

Select a Location (Node) for Force Excitation : 4

LOX SLOSH MASS	1	227	-64.672	0.0
LH2 SLOSH MASS	2	228	-125.338	0.0
Shuttle Main Engine # 1	3	2077	-182.16	0.0
Shuttle Main Engine # 2	4	2243	-184.1	-4.41
Shuttle Main Engine # 3	5	2080	-184.1	4.41
Right Coulomb Damper (payload side)	6	294	-166.08	6.99
Left Coulomb Damper (payload side)	7	3103	-166.08	-6.99
Orbiter IMU/Accelerom (right)	8	2311	-93.62	0.66
Orbiter IMU/Accelerom (left)	9	2308	-93.62	-0.66
Aft Payload Gyro (left)	10	2168	-108.55	-1.08
Aft Payload Gyro (right)	11	2172	-108.55	1.08
Right Coulomb Damper (vehicle side)	12	3101	-166.08	7.29
Left Coulomb Damper (vehicle side)	13	3102	-166.08	-7.29
Forward Payload Gyro	14	1491	-57.75	-3.33

OK
Cancel

Axis
Along-X
Along-Y
Along-Z

Direction
+ (positive)
- (negative)

In one of the previous dialogs we also specified to use 3 translational sensors for mode comparison. For symmetric (pitch) structural measurement we may choose two of the translational sensors to measure the left and right coulomb damper extensions on the payload side, and the third sensor located at the accelerometer (node #8). All three sensors are measuring in the +z direction.

Table of Vehicle Structure FEM Nodes

In mode selection, in order to calculate the relative mode strength of a number of modes in a specified direction you must define some node points in the Nastran model where the excitation forces or torques will be applied and also the forcing directions.

Similarly, you must also define the sensor points (translations or rotations) and the sensing directions.

Select a Location (Node) for Translation Sensor 1

LOX SLOSH MASS	1	227	-64.672	0.0
LH2 SLOSH MASS	2	228	-125.338	0.0
Shuttle Main Engine # 1	3	2077	-182.16	0.0
Shuttle Main Engine # 2	4	2243	-184.1	-4.41
Shuttle Main Engine # 3	5	2080	-184.1	4.41
Right Coulomb Damper (payload side)	6	294	-166.08	6.99
Left Coulomb Damper (payload side)	7	3103	-166.08	-6.99
Orbiter IMU/Accelerom (right)	8	2311	-93.62	0.66
Orbiter IMU/Accelerom (left)	9	2308	-93.62	-0.66
Aft Payload Gyro (left)	10	2168	-108.55	-1.08
Aft Payload Gyro (right)	11	2172	-108.55	1.08
Right Coulomb Damper (vehicle side)	12	3101	-166.08	7.29
Left Coulomb Damper (vehicle side)	13	3102	-166.08	-7.29
Forward Payload Gyro	14	1491	-57.75	-3.33

OK
Cancel

Axis
Along-X
Along-Y
Along-Z

Direction
+ (positive)
- (negative)

Table of Vehicle Structure FEM Nodes

In mode selection, in order to calculate the relative mode strength of a number of modes in a specified direction you must define some node points in the Nastran model where the excitation forces or torques will be applied and also the forcing directions.

Similarly, you must also define the sensor points (translations or rotations) and the sensing directions.

Select a Location (Node) for Translation Sensor 2

LOX SLOSH MASS	1	227	-64.672	0.0
LH2 SLOSH MASS	2	228	-125.338	0.0
Shuttle Main Engine # 1	3	2077	-182.16	0.0
Shuttle Main Engine # 2	4	2243	-184.1	-4.41
Shuttle Main Engine # 3	5	2080	-184.1	4.41
Right Coulomb Damper (payload side)	6	294	-166.08	6.99
Left Coulomb Damper (payload side)	7	3103	-166.08	-6.99
Orbiter IMU/Accelerom (right)	8	2311	-93.62	0.66
Orbiter IMU/Accelerom (left)	9	2308	-93.62	-0.66
Aft Payload Gyro (left)	10	2168	-108.55	-1.08
Aft Payload Gyro (right)	11	2172	-108.55	1.08
Right Coulomb Damper (vehicle side)	12	3101	-166.08	7.29
Left Coulomb Damper (vehicle side)	13	3102	-166.08	-7.29
Forward Payload Gyro	14	1491	-57.75	-3.33

OK
Cancel

Axis
Along-X
Along-Y
Along-Z

Direction
+ (positive)
- (negative)

We have now completed the definition of the excitation and sensor points to be used in one of our mode strength comparison cases. However, the mode selection process is not finished yet because the program needs additional information from the user before it can generate the reduced set of modes in the input data file. The selected set of modes will consist of the selected dominant mode frequencies and the mode shapes only at the locations that correspond to those which are defined in the vehicle input data, such as, the engine gimbals, the damper attachment points, the sensors, etc. This requires a

similar node identification process where we must select structure nodes that correspond to the 3 TVC engines, the 2 sloshing propellant tanks, the 4 Coulomb damper attachment points which are represented as thrusters in the vehicle data, and the sensors which are specified in the vehicle input data. The program will open up dialogs similar to the previous and it will ask the user to identify those locations. The nodes selection menus are slightly different this time using a different color because they are for a different purpose. Nodes number 3 to 5 are selected for the TVC engines 1 to 3. Notice that, the 4 Coulomb damper force application points are referred to as “Thrusters” because they apply force. Thrusters 4 and 5 correspond to the left and right Coulomb damper force application points on the vehicle side (nodes 13 and 12). Thrusters 6 and 7 correspond to the left and right Coulomb damper force application points on the payload side (nodes 7 and 6). The thrusters are defined as throttling, which means that ± 1 corresponds to max force ± 350 (lb).

Table of Vehicle Structure FEM Nodes

You must now identify some points on the finite element model that correspond to the important locations on the vehicle (as specified in the vehicle data) where the forces are being applied and the motion is being sensed. Such as TVC gimbals, gyros, etc.

Select a Location (Node) for Thruster Engine : 1

LOX SLOSH MASS	1	227	-64.672	0.0
LH2 SLOSH MASS	2	228	-125.338	0.0
Shuttle Main Engine # 1	3	2077	-182.16	0.0
Shuttle Main Engine # 2	4	2243	-184.1	-4.41
Shuttle Main Engine # 3	5	2080	-184.1	4.41
Right Coulomb Damper (payload side)	6	294	-166.08	6.99
Left Coulomb Damper (payload side)	7	3103	-166.08	-6.99
Orbiter IMU/Accelerom (right)	8	2311	-93.62	0.66
Orbiter IMU/Accelerom (left)	9	2308	-93.62	-0.66
Aft Payload Gyro (left)	10	2168	-108.55	-1.08
Aft Payload Gyro (right)	11	2172	-108.55	1.08
Right Coulomb Damper (vehicle side)	12	3101	-166.08	7.29
Left Coulomb Damper (vehicle side)	13	3102	-166.08	-7.29
Forward Payload Gyro	14	1491	-57.75	-3.33

Table of Vehicle Structure FEM Nodes

You must now identify some points on the finite element model that correspond to the important locations on the vehicle (as specified in the vehicle data) where the forces are being applied and the motion is being sensed. Such as TVC gimbals, gyros, etc.

Select a Location (Node) for Thruster Engine : 4

LOX SLOSH MASS	1	227	-64.672	0.0
LH2 SLOSH MASS	2	228	-125.338	0.0
Shuttle Main Engine # 1	3	2077	-182.16	0.0
Shuttle Main Engine # 2	4	2243	-184.1	-4.41
Shuttle Main Engine # 3	5	2080	-184.1	4.41
Right Coulomb Damper (payload side)	6	294	-166.08	6.99
Left Coulomb Damper (payload side)	7	3103	-166.08	-6.99
Orbiter IMU/Accelerom (right)	8	2311	-93.62	0.66
Orbiter IMU/Accelerom (left)	9	2308	-93.62	-0.66
Aft Payload Gyro (left)	10	2168	-108.55	-1.08
Aft Payload Gyro (right)	11	2172	-108.55	1.08
Right Coulomb Damper (vehicle side)	12	3101	-166.08	7.29
Left Coulomb Damper (vehicle side)	13	3102	-166.08	-7.29
Forward Payload Gyro	14	1491	-57.75	-3.33

Table of Vehicle Structure FEM Nodes

You must now identify some points on the finite element model that correspond to the important locations on the vehicle (as specified in the vehicle data) where the forces are being applied and the motion is being sensed. Such as TVC gimbals, gyros, etc.

Select a Location (Node) for Thruster Engine : 7

LOX SLOSH MASS	1	227	-64.672	0.0
LH2 SLOSH MASS	2	228	-125.338	0.0
Shuttle Main Engine # 1	3	2077	-182.16	0.0
Shuttle Main Engine # 2	4	2243	-184.1	-4.41
Shuttle Main Engine # 3	5	2080	-184.1	4.41
Right Coulomb Damper (payload side)	6	294	-166.08	6.99
Left Coulomb Damper (payload side)	7	3103	-166.08	-6.99
Orbiter IMU/Accelerom (right)	8	2311	-93.62	0.66
Orbiter IMU/Accelerom (left)	9	2308	-93.62	-0.66
Aft Payload Gyro (left)	10	2168	-108.55	-1.08
Aft Payload Gyro (right)	11	2172	-108.55	1.08
Right Coulomb Damper (vehicle side)	12	3101	-166.08	7.29
Left Coulomb Damper (vehicle side)	13	3102	-166.08	-7.29
Forward Payload Gyro	14	1491	-57.75	-3.33

Node 10 (Aft Payload Gyro #2168) is used for the 3 rate gyro locations (roll, pitch, yaw).

Table of Vehicle Structure FEM Nodes

You must now identify some points on the finite element model that correspond to the important locations on the vehicle (as specified in the vehicle data) where the forces are being applied and the motion is being sensed. Such as TVC gimbals, gyros, etc.

Select a Location (Node) for Gyro/Rate Sensor : 1

LOX SLOSH MASS	1	227	-64.672	0.0
LH2 SLOSH MASS	2	228	-125.338	0.0
Shuttle Main Engine # 1	3	2077	-182.16	0.0
Shuttle Main Engine # 2	4	2243	-184.1	-4.41
Shuttle Main Engine # 3	5	2080	-184.1	4.41
Right Coulomb Damper (payload side)	6	294	-166.08	6.99
Left Coulomb Damper (payload side)	7	3103	-166.08	-6.99
Orbiter IMU/Accelerom (right)	8	2311	-93.62	0.66
Orbiter IMU/Accelerom (left)	9	2308	-93.62	-0.66
Aft Payload Gyro (left)	10	2168	-108.55	-1.08
Aft Payload Gyro (right)	11	2172	-108.55	1.08
Right Coulomb Damper (vehicle side)	12	3101	-166.08	7.29
Left Coulomb Damper (vehicle side)	13	3102	-166.08	-7.29
Forward Payload Gyro	14	1491	-57.75	-3.33

Node 8 (Orbiter Right Accelerometer #2311) is used for the normal and lateral accelerometers. The displacement and velocity outputs at the damper attachments are also referred to as “accelerometers”. Accelerometers 3 & 4 are the left and right damper displacement sensors on the vehicle side. Accelerometers 5 & 6 are the left and right damper displacements sensors on the payload side. Accelerometers 7 & 8 are the left and right damper velocity sensors on the vehicle side. Accelerometers 9 & 10 are the left and right damper velocity sensors on the payload side.

Table of Vehicle Structure FEM Nodes

You must now identify some points on the finite element model that correspond to the important locations on the vehicle (as specified in the vehicle data) where the forces are being applied and the motion is being sensed. Such as TVC gimbals, gyros, etc.

Select a Location (Node) for Accelerometer : 1

LOX SLOSH MASS	1	227	-64.672	0.0
LH2 SLOSH MASS	2	228	-125.338	0.0
Shuttle Main Engine # 1	3	2077	-182.16	0.0
Shuttle Main Engine # 2	4	2243	-184.1	-4.41
Shuttle Main Engine # 3	5	2080	-184.1	4.41
Right Coulomb Damper (payload side)	6	294	-166.08	6.99
Left Coulomb Damper (payload side)	7	3103	-166.08	-6.99
Orbiter IMU/Accelerom (right)	8	2311	-93.62	0.66
Orbiter IMU/Accelerom (left)	9	2308	-93.62	-0.66
Aft Payload Gyro (left)	10	2168	-108.55	-1.08
Aft Payload Gyro (right)	11	2172	-108.55	1.08
Right Coulomb Damper (vehicle side)	12	3101	-166.08	7.29
Left Coulomb Damper (vehicle side)	13	3102	-166.08	-7.29
Forward Payload Gyro	14	1491	-57.75	-3.33

OK

Table of Vehicle Structure FEM Nodes

You must now identify some points on the finite element model that correspond to the important locations on the vehicle (as specified in the vehicle data) where the forces are being applied and the motion is being sensed. Such as TVC gimbals, gyros, etc.

Select a Location (Node) for Accelerometer : 3

LOX SLOSH MASS	1	227	-64.672	0.0
LH2 SLOSH MASS	2	228	-125.338	0.0
Shuttle Main Engine # 1	3	2077	-182.16	0.0
Shuttle Main Engine # 2	4	2243	-184.1	-4.41
Shuttle Main Engine # 3	5	2080	-184.1	4.41
Right Coulomb Damper (payload side)	6	294	-166.08	6.99
Left Coulomb Damper (payload side)	7	3103	-166.08	-6.99
Orbiter IMU/Accelerom (right)	8	2311	-93.62	0.66
Orbiter IMU/Accelerom (left)	9	2308	-93.62	-0.66
Aft Payload Gyro (left)	10	2168	-108.55	-1.08
Aft Payload Gyro (right)	11	2172	-108.55	1.08
Right Coulomb Damper (vehicle side)	12	3101	-166.08	7.29
Left Coulomb Damper (vehicle side)	13	3102	-166.08	-7.29
Forward Payload Gyro	14	1491	-57.75	-3.33

OK

Finally, nodes 1 & 2 are defined to be the slosh mass locations for the liquid oxygen and the liquid hydrogen propellant tanks.

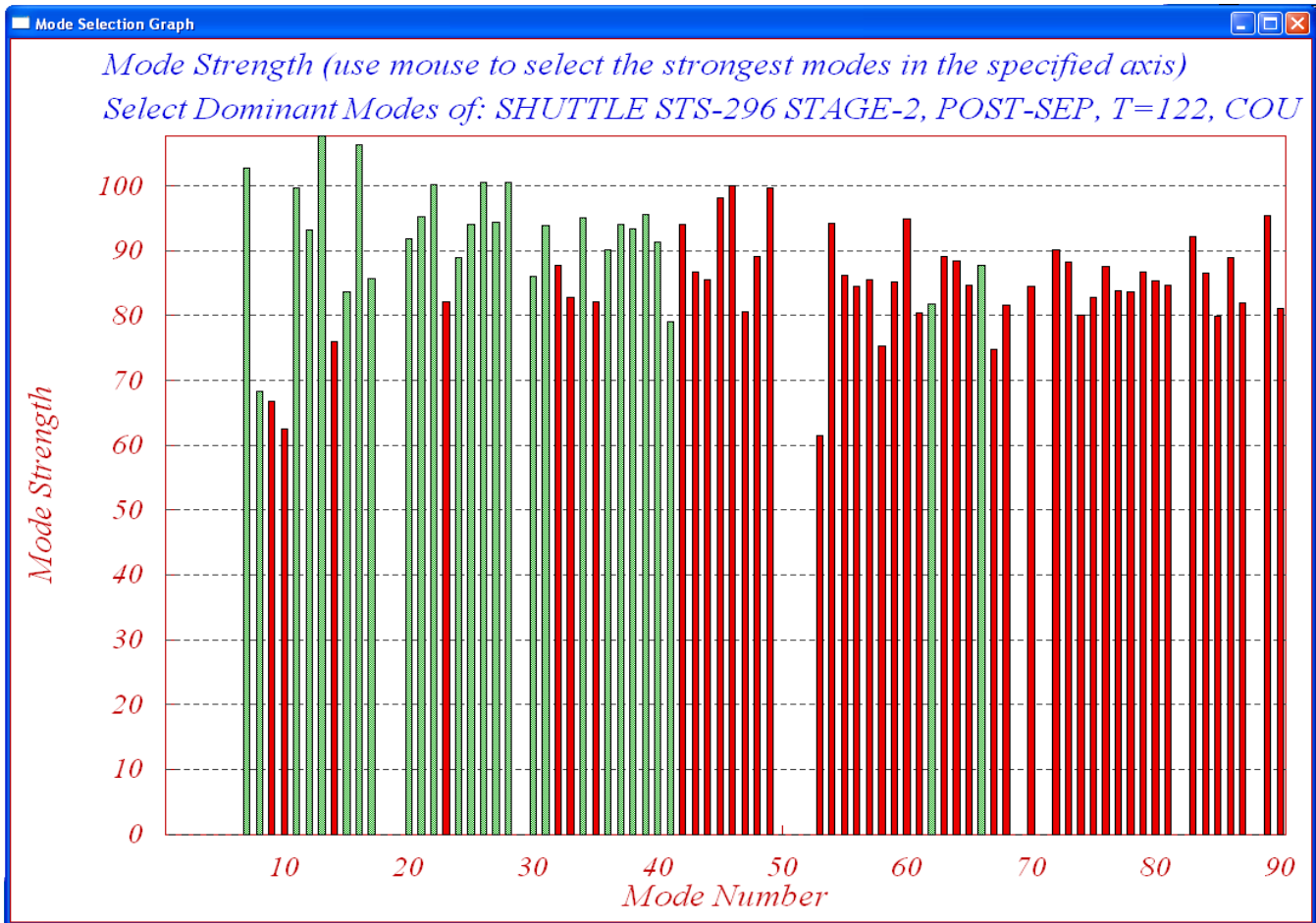
You must now identify some points on the finite element model that correspond to the important locations on the vehicle (as specified in the vehicle data) where the forces are being applied and the motion is being sensed. Such as TVC gimbals, gyros, etc.

Select a Location (Node) for Slosh Mass Locat.: 1 OK

LOX SLOSH MASS	1	227	-64.672	0.0
LH2 SLOSH MASS	2	228	-125.338	0.0
Shuttle Main Engine # 1	3	2077	-182.16	0.0
Shuttle Main Engine # 2	4	2243	-184.1	-4.41
Shuttle Main Engine # 3	5	2080	-184.1	4.41
Right Coulomb Damper (payload side)	6	294	-166.08	6.99
Left Coulomb Damper (payload side)	7	3103	-166.08	-6.99
Orbiter IMU/Accelerom (right)	8	2311	-93.62	0.66
Orbiter IMU/Accelerom (left)	9	2308	-93.62	-0.66
Aft Payload Gyro (left)	10	2168	-108.55	-1.08
Aft Payload Gyro (right)	11	2172	-108.55	1.08
Right Coulomb Damper (vehicle side)	12	3101	-166.08	7.29
Left Coulomb Damper (vehicle side)	13	3102	-166.08	-7.29
Forward Payload Gyro	14	1491	-57.75	-3.33

The mode selection program reads the mode shapes and slopes at the selected locations and performs a mode strength comparison from the excitation points and directions to the sensor points and directions. When the comparison is complete it saves the relative mode strength of each mode as a function of frequency in file “*Modsel.Dat*” and expects the user to manually select the dominant modes. It opens a mode comparison plot for manually selecting the modes. Each mode appears as a vertical red bar of mode strength plotted against the mode numbers, and the height of each bar is logarithmically proportional to its modal strength. The strong modes appear tall and the weak modes are short. The user can select some of the strongest modes to be retained manually, by pointing the mouse cursor on a bar and clicking the mouse. The modes change color from red to green when they are selected. Notice that the first 6 rigid-body modes are not shown. When you finish selecting the modes press the “*Enter*” button on the keyboard and it will save the selected modal data set in the input data file.

For this analysis we selected 27 flexible modes as a result of multiple flex mode comparisons that were performed between different excitation and sensor points using symmetric and anti-symmetric excitations and measurements. In some cases we also included rotational measurements to evaluate sensitivity at the gyros. The selected modes from the combined analysis are: 7, 8, 11, 12, 13, 15, 16, 17, 20, 21, 22, 24, 25, 26, 27, 28, 30, 31, 34, 36, 37, 38, 39, 40, 41, 62, and 66.



A short description regarding the nature of the selected modal data is also entered by means of a text dialog. Information such as, conditions, actuator and sensor locations, directions, etc. are included as comment lines for reference below the title of the selected modes. The selected 27 modes are saved in file "Stg2_Damper.Inp". The default title of the selected modes set was modified to "Shuttle Second Stage with Payload Damper, at T=123 sec, Mixed Modes". The title of the selected modes must also be included in the last line of the vehicle input data, below the line "Number of Modes: 27", in order for the flight vehicle modeling program to associate the modes with the vehicle data. The selected modes are now ready to be combined with the vehicle data and to create the flexible vehicle state model.

The selected set of modal data in file: "Stg2_Damper.Inp" that includes 27 structural modes. Only the first two modes are shown.

SELECTED MODAL DATA AND LOCATIONS USING MULTIPLE CRITERIA

Shuttle Second Stage with Payload Damper, at T=123 sec, Mixed Modes

! The Finite Elements Model does not include the Coulong Damper.
 ! The model includes four nodes that connect to the two ends of the
 ! two dampers. Modes were selected using a compilation of many criteria
 ! (a)- from TVC engines to pitch gyro,
 ! (b)- symmetric forces on the vehicle along Z at the 2 damper attachments
 ! to symmetric accelerations at the payload attachments.
 ! (c)- antisymmetric Z-forces on the vehicle at the 2 damper attachments
 ! to anti-symmetric accelerations at the payload attachments.

MODE # 1/ 7, Frequency (rad/sec), Damping (zeta), Generalized Mass=	9.0752	0.50000E-02	43216.			
DEFINITION OF LOCATIONS (NODES)	phi along X	phi along Y	phi along Z	sigm about X	sigm about Y	sigm about Z
Modal Data at the 7 Engines, (x,y,z)...						
Shuttle Main Engine # 1	2077	0.15362D+00	0.12782D-02	-0.24250D+00	0.69584D-04	-0.89453D-02
Shuttle Main Engine # 2	2243	0.79232D-01	0.13871D-02	-0.25930D+00	-0.43284D-04	-0.88351D-02
Shuttle Main Engine # 3	2080	0.79451D-01	0.12117D-02	-0.26014D+00	0.79560D-04	-0.97774D-02
Left Coulomb Damper (vehicle s	3102	0.00000D+00	0.13251D-01	-0.81907D-01	0.00000D+00	0.00000D+00
Right Coulomb Damper (vehicle	3101	0.00000D+00	-0.10628D-01	-0.81643D-01	0.00000D+00	0.00000D+00
Left Coulomb Damper (payload	3103	0.11840D+00	0.39883D-03	-0.20333D+01	0.00000D+00	0.00000D+00
Right Coulomb Damper (payload	294	0.11514D+00	-0.11015D-01	-0.20360D+01	0.00000D+00	0.00000D+00
Modal Data at the 3 Gyros ...						
Aft Payload Gyro (left)	2168	0.44584D-01	0.00000D+00	0.00000D+00	0.24427D-03	-0.10604D-01
Aft Payload Gyro (left)	2168	0.44584D-01	0.00000D+00	0.00000D+00	0.24427D-03	-0.10604D-01
Aft Payload Gyro (left)	2168	0.44584D-01	0.00000D+00	0.00000D+00	0.24427D-03	-0.10604D-01
Modal Data at the 10 Accelerometers, along (x,y,z)...						
Orbiter IMU/Accelerom (right)	2311	0.00000D+00	0.12908D-02	-0.98519D-02		
Orbiter IMU/Accelerom (right)	2311	0.00000D+00	0.12908D-02	-0.98519D-02		
Left Coulomb Damper (vehicle s	3102	0.00000D+00	0.13251D-01	-0.81907D-01		
Right Coulomb Damper (vehicle	3101	0.00000D+00	-0.10628D-01	-0.81643D-01		
Left Coulomb Damper (payload	3103	0.11840D+00	0.39883D-03	-0.20333D+01		
Right Coulomb Damper (payload	294	0.11514D+00	-0.11015D-01	-0.20360D+01		
Left Coulomb Damper (vehicle s	3102	0.00000D+00	0.13251D-01	-0.81907D-01		
Right Coulomb Damper (vehicle	3101	0.00000D+00	-0.10628D-01	-0.81643D-01		
Left Coulomb Damper (payload	3103	0.11840D+00	0.39883D-03	-0.20333D+01		
Right Coulomb Damper (payload	294	0.11514D+00	-0.11015D-01	-0.20360D+01		
Modal Data at the 2 Slosh Masses...						
LOX SLOSH MASS	227	0.00000D+00	-0.23727D-03	-0.32455D-01	0.00000D+00	0.00000D+00
LH2 SLOSH MASS	228	0.00000D+00	-0.38542D-03	-0.79081D-01	0.00000D+00	0.00000D+00
Modal Data at the Disturbance Point						
Shuttle Main Engine # 1	2077	0.15362D+00	0.12782D-02	-0.24250D+00	0.69584D-04	-0.89453D-02

MODE # 2/ 8, Frequency (rad/sec), Damping (zeta), Generalized Mass=	9.4117	0.50000E-02	43216.			
DEFINITION OF LOCATIONS (NODES)	phi along X	phi along Y	phi along Z	sigm about X	sigm about Y	sigm about Z
Modal Data at the 7 Engines, (x,y,z)...						
Shuttle Main Engine # 1	2077	-0.69673D-03	-0.11869D+00	0.21129D-02	-0.35287D-02	0.78575D-04
Shuttle Main Engine # 2	2243	0.34073D-03	-0.89213D-01	0.17570D-01	-0.35216D-02	-0.21202D-04
Shuttle Main Engine # 3	2080	-0.12625D-02	-0.89319D-01	-0.13351D-01	-0.34372D-02	-0.68072D-04
Left Coulomb Damper (vehicle s	3102	0.00000D+00	-0.94655D-01	0.24381D-01	0.00000D+00	0.00000D+00
Right Coulomb Damper (vehicle	3101	0.00000D+00	-0.94564D-01	-0.21434D-01	0.00000D+00	0.00000D+00
Left Coulomb Damper (payload	3103	0.17086D-01	0.44947D-01	-0.61580D-01	0.00000D+00	0.00000D+00
Right Coulomb Damper (payload	294	-0.18282D-01	0.45011D-01	0.55888D-01	0.00000D+00	0.00000D+00
Modal Data at the 3 Gyros ...						
Aft Payload Gyro (left)	2168	0.11844D-03	0.00000D+00	0.00000D+00	-0.33881D-02	0.61501D-04
Aft Payload Gyro (left)	2168	0.11844D-03	0.00000D+00	0.00000D+00	-0.33881D-02	0.61501D-04
Aft Payload Gyro (left)	2168	0.11844D-03	0.00000D+00	0.00000D+00	-0.33881D-02	0.61501D-04
Modal Data at the 10 Accelerometers, along (x,y,z)...						
Orbiter IMU/Accelerom (right)	2311	0.00000D+00	-0.10966D+00	-0.25398D-02		
Orbiter IMU/Accelerom (right)	2311	0.00000D+00	-0.10966D+00	-0.25398D-02		
Left Coulomb Damper (vehicle s	3102	0.00000D+00	-0.94655D-01	0.24381D-01		
Right Coulomb Damper (vehicle	3101	0.00000D+00	-0.94564D-01	-0.21434D-01		
Left Coulomb Damper (payload	3103	0.17086D-01	0.44947D-01	-0.61580D-01		
Right Coulomb Damper (payload	294	-0.18282D-01	0.45011D-01	0.55888D-01		
Left Coulomb Damper (vehicle s	3102	0.00000D+00	-0.94655D-01	0.24381D-01		
Right Coulomb Damper (vehicle	3101	0.00000D+00	-0.94564D-01	-0.21434D-01		
Left Coulomb Damper (payload	3103	0.17086D-01	0.44947D-01	-0.61580D-01		
Right Coulomb Damper (payload	294	-0.18282D-01	0.45011D-01	0.55888D-01		
Modal Data at the 2 Slosh Masses...						
LOX SLOSH MASS	227	0.00000D+00	-0.15104D-02	0.58053D-04	0.00000D+00	0.00000D+00
LH2 SLOSH MASS	228	0.00000D+00	-0.21983D-02	0.91942D-03	0.00000D+00	0.00000D+00
Modal Data at the Disturbance Point						
Shuttle Main Engine # 1	2077	-0.69673D-03	-0.11869D+00	0.21129D-02	-0.35287D-02	0.78575D-04

2 Generating the Flexible Vehicle with Payload State-Space Model

The vehicle model is defined in the input data file “*Stg2_Damper.Inp*” which is in folder “*Flixan\Examples\ Payload Damper*”. The data set includes: trajectory data, mass properties, and aero data corresponding to post SRB separation, which happens at $t=123$ seconds after lift-off. The flags in the first line below the comments indicate that: the output rates are vehicle body rates, the attitudes are integrals of body rates (not Euler angles), the model will not include aeroelasticity data, and no turn-coordination terms are included in the output rates. The vehicle has three gimbaling Shuttle main engines with the tail-wags-dog option turned on. The four forces generated on the vehicle and on the payload sides by the two Coulomb dampers are represented by four jets of variable thrust. Note that the flexible payload is included in finite elements model but the coulomb dampers are not connected and the ends of the structure across the dampers are free. The four thrusters are defined as “Throttling” and are normalized to ± 350 (lb) maximum thrust, which is the damper breakout force. That is, each thruster is defined to be generating a force which is limited to ± 350 pounds maximum when the corresponding input varies between ± 1 . Thrusters 4 and 5 generate the left and right Coulomb damper forces on the vehicle side in the $+Z$ direction ($+1$ corresponds to a force of $+350$ lb), and thrusters 6 and 7 generate the left and right Coulomb damper forces on the payload side in the $-Z$ direction ($+1$ corresponds to a force of -350 lb). A special function “*Coulomb-Damper.m*” will be used in the simulations to generate the damper force as a function of the relative motion at the two ends of the damper.

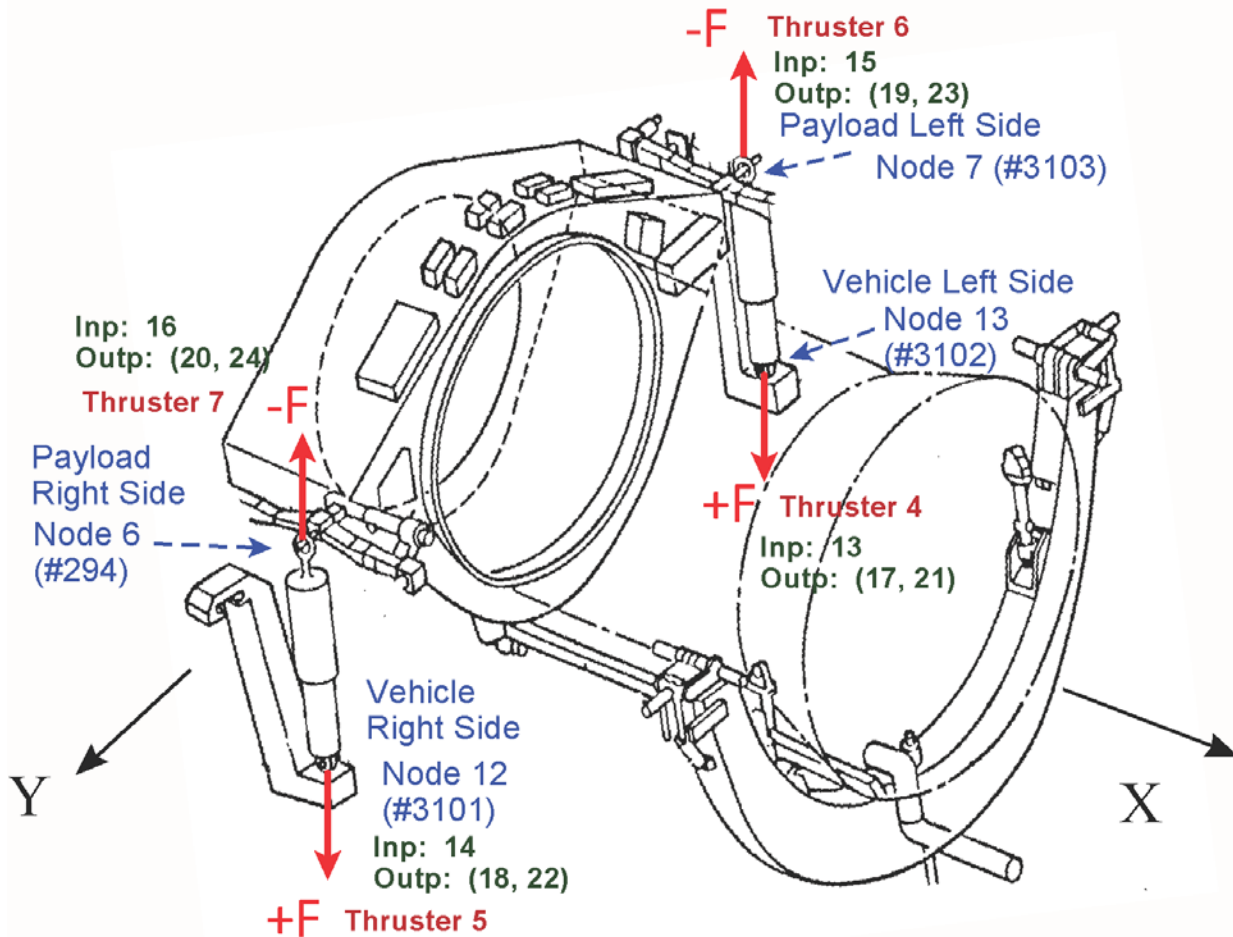
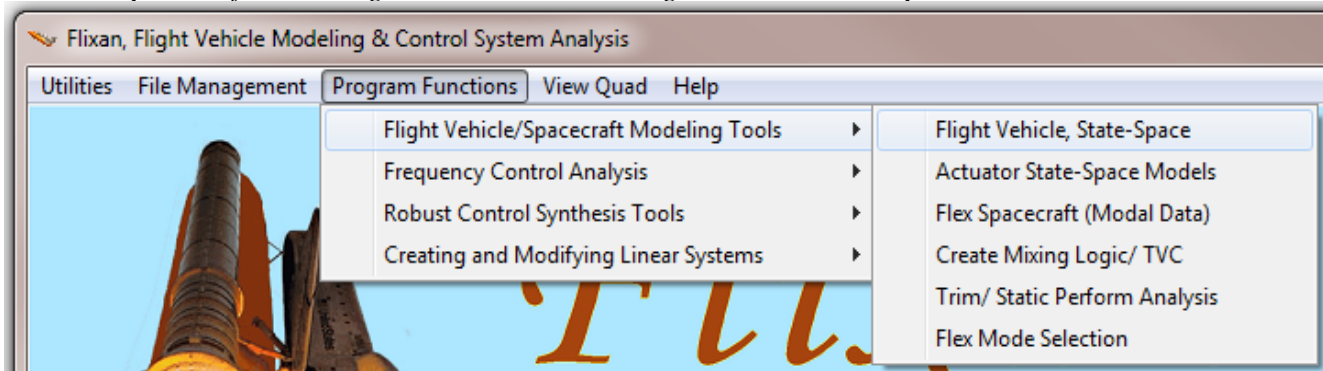


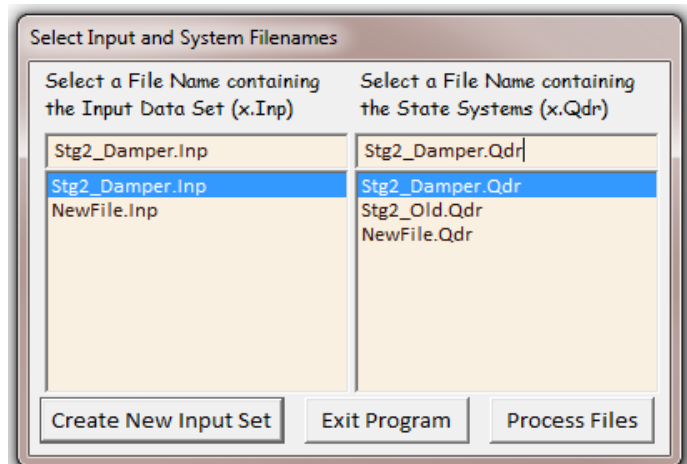
Figure 3 Shows the 4 Coulomb Damper attachment points, the locations of the dynamic model Inputs and Outputs, and the forces on the vehicle and on the payload sides generated by the dampers compression.

There are three rate gyros and two accelerometers on the vehicle measuring rigid and flex motion and used for flight control. There are eight additional measurements defined as “accelerometers”, but in fact they are position and velocity sensors at the two ends of the dampers. The first four measure flex displacements alone (rigid-body motion is excluded), at the four damper attachments, and the other four measure flex velocities only (rigid-body motion is excluded) at the same four attachments. The four displacement and four velocity measurements at the four damper attachments are defined to measure only flexibility “Pos.Flex” and “Vel.Flex” in the Z directions. This definition excludes the rigid-body components. The relative displacements and velocities at each damper will be used in the simulation by the Matlab damper function to calculate the normalized reaction forces at the two damper attachments. The vehicle model contains also two slosh modes that represent sloshing of the liquid oxygen and liquid hydrogen propellants inside the tanks. The model will also include the selected set of 27 structural modes which was prepared in Section 1, having a title: “*Shuttle Second Stage with Payload Damper, at T=123 sec, Mixed Modes*”.

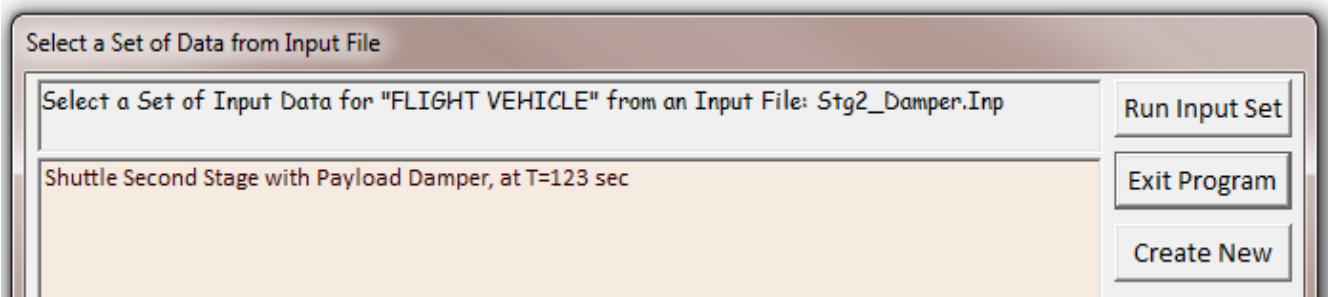
The Flixan flight vehicle modeling program is used to generate the flexible vehicle state-space model. Begin the Flixan program and choose the directory: “\Flixan\ Examples\ Payload Damper”. The Flixan main menu comes up and the program is selected by clicking on “Program Functions”, then “Flight Vehicle/ Spacecraft Modeling Tools”, and then “Flight Vehicle State-Space Models”, as shown below.



From the filenames selection menu choose the input file “*Stg2_Damper.Inp*” that contains the vehicle data, and the output systems file “*Stg2_Damper.Qdr*”, and click on “Process Files”.



The menu below shows the titles of the flight vehicle data-sets which are already saved in the input file. Select the vehicle set “*Shuttle Second Stage with Payload Damper, at T=123 sec*” and click on “Run Input Set”.



The following dialog appears showing the various vehicle parameters. Click on “Run” and the program will combine the vehicle data with the flex data-set that includes the selected 27 structural modes to create the flexible vehicle/ payload state-space model. It will save it in file “*Stg2-Damper.Qdr*” using the same title as the input data “*Shuttle Second Stage with Payload Damper, at T=123 sec*”.

Flight Vehicle Parameters

Vehicle System Title
Shuttle Second Stage with Payload Damper, at T=123 sec

Number of Vehicle Effectors
 Gimballing Engines or Jets. Include Tail-Wags-Dog? WITH TWD / WITHOUT TWD
 Rotating Control Surfaces. Include Tail-Wags-Dog? WITH TWD / WITHOUT TWD
 Reaction Wheels? **Momentum Control Devices**
 Single Gimbal CMGs? Include a 3-axes Stabilized Double Gimbal CMG System? Yes/No

Number of Sensors
 Gyros
 Acceleromet
 Aero Vanes
 External Torques

Modeling Options (Flags)
 Output Rates in: Body Axes, Stability Axes
 Turn Coordination?: Include Turn Coordination, Without Turn Coordination
 Aero-Elasticity Options: Include GAFD, H-param Flex Coupl. data only, Neither Gafid nor Hpar
 Attitude Angles: Euler Angles, Integrals of Rates, LVLH Attitude

Number of Modes
 Structure Bending
 Fuel Sloshing:

Buttons: Edit Input File, Exit, Update Data, Run, Save in File

Reaction/Wheels | Single Gimbal CMGs | Double Gimbal CMG System | Slewing Appendages | Gyros | Accelerometer | Aero Sensors | Fuel Slosh | Flex Modes | User Notes
 Mass Properties | Trajectory Data | Gust/ Aero Paramet. | Aero Force Coeffs | Aero Moment Coeffs | Control Surfaces | Gimbal Engines/ RCS | External Torques

This Vehicle has 7 Thruster Engines Engine No: 4 Left Dampr Vehi Engine/ Thruster Jet Definition

Thrust in (lb): Nominal Thrust Maximum Thrust
 Maximum Deflections (deg): Pitch, Delta_Y max Yaw, Delta_Z max
 Nominal Position Angles (deg): Azimuth, Delta_Zo Elevation, Delta_Yo
 Engine Orientation Angles with respect to the vehicle X axis

Engine Mass Properties: Engine Mass in (Slugs) Moment of Inertia about the Gimbal (slug-ft^2) Moment Arm (ft), Engine CG to Gimbal
 Location of Engine Gimbal (feet): X_gimbal Y_gimbal Z_gimbal
 Gimballing or Throttling?: Is the Engine Gimballing? Yes/No Can it Vary its Thrust like a Jet? Yes/No

The definitions of the vehicle state-space variables are also included in the systems file, below the state-space matrices. The inputs to the model are 3 engine pitch and yaw deflections and the 3 engine pitch and yaw accelerations. There are also four throttles (inputs 13 to 16) which are applied at the attachment points of the two dampers, two on the vehicle and two on the payload sides. They represent the normalized reaction forces generated by the coulomb damper extensions and they must be equal and opposite on each side (see Figure 3). The last input (17) is a wind gust velocity disturbance in (ft/sec) striking the vehicle in a direction that is specified in the vehicle data. The gust direction is perpendicular to the x-axis and at 45 deg azimuth (that is between the +Z and the +Y right side of the vehicle).

The vehicle outputs consist of: rigid body attitudes and rates, angles of attack and sideslip, rate gyro measurements (including flexibility), normal and lateral accelerations at the accelerometers (with flex). Outputs (17-20) are the structural displacements at the 4 ends of the Coulomb dampers, and outputs (21-24) are the structural velocities at the same 4 ends of the two Coulomb dampers. Outputs (25-27) are the pitch load-torques and outputs (28-30) are the yaw load-torques at the three TVC gimbals as a result of the vehicle normal and lateral accelerations. The dampers are non-linear devices and they will be introduced later in the DF analysis and simulations. The data-set below is the Shuttle vehicle parameters during second stage, at t=123 seconds after lift-off. It is included in file “*Stg2-Damper.Inp*”, and was used to generate the flexible vehicle state-space model.

FLIGHT VEHICLE INPUT DATA

Shuttle Second Stage with Payload Damper, at T=123 sec

! This is a Second Stage Shuttle Ascent model at T=123 sec, after solid booster separation.
! It will be used in flexible payload analysis with a non-linear Coulomb Damper. There are
! two dampers whose two ends are attached to both the vehicle and the payload. Seven engines
! are defined. Only the first 3 engines are real, the actual 3 SSME's. Engines 4-7 are only
! force application points used to apply the coulomb damper forces, both on the payload and
! on the vehicle. There are 10 translational sensors. The first two are accelerometers in
! Z and Y directions. Sensors 3-6 measure Displacement in the Z direction, and sensors 7-10
! measure Velocity in the Z direction at the two ends of the two dampers. They measure the
! relative motion between vehicle and payload across the dampers used for calculating the
! damper forces.

Body Axes Output,Attitude=Rate Integral,Without GAFD, No Turn Coordination

Vehicle Mass (lb-sec^2/ft), Gravity Accelerat. (g) (ft/sec^2), Earth Radius (Re) (ft) : 0.41820E+05 32.1 0.20896E+08
Moments and products of Inertias Ixx, Iyy, Izz, Ixy, Ixz, Iyz, in (lb-sec^2-ft) : 0.6047E+7 0.8733E+8 0.8295E+8
CG location with respect to the Vehicle Reference Point, Xcg, Ycg, Zcg, in (feet) : -95.194 0.0619 -38.847
Vehicle Mach Number, Velocity Vo (ft/sec), Dynamic Pressure (psf), Altitude (feet) : 4.25 4217.4 31.37 0.1531E+06
Inertial Acceleration Vo_dot, Sensed Body Axes Accelerations Ax,Ay,Az (ft/sec^2) : 28.77 28.87 0.14 8.484
Angles of Attack and Sideslip (deg), alpha, beta rates (deg/sec) : 2.78 0.1 0.0 0.0
Vehicle Attitude Euler Angles, Phi_o,Thet_o,Psi_o (deg), Body Rates Po,Qo,Ro (deg/sec) : -178.6 26.3 90.4 0.043 0.2825 -0.026
Wind Gust Vel wrt Vehicle (Azim & Elev) angles, or Force (lb), location, Torque (ft-lb) : Gust 45.0 90.0
Surface Reference Area (feet^2), Mean Aerodynamic Chord (ft), Wing Span in (feet) : 2690.0 39.56 78.05
Aero Moment Reference Center (Xmrc,Ymrc,Zmrc) Location in (ft), {Partial_rho/ Partial_H} : -95.194 0.0619 -38.847 0.0000
Aero Force Coef/Deriv (1/deg), Along -X, {Cao,Ca_alf,PCa/PV,PCa/Ph,Ca_alfdot,Ca_q,Ca_bet} : 0.1435 0.00314 0.00 0.0 0.0
Aero Force Coeff/Derivat (1/deg), Along Y, {Cyo,Cy_bet,Cy_r,Cy_alf,Cy_p,Cy_betdot,Cy_V} : -0.003 -0.0317 0.0 -0.00226 0.0000
Aero Force Coeff/Deriv (1/deg), Along Z, {Czo,Cz_alf,Cz_q,Cz_bet,PCz/Ph,Cz_alfdot,PCz/PV} : 0.013 -0.02928 0.00 0.0000 0.0000
Aero Moment Coeff/Derivat (1/deg), Roll: {Clo, Cl_beta, Cl_betdot, Cl_p, Cl_r, Cl_alfa} : -0.00173 -0.00451 0.00 0.00
Aero Moment Coeff/Deriv (1/deg), Pitch: {Cmo,Cm_alfa,Cm_alfdot,Cm_bet,Cm_q,PCm/PV,PCm/Ph} : 0.05586 -0.01484 0.0 0.0 0.0000
Aero Moment Coeff/Derivat (1/deg), Yaw : {Cno,Cn_beta, Cn_betdot, Cn_p, Cn_r, Cn_alfa} : 0.00152 0.0086 0.0 0.00 0.0

Number of Thruster Engines, Include or Not the Tail-Wags-Dog and Load-Torque Dynamics ? : 7 WITH TWD

TVC Engine No: 1 (Gimbaling Throttling Single_Gimbal) : SSME Top-Cent Gimbaling only
Engine Nominal Thrust, and Maximum Thrust in (lb) (for throttling) : 488688.0 488688.0
Mounting Angles wrt Vehicle (Dyn,Dzn), Maximum Deflections from Mount (Dymax,Dzmax) (deg) : -14.0 0.0 10.0 10.0
Eng Mass (slug), Inertia about Gimbal (lb-sec^2-ft), Moment Arm, engine CG to gimbal (ft) : 210.0 4032.0 3.0
Gimbal location with respect to the Vehicle Reference Axes, Xgimb, Ygimb, Zgimb, in (ft) : -182.16 0.0 -64.94
TVC Engine No: 2 (Gimbaling Throttling Single_Gimbal) : SSME Left Gimbaling only
Engine Nominal Thrust, and Maximum Thrust in (lb) (for throttling) : 488688.0 488688.0
Mounting Angles wrt Vehicle (Dyn,Dzn), Maximum Deflections from Mount (Dymax,Dzmax) (deg) : -10.8 3.5 10.0 10.0
Eng Mass (slug), Inertia about Gimbal (lb-sec^2-ft), Moment Arm, engine CG to gimbal (ft) : 210.0 4032.0 3.0
Gimbal location with respect to the Vehicle Reference Axes, Xgimb, Ygimb, Zgimb, in (ft) : -184.1 -4.4 -56.33
TVC Engine No: 3 (Gimbaling Throttling Single_Gimbal) : SSME Right Gimbaling only
Engine Nominal Thrust, and Maximum Thrust in (lb) (for throttling) : 488688.0 488688.0
Mounting Angles wrt Vehicle (Dyn,Dzn), Maximum Deflections from Mount (Dymax,Dzmax) (deg) : -10.8 -3.5 10.0 10.0
Eng Mass (slug), Inertia about Gimbal (lb-sec^2-ft), Moment Arm, engine CG to gimbal (ft) : 210.0 4032.0 3.0
Gimbal location with respect to the Vehicle Reference Axes, Xgimb, Ygimb, Zgimb, in (ft) : -184.1 +4.4 -56.33
Engine No: 4 (Gimbaling Throttling Single_Gimbal) : Left Dampr Vehi Throttling
Engine Nominal Thrust, and Maximum Thrust in (lb) (for throttling) : 0.0 350.0
Mounting Angles wrt Vehicle (Dyn,Dzn), Maximum Deflections from Mount (Dymax,Dzmax) (deg) : -90.0 0.0 0.0 0.0
Eng Mass (slug), Inertia about Gimbal (lb-sec^2-ft), Moment Arm, engine CG to gimbal (ft) : 0.0 0.0 0.0 0.0
Gimbal location with respect to the Vehicle Reference Axes, Xgimb, Ygimb, Zgimb, in (ft) : -166.08 -7.29 -65.91
Engine No: 5 (Gimbaling Throttling Single_Gimbal) : Right Dampr Vehi Throttling
Engine Nominal Thrust, and Maximum Thrust in (lb) (for throttling) : 0.0 350.0
Mounting Angles wrt Vehicle (Dyn,Dzn), Maximum Deflections from Mount (Dymax,Dzmax) (deg) : -90.0 0.0 0.0 0.0
Eng Mass (slug), Inertia about Gimbal (lb-sec^2-ft), Moment Arm, engine CG to gimbal (ft) : 0.0 0.0 0.0 0.0
Gimbal location with respect to the Vehicle Reference Axes, Xgimb, Ygimb, Zgimb, in (ft) : -166.08 +7.29 -65.91
Engine No: 6 (Gimbaling Throttling Single_Gimbal) : Left Dampr Payld Throttling
Engine Nominal Thrust, and Maximum Thrust in (lb) (for throttling) : 0.0 350.0
Mounting Angles wrt Vehicle (Dyn,Dzn), Maximum Deflections from Mount (Dymax,Dzmax) (deg) : +90.0 0.0 0.0 0.0
Eng Mass (slug), Inertia about Gimbal (lb-sec^2-ft), Moment Arm, engine CG to gimbal (ft) : 0.0 0.0 0.0 0.0
Gimbal location with respect to the Vehicle Reference Axes, Xgimb, Ygimb, Zgimb, in (ft) : -166.08 -7.00 -67.83
Engine No: 7 (Gimbaling Throttling Single_Gimbal) : Right Dampr Payld Throttling
Engine Nominal Thrust, and Maximum Thrust in (lb) (for throttling) : 0.0 350.0
Mounting Angles wrt Vehicle (Dyn,Dzn), Maximum Deflections from Mount (Dymax,Dzmax) (deg) : +90.0 0.0 0.0 0.0
Eng Mass (slug), Inertia about Gimbal (lb-sec^2-ft), Moment Arm, engine CG to gimbal (ft) : 0.0 0.0 0.0 0.0
Gimbal location with respect to the Vehicle Reference Axes, Xgimb, Ygimb, Zgimb, in (ft) : -166.08 +7.00 -67.83

Number of Gyros, (Attitude and Rate) : 3
Gyro No 1 Axis:(Pitch,Yaw,Roll), (Attitude, Rate, Accelerat), Sensor Location in (feet) : Roll Rate -93.62 0.0 -61.53
Gyro No 2 Axis:(Pitch,Yaw,Roll), (Attitude, Rate, Accelerat), Sensor Location in (feet) : Pitch Rate -93.62 0.0 -61.53
Gyro No 3 Axis:(Pitch,Yaw,Roll), (Attitude, Rate, Accelerat), Sensor Location in (feet) : Yaw Rate -93.62 0.0 -61.53

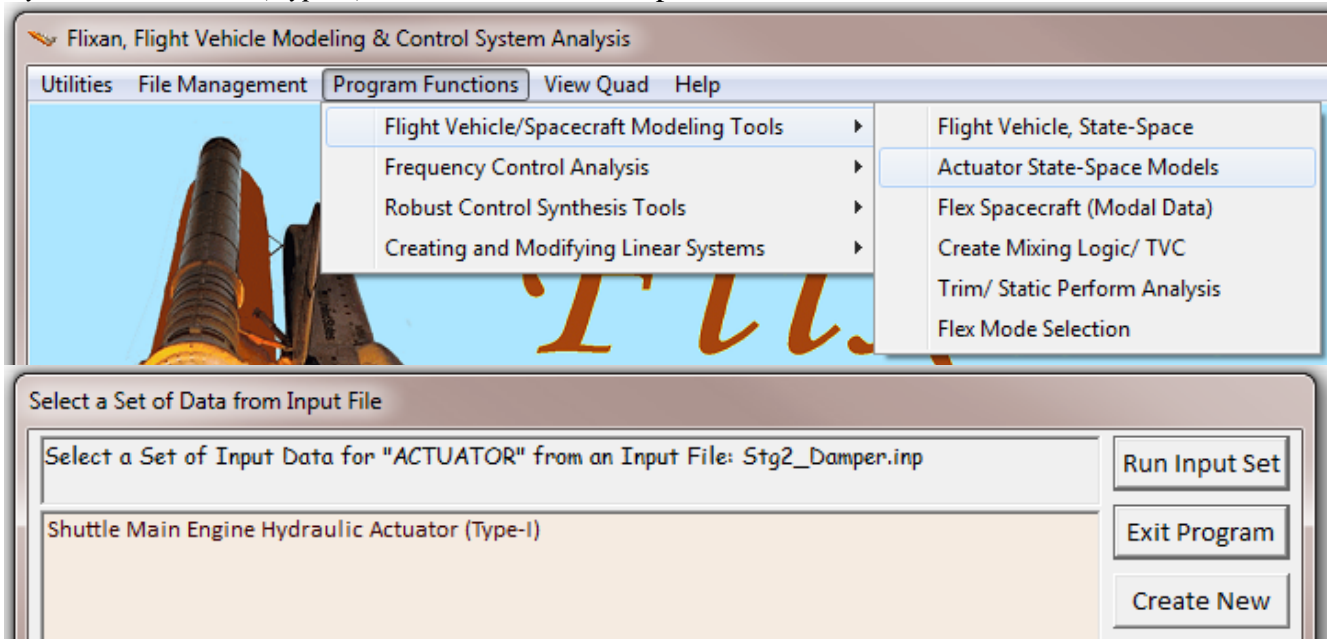
Number of Accelerometers, Along Axis: (x,y,z) : 10
Acceleromet No 1 Axis:(X,Y,Z), (Z Acceleration, Flex and Rigid), (N2311) : Z-axis Accelerat. -93.62 0.0 -61.53
Acceleromet No 2 Axis:(X,Y,Z), (Y Acceleration, Flex and Rigid), (N2311) : Y-axis Accelerat. -93.62 0.0 -61.53
Acceleromet No 3 Axis:(X,Y,Z), (Flex Position Only, No Rig-Body), (Vehicle Left N3102) : Z-axis Pos.Flex -166.08 -7.29 -65.9
Acceleromet No 4 Axis:(X,Y,Z), (Flex Position Only, No Rig-Body), (Vehicle Rght N3101) : Z-axis Pos.Flex -166.08 +7.29 -65.9
Acceleromet No 5 Axis:(X,Y,Z), (Flex Position Only, No Rig-Body), (Payload Left N3103) : Z-axis Pos.Flex -166.08 -7.00 -67.8
Acceleromet No 6 Axis:(X,Y,Z), (Flex Position Only, No Rig-Body), (Payload Right N294) : Z-axis Pos.Flex -166.08 +7.00 -67.8
Acceleromet No 7 Axis:(X,Y,Z), (Flex Velocity Only, No Rig-Body), (Vehicle Left N3102) : Z-axis Vel.Flex -166.08 -7.29 -65.9
Acceleromet No 8 Axis:(X,Y,Z), (Flex Velocity Only, No Rig-Body), (Vehicle Rght N3101) : Z-axis Vel.Flex -166.08 +7.29 -65.9
Acceleromet No 9 Axis:(X,Y,Z), (Flex Velocity Only, No Rig-Body), (Payload Left N3103) : Z-axis Vel.Flex -166.08 -7.00 -67.8
Acceleromet No 10 Axis:(X,Y,Z), (Flex Velocity Only, No Rig-Body), (Payload Right N294) : Z-axis Vel.Flex -166.08 +7.00 -67.8

Number of Slosh Modes : 2
LOX Slosh Mass (slugs), Frequ Wy,Wz 1g (rad/s), Damp (zeta-y-z), Locat {Xsl,Ysl,Zsl} (ft) : 6024.4 2.21 2.215 0.002 0.002 -64.67
LH2 Slosh Mass (slugs), Frequ Wy,Wz 1g (rad/s), Damp (zeta-y-z), Locat {Xsl,Ysl,Zsl} (ft) : 511.06 2.10 2.102 0.005 0.005 -125.3

Number of Bending Modes : 27
Shuttle Second Stage with Payload Damper, at T=123 sec, Mixed Modes

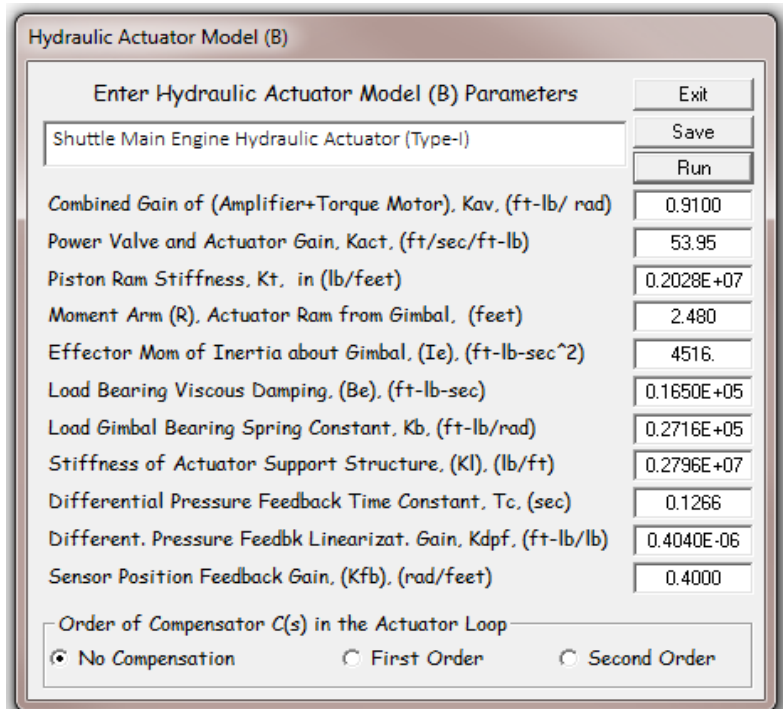
3 Actuator Model

The actuator model is common to all three engines and it is used for gimbaling in both pitch and yaw direction. It is, therefore, repeated 6 times for the 6 gimbaling DOFs. The actuator type is a hydraulic Model-B, which is documented in the actuators section. The input parameters for this actuator are in the input data file “*Stg2_Damper.Inp*” and the actuator title is “*Shuttle Main Engine Hydraulic Actuator (Type-I)*”. The actuator modeling program is used to create the state-space model from the actuator data. To run the actuator program, from the Flixan main menu choose “*Program Functions*”, “*Flight Vehicle/ Spacecraft Modeling*”, and then “*Actuator State-Space Models*”. From the filenames selection menu choose the input vehicle data file “*Stg2_Damper.Inp*” and the output systems file “*Stg2_Damper.Qdr*”. From the next menu select the title of the actuator model “*Shuttle Main Engine Hydraulic Actuator (Type-I)*” and click on “*Run Input Set*”.



The following dialog comes up showing the actuator parameters. Click on “Run” and the program will create the actuator state-space model and save it in file “*Stg2_Damper.Qdr*” using the same title as the input data.

The inputs to the actuator state-space model are: engine deflection commands in (rad) and load-torque feedback in (ft-lb). The outputs are: engine deflection in (rad), deflection rate in (rad/sec), and acceleration.



4 Creating the TVC/ Actuator Subsystem

We must now create a new subsystem that combines the six identical actuator subsystems with the thrust vector control matrix. It has 3 pitch and 3 yaw TVC actuators. It connects between the flight control output and the vehicle dynamic model. The system's block diagram is shown in Figure 4. The first 3 inputs are the roll, pitch, and yaw commands that go to the TVC matrix that converts the 3 flight control demands to engine deflection commands. There are also 3 pitch and 3 yaw load-torque inputs at the TVC gimbals. The system outputs are 6 gimbal deflections and 6 gimbal accelerations that drive the three Space Shuttle Main Engines (SSMEs) in pitch and yaw. The gimbal accelerations generate the forces required for the implementation of the tail-wags-dog dynamics. The state-space model of a single actuator block was described in Section 3 and was saved in systems file: "Stg2_Damper.Qdr".

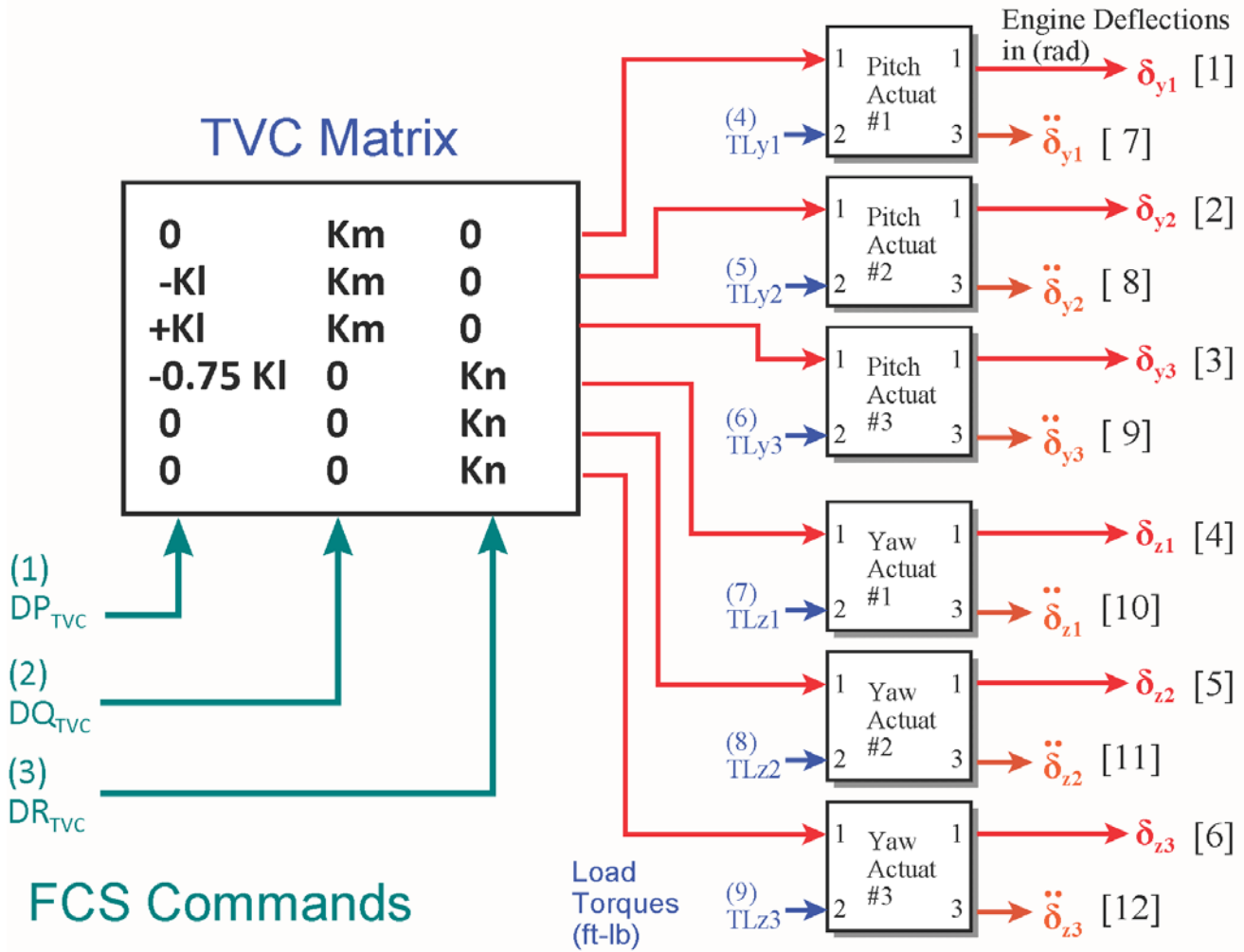
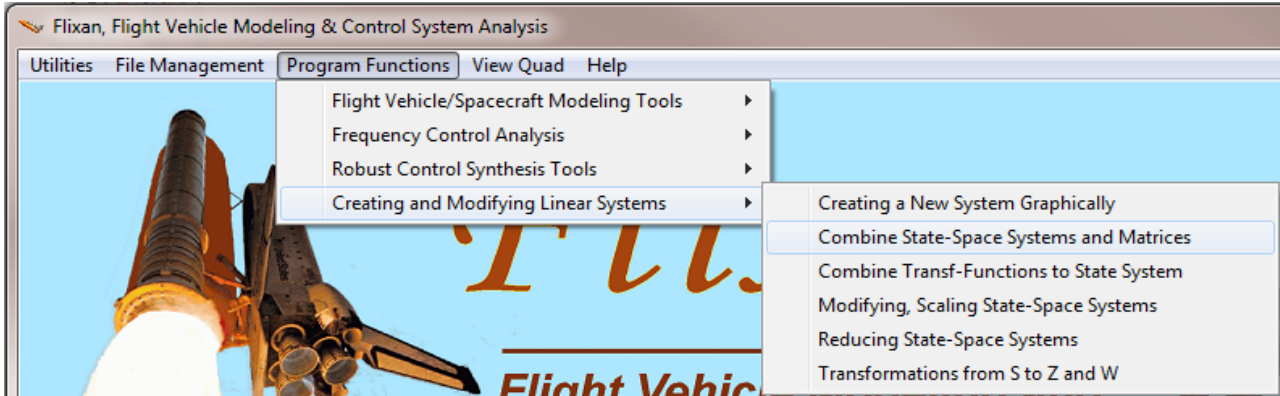


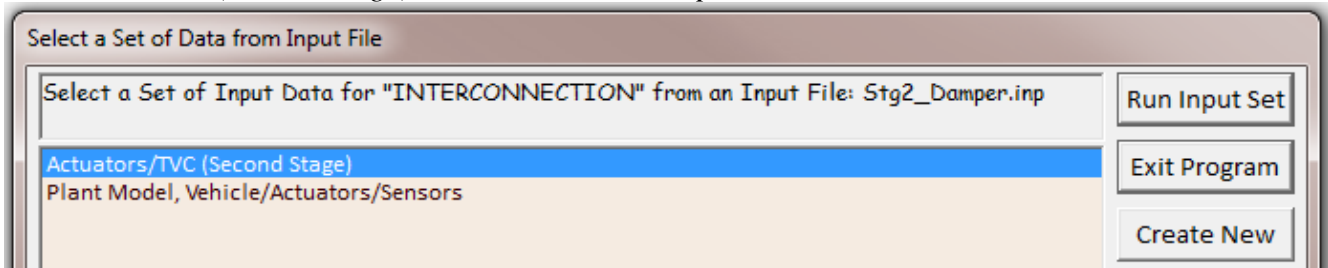
Figure 4 TVC/ Actuators Subsystem

The first three inputs to the TVC/ Actuator subsystem comprise the flight control demands vector [DP_{TVC} , DQ_{TVC} , DR_{TVC}] which is multiplied by the TVC matrix and it is transformed to 3 pitch (δ_{y1} , δ_{y2} , δ_{y3}), and 3 yaw (δ_{z1} , δ_{z2} , δ_{z3}) actuator deflection commands that go to input #1 of the corresponding actuators. Inputs (4-6) are the pitch load-torques (TLy_i), and inputs (7-9) are the yaw load-torques (TLz_i) for the three TVC engines. They come from the vehicle model and go to the second input of the actuators. Outputs (1-6) are: pitch (δ_{y1} - δ_{y3}), and yaw (δ_{z1} - δ_{z3}) engine deflections in radians. Outputs (7-12) are pitch and yaw engine accelerations in (rad/sec^2).

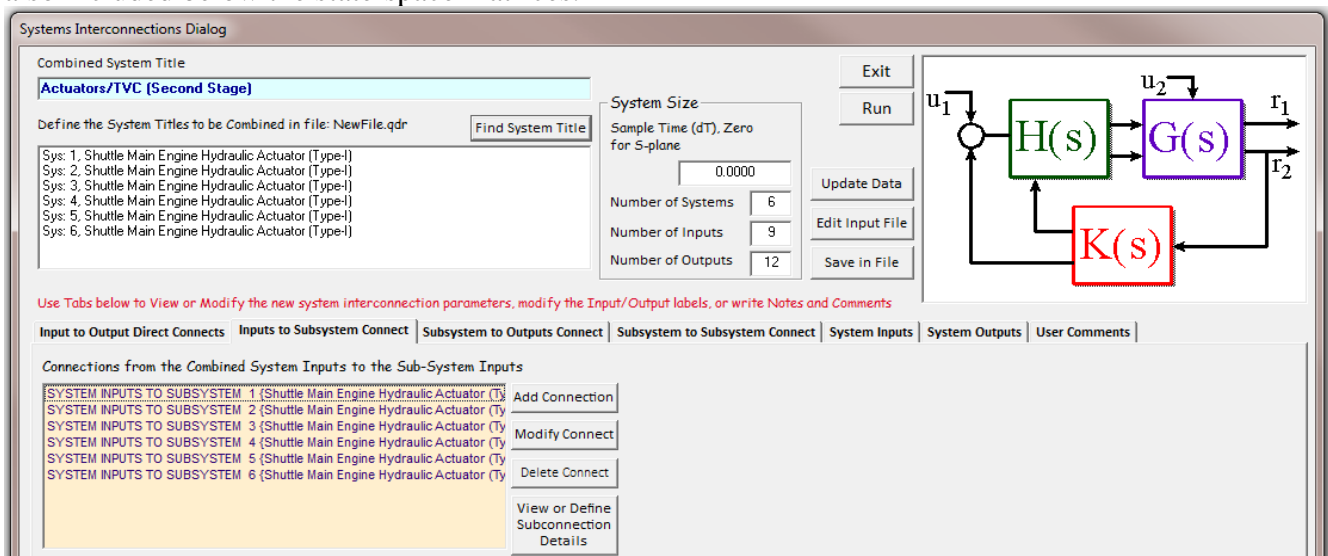
This system was created using the Flixan systems combination program. The interconnection data for the program is in file “Stg2_Damper.Inp”. Its title is “Actuators/TVC (Second Stage)”. The six systems to be combined are the same actuator model “Shuttle Main Engine Hydraulic Actuator (Type-I)” which is repeated six times (two gimbaling directions per engine). From the Flixan main menu select “Program Functions”, “Creating and Modifying Linear Systems” and “Combine State-Space Systems and Matrices”.



From the filenames selection menu choose the input vehicle data file “Stg2_Damper.Inp” and the output systems file “Stg2_Damper.Qdr”. The following menu shows the titles of the “Systems Interconnection” data-sets which are already saved in file “Stg2_Damper.Inp”. Select the title “Actuators/TVC (Second Stage)” and click on “Run Input Set”.



The following dialog shows the interconnection data in this set between the TVD and the 6 actuators. Click on “Run” to process the data and combine the systems. The new system: “Actuators/ TVC (Second Stage)” will be added in the systems file “Stg2_Damper.Qdr”. Its input/ output definitions are also included below the state-space matrices.



Actuators/TVC systems interconnection set in file "Stg2_Damper.Inp".

INTERCONNECTION OF SYSTEMS

Actuators/TVC (Second Stage)

! The Following System Consists of Pitch and Yaw Actuators and the TVC For the 3 Engines.
! The System Inputs are the 3 flight control commands: DPTVC, DQTVC, DRTVC, the 3
! pitch load-torques: TLY1, TLY2, TLY3, and the 3 yaw load-torques: TLZ1, TLZ2, TLZ3
! The First 6 Outputs are Pitch and Yaw Deflections.
! The Last 6 Outputs are Pitch and Yaw Accelerations

Titles of Systems to be Combined

Title 1 Shuttle Main Engine Hydraulic Actuator (Type-I)
Title 2 Shuttle Main Engine Hydraulic Actuator (Type-I)
Title 3 Shuttle Main Engine Hydraulic Actuator (Type-I)
Title 4 Shuttle Main Engine Hydraulic Actuator (Type-I)
Title 5 Shuttle Main Engine Hydraulic Actuator (Type-I)
Title 6 Shuttle Main Engine Hydraulic Actuator (Type-I)

```
SYSTEM INPUTS TO SUBSYSTEM 1                                DY1
System Input 2 to Subsystem 1, Input 1, Gain= 1.071
System Input 4 to Subsystem 1, Input 2, Gain= 1.0           TLY1
.....
SYSTEM INPUTS TO SUBSYSTEM 2                                DY2
System Input 1 to Subsystem 2, Input 1, Gain= -0.45        KLMPS
System Input 2 to Subsystem 2, Input 1, Gain= 1.071        KMMPS
System Input 5 to Subsystem 2, Input 2, Gain= 1.0           TLY2
.....
SYSTEM INPUTS TO SUBSYSTEM 3                                DY3
System Input 1 to Subsystem 3, Input 1, Gain= +0.45        KLMPS
System Input 2 to Subsystem 3, Input 1, Gain= 1.071        KMMPS
System Input 6 to Subsystem 3, Input 2, Gain= 1.0           TLY3
.....
SYSTEM INPUTS TO SUBSYSTEM 4                                DZ1
System Input 1 to Subsystem 4, Input 1, Gain= -0.337       KLMPS*0.75
System Input 3 to Subsystem 4, Input 1, Gain= 1.13         KNMPS
System Input 7 to Subsystem 4, Input 2, Gain= 1.0           TLZ1
.....
SYSTEM INPUTS TO SUBSYSTEM 5                                DZ2
System Input 3 to Subsystem 5, Input 1, Gain= 1.13         KNMPS
System Input 8 to Subsystem 5, Input 2, Gain= 1.0           TLZ2
.....
SYSTEM INPUTS TO SUBSYSTEM 6                                DZ3
System Input 3 to Subsystem 6, Input 1, Gain= 1.13         KNMPS
System Input 9 to Subsystem 6, Input 2, Gain= 1.0           TLZ3
.....
SYSTEM OUTPUTS FROM SUBSYSTEM 1
System Output 1 from Subsystem 1, Output 1, Gain= 1.0      dy1
System Output 7 from Subsystem 1, Output 3, Gain= 1.0      dy1_dd
.....
SYSTEM OUTPUTS FROM SUBSYSTEM 2
System Output 2 from Subsystem 2, Output 1, Gain= 1.0      dy2
System Output 8 from Subsystem 2, Output 3, Gain= 1.0      dy2_dd
.....
SYSTEM OUTPUTS FROM SUBSYSTEM 3
System Output 3 from Subsystem 3, Output 1, Gain= 1.0      dy3
System Output 9 from Subsystem 3, Output 3, Gain= 1.0      dy3_dd
.....
SYSTEM OUTPUTS FROM SUBSYSTEM 4
System Output 4 from Subsystem 4, Output 1, Gain= 1.0      dz1
System Output 10 from Subsystem 4, Output 3, Gain= 1.0     dz1_dd
.....
SYSTEM OUTPUTS FROM SUBSYSTEM 5
System Output 5 from Subsystem 5, Output 1, Gain= 1.0      dz2
System Output 11 from Subsystem 5, Output 3, Gain= 1.0     dz2_dd
.....
SYSTEM OUTPUTS FROM SUBSYSTEM 6
System Output 6 from Subsystem 6, Output 1, Gain= 1.0      dz3
System Output 12 from Subsystem 6, Output 3, Gain= 1.0     dz3_dd
.....
```

Definitions of Inputs = 9

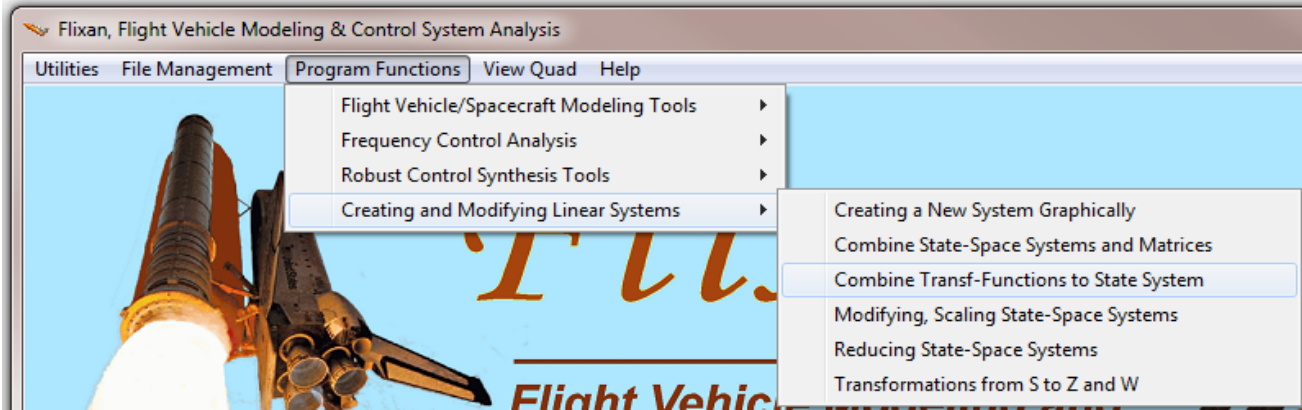
Roll FCS Command (DPTVC)
Pitch FCS Command (DQTVC)
Yaw FCS Command (DRTVC)
Engine 1 Pitch Load-Torque TLY1
Engine 2 Pitch Load-Torque TLY2
Engine 3 Pitch Load-Torque TLY3
Engine 1 Yaw Load-Torque TLZ1
Engine 2 Yaw Load-Torque TLZ2
Engine 3 Yaw Load-Torque TLZ3

Definitions of Outputs = 12

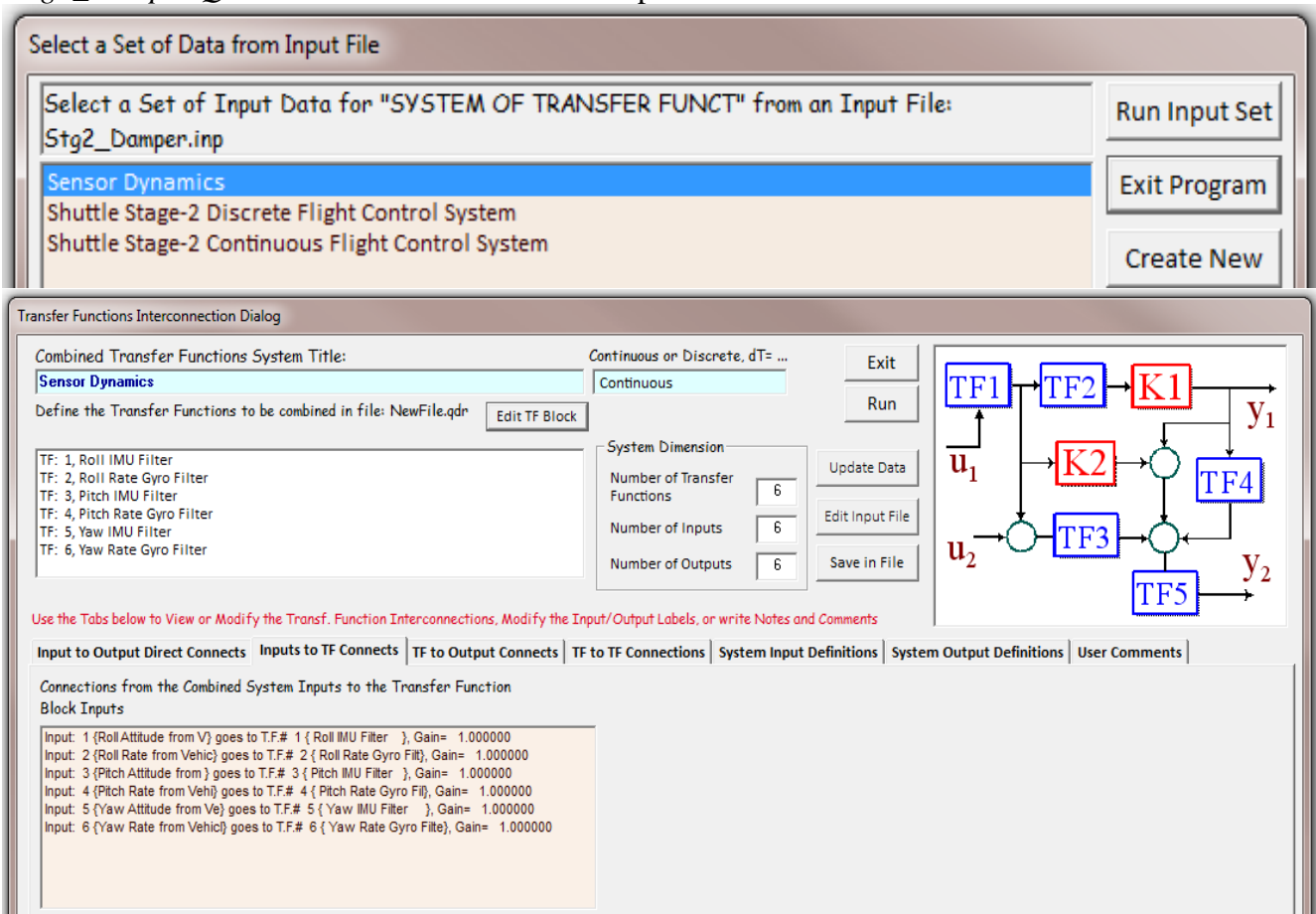
Engine 1 Pitch Deflection (rad)
Engine 2 Pitch Deflection (rad)
Engine 3 Pitch Deflection (rad)
Engine 1 Yaw Deflection (rad)
Engine 2 Yaw Deflection (rad)
Engine 3 Yaw Deflection (rad)
Engine 1 Pitch Accelerat (rad/sec^2)
Engine 2 Pitch Accelerat (rad/sec^2)
Engine 3 Pitch Accelerat (rad/sec^2)
Engine 1 Yaw Accelerat (rad/sec^2)
Engine 2 Yaw Accelerat (rad/sec^2)
Engine 3 Yaw Accelerat (rad/sec^2)

5 Flight Control Sensors

The IMU and rate gyro sensor dynamics are implemented as transfer function blocks which are converted to a state-space subsystem that is combined later with the vehicle model. The sensor transfer function data are defined in file “*Stg2_Damper.Inp*” and its title is “*Sensor Dynamics*”. The transfer functions combination program is used to combine them together and to create a state-space system.



From the filenames selection menu choose the input vehicle data file “*Stg2_Damper.Inp*” and the output systems file “*Stg2_Damper.Qdr*”. The following menu shows the transfer-function data-sets which are already saved in the input file. Select the title “*Sensor Dynamics*” and click on “Run Input Set”. The following dialog comes up showing the transfer function interconnections. Click on “Run” button and the program will convert the set to a state-space model and save it in file “*Stg2_Damper.Qdr*” under the same title as the input data.



Sensor dynamics transfer-functions interconnection set located in file “Stg2_Damper.Inp”.

SYSTEM OF TRANSFER FUNCTIONS ...

Sensor Dynamics

! Roll, Pitch, Yaw Attitude and Rate Sensors used for Flight Control

Continuous

```
TF. Block # 1 Roll IMU Filter                    Order of Numer, Denom= 1 1
Numer 0.00000      7.00000
Denom 1.00000      7.00000
TF. Block # 2 Roll Rate Gyro Filter              Order of Numer, Denom= 1 1
Numer 0.00000      50.0000
Denom 1.00000      50.0000
TF. Block # 3 Pitch IMU Filter                   Order of Numer, Denom= 1 1
Numer 0.00000      7.00000
Denom 1.00000      7.00000
TF. Block # 4 Pitch Rate Gyro Filter             Order of Numer, Denom= 1 1
Numer 0.00000      50.0000
Denom 1.00000      50.0000
TF. Block # 5 Yaw IMU Filter                     Order of Numer, Denom= 1 1
Numer 0.00000      7.00000
Denom 1.00000      7.00000
TF. Block # 6 Yaw Rate Gyro Filter              Order of Numer, Denom= 1 1
Numer 0.00000      50.0000
Denom 1.00000      50.0000
```

Block #, from Input #, Gain:

```
 1   1   1.0
 2   2   1.0
 3   3   1.0
 4   4   1.0
 5   5   1.0
 6   6   1.0
```

.....
Outpt #, from Block #, Gain:

```
 1   1   1.0
 2   2   1.0
 3   3   1.0
 4   4   1.0
 5   5   1.0
 6   6   1.0
```

.....
Definitions of Inputs = 6

```
Roll Attitude from Vehicle
Roll Rate from Vehicle
Pitch Attitude from Vehicle
Pitch Rate from Vehicle
Yaw Attitude from Vehicle
Yaw Rate from Vehicle
```

.....
Definitions of Outputs = 6

```
Roll Attitude to FCS
Roll Rate to FCS
Pitch Attitude to FCS
Pitch Rate to FCS
Yaw Attitude to FCS
Yaw Rate to FCS
```

6 Combined Plant Model Consisting of: Vehicle, Actuators, Sensors, and TVC

Figure 5 shows the combined plant model comprising of the three previously generated subsystems. The Shuttle vehicle model is combined with the actuator/ TVC and the sensor subsystems. The plant inputs (1-3) are coming from the flight control system. Inputs 5 and 6 represent the forces in (lb) which are generated at the attachments of the left and right coulomb dampers. The left damper force is applied to vehicle inputs 13 and 15, representing equal and opposite forces acting at the two ends of the damper on the vehicle and on the payload sides. The force is positive when the device extends, as shown in Figure 3. Similarly, the right damper force is applied to vehicle inputs 14 and 16, representing equal and opposite forces acting at the two ends of the right damper. The actuator outputs are connected to the vehicle inputs. They consist of pitch and yaw engine deflections in (radians), and pitch and yaw engine accelerations in (rad/sec^2). The engine accelerations are needed in the vehicle model for the tail-wags-dog implementation. Input (4) is a wind gust velocity disturbance in (ft/sec) which can be applied to create disturbances on the vehicle. This type of disturbance involves aerodynamics and it was not used in this flight condition because the dynamic pressure is low since the vehicle is almost out of the atmosphere.

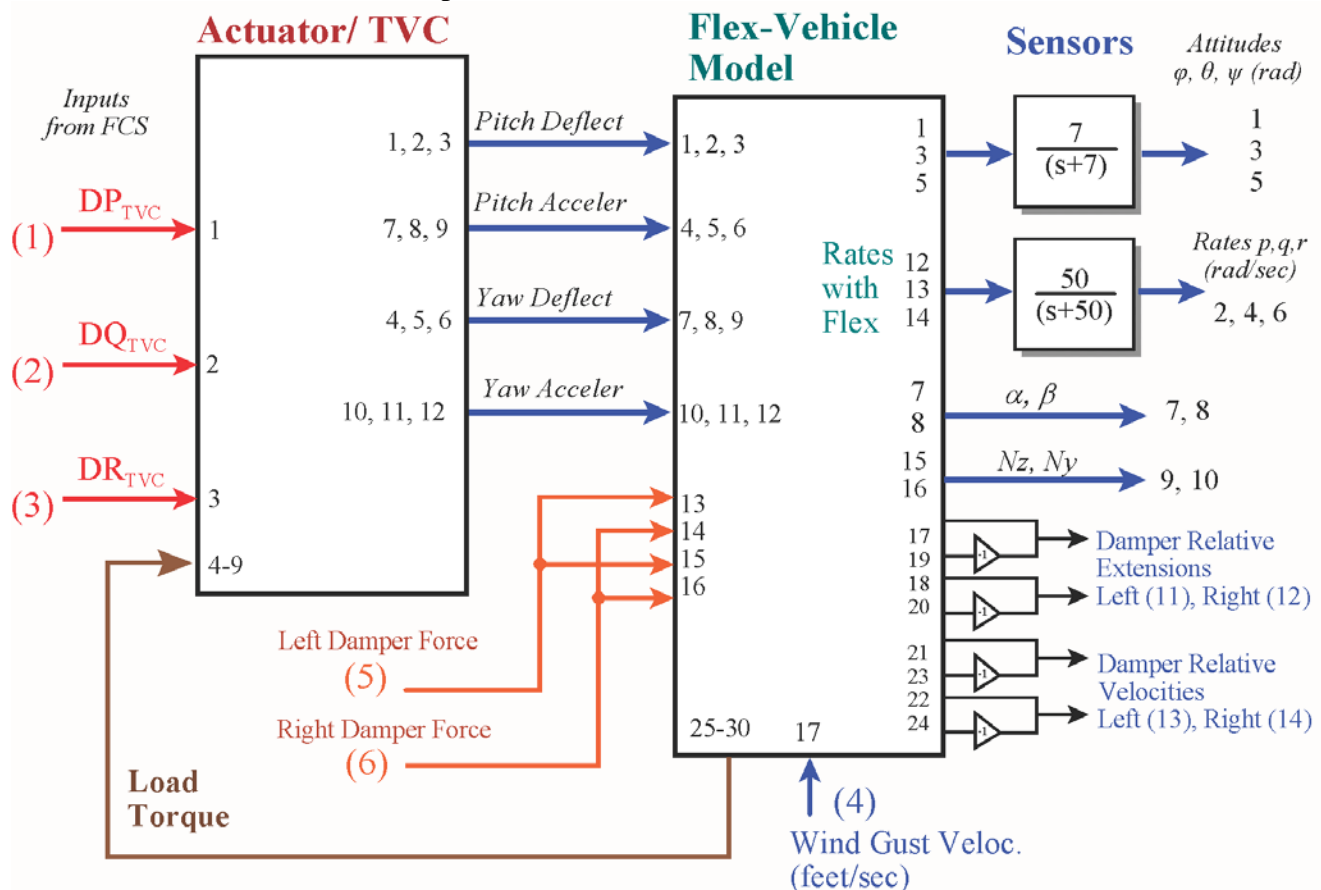
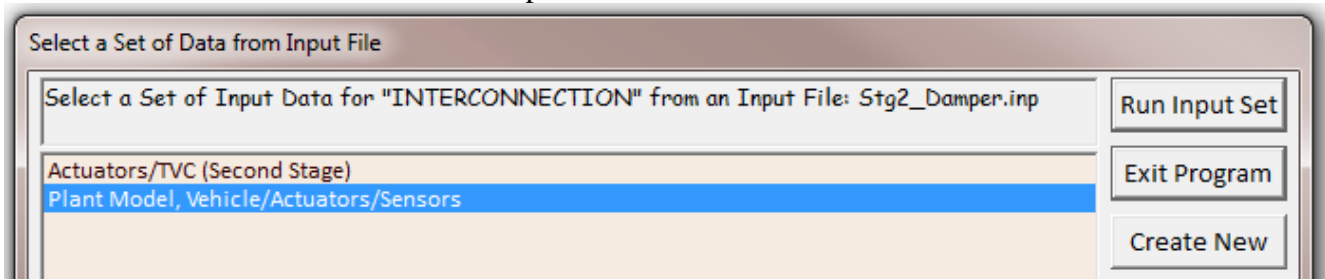


Figure 5 Combined Plant Model Consisting of: Actuators, TVC, Vehicle, and Sensor Dynamics

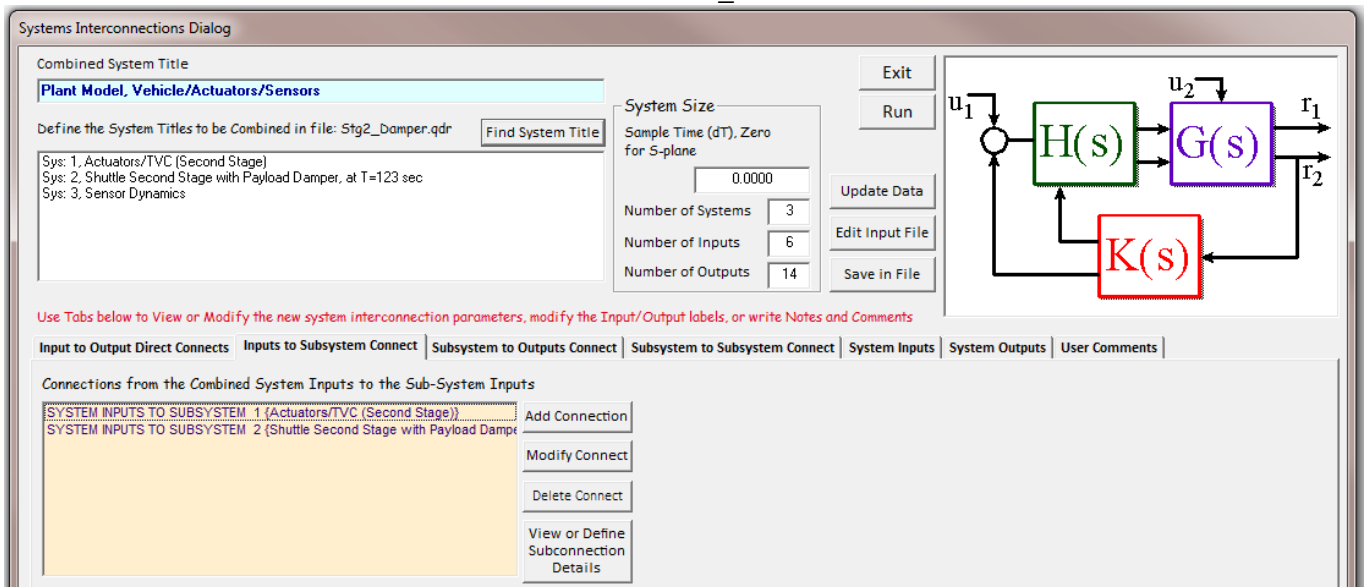
Disturbance inputs in the simulations are introduced by applying 4 equal forces at the coulomb damper attachments, thus exciting the payload flex motion relative to the vehicle without disturbing the rigid vehicle motion. The roll, pitch, and yaw vehicle attitudes (outputs 1 to 3) do not include structural bending. They represent IMU measurements and they are filtered by first order lag attitude sensor filters having a cut-off frequency of 7 rad/sec . The vehicle body rate outputs: (12, 13, 14) represent rate

gyro measurements which include structural bending. They are attenuated by the rate gyros that have a cut-off frequency of 50 rad/sec. The combined plant output 11 represents the relative displacement in (feet) across the left coulomb damper in the z direction. That is, bottom left z-displacement minus top left z-displacement. Similarly plant output 12 represents the relative displacement across the right damper. Also by the same logic, the plant outputs 13 and 14 represent relative velocities in (ft/sec) in the z direction across the left and the right dampers respectively. The load-torque is a mechanical feedback loop that represents external loading on the actuators caused by the vehicle acceleration at the gimbals, both rotational and translational.

The Flxan systems combination program is used again to combine the three continuous subsystems together as shown in Figure 5. The interconnections data-set title for this system is “*Plant Model, Vehicle/Actuators/Sensors*”, and it is also located in file “*Stg2_Damper.Inp*”. The vehicle, actuators, TVC, and sensor subsystems are already in systems file “*Stg2_Damper.Qdr*”. Run the systems combination program and from the filenames selection menu choose the input vehicle data file “*Stg2_Damper.Inp*” and the output systems file “*Stg2_Damper.Qdr*”. The following menu shows the system interconnection sets which are in the input file. Select the second title “*Plant Model, Vehicle/Actuators/Sensors*” and click on “Run Input Set”.



The program opens the systems interconnection dialog showing the subsystem connections as defined in figure 5. Click on the “Run” button to combine the systems. The combined plant with its input and output definitions is also saved in file “*Stg2_Damper.Qdr*” with the same title “*Plant Model, Vehicle/Actuators/Sensors*”. This continuous plant system is also converted to Matlab m-file function format to be used in simulation models. Its title is “*Plant_Flxcont.m*”.



Plant model interconnection set in file “*Stg2_Damper.Inp*” consisting of the Shuttle vehicle, actuators, TVC, and sensor subsystems combined as in Figure 5.

```

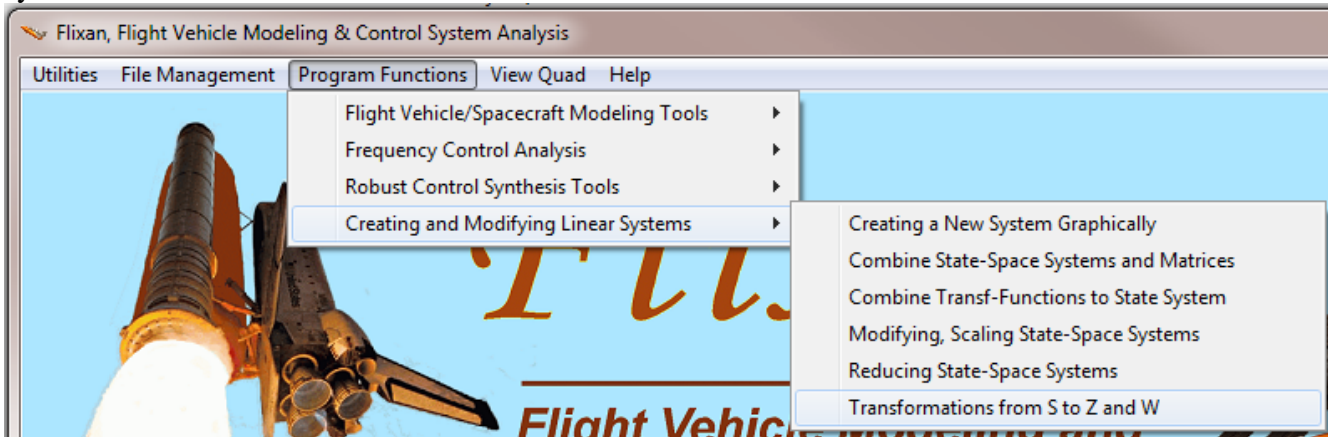
INTERCONNECTION OF SYSTEMS .....
Plant Model, Vehicle/Actuators/Sensors
! Combined Model of Vehicle, Actuators, TVC, and Sensor dynamics
!
Titles of Systems to be Combined
Title 1 Actuators/TVC (Second Stage)
Title 2 Shuttle Second Stage with Payload Damper, at T=123 sec
Title 3 Sensor Dynamics
SYSTEM INPUTS TO SUBSYSTEM 1
System Input 1 to Subsystem 1, Input 1, Gain= 1.0
System Input 2 to Subsystem 1, Input 2, Gain= 1.0
System Input 3 to Subsystem 1, Input 3, Gain= 1.0
.....
SYSTEM INPUTS TO SUBSYSTEM 2
System Input 4 to Subsystem 2, Input 17, Gain= 1.0
System Input 5 to Subsystem 2, Input 13, Gain= 1.0
System Input 5 to Subsystem 2, Input 15, Gain= 1.0
System Input 6 to Subsystem 2, Input 14, Gain= 1.0
System Input 6 to Subsystem 2, Input 16, Gain= 1.0
.....
SYSTEM OUTPUTS FROM SUBSYSTEM 3
Via Matrix +I6
.....
SYSTEM OUTPUTS FROM SUBSYSTEM 2
System Output 7 from Subsystem 2, Output 7, Gain= 1.0
System Output 8 from Subsystem 2, Output 8, Gain= 1.0
System Output 9 from Subsystem 2, Output 15, Gain= 1.0
System Output 10 from Subsystem 2, Output 16, Gain= 1.0
System Output 11 from Subsystem 2, Output 17, Gain= 1.0
System Output 11 from Subsystem 2, Output 19, Gain=-1.0
System Output 12 from Subsystem 2, Output 18, Gain= 1.0
System Output 12 from Subsystem 2, Output 20, Gain=-1.0
System Output 13 from Subsystem 2, Output 21, Gain= 1.0
System Output 13 from Subsystem 2, Output 23, Gain=-1.0
System Output 14 from Subsystem 2, Output 22, Gain= 1.0
System Output 14 from Subsystem 2, Output 24, Gain=-1.0
.....
SUBSYSTEM NO 1 GOES TO SUBSYSTEM NO 2
Subsystem 1, Output 1 to Subsystem 2, Input 1, Gain= 1.0
Subsystem 1, Output 2 to Subsystem 2, Input 2, Gain= 1.0
Subsystem 1, Output 3 to Subsystem 2, Input 3, Gain= 1.0
Subsystem 1, Output 7 to Subsystem 2, Input 4, Gain= 1.0
Subsystem 1, Output 8 to Subsystem 2, Input 5, Gain= 1.0
Subsystem 1, Output 9 to Subsystem 2, Input 6, Gain= 1.0
Subsystem 1, Output 4 to Subsystem 2, Input 7, Gain= 1.0
Subsystem 1, Output 5 to Subsystem 2, Input 8, Gain= 1.0
Subsystem 1, Output 6 to Subsystem 2, Input 9, Gain= 1.0
Subsystem 1, Output 10 to Subsystem 2, Input 10, Gain= 1.0
Subsystem 1, Output 11 to Subsystem 2, Input 11, Gain= 1.0
Subsystem 1, Output 12 to Subsystem 2, Input 12, Gain= 1.0
.....
SUBSYSTEM NO 2 GOES TO SUBSYSTEM NO 3
Subsystem 2, Output 1 to Subsystem 3, Input 1, Gain= 1.0
Subsystem 2, Output 3 to Subsystem 3, Input 3, Gain= 1.0
Subsystem 2, Output 5 to Subsystem 3, Input 5, Gain= 1.0
Subsystem 2, Output 12 to Subsystem 3, Input 2, Gain= 1.0
Subsystem 2, Output 13 to Subsystem 3, Input 4, Gain= 1.0
Subsystem 2, Output 14 to Subsystem 3, Input 6, Gain= 1.0
.....
SUBSYSTEM NO 2 GOES TO SUBSYSTEM NO 1
Subsystem 2, Output 25 to Subsystem 1, Input 4, Gain= 1.0
Subsystem 2, Output 26 to Subsystem 1, Input 5, Gain= 1.0
Subsystem 2, Output 27 to Subsystem 1, Input 6, Gain= 1.0
Subsystem 2, Output 28 to Subsystem 1, Input 7, Gain= 1.0
Subsystem 2, Output 29 to Subsystem 1, Input 8, Gain= 1.0
Subsystem 2, Output 30 to Subsystem 1, Input 9, Gain= 1.0
.....
Definitions of Inputs = 6
Roll FCS Command (DP-TVC)
Pitch FCS Command (DQ-TVC)
Yaw FCS Command (DR-TVC)
Wind-Gust Velocity (ft/sec)
Left Coulomb Damper Force
Right Coulomb Damper Force

Definitions of Outputs = 14
Roll Attitude to FCS
Roll Rate to FCS
Pitch Attitude to FCS
Pitch Rate to FCS
Yaw Attitude to FCS
Yaw Rate to FCS
Angle of Attack, alpha (rad)
Angle of Sideslip, beta (rad)
Normal Accelerometer, Nz (ft/sec^2)
Lateral Accelerometer, Ny (ft/sec^2)
Left Damper Extension (ft)
Right Damper Extension (ft)
Left Damper Rate (ft/sec)
Right Damper Rate (ft/sec)
-----
Data-Set ID Line
Actuator
DP_tvc
DQ_tvc
DR_tvc
Vehicle
V-Gust
Coul_Damp Force Bot Left 3102
Coul_Damp Force Top Left 3103
Coul_Damp Force Bot Rght 3103
Coul_Damp Force Top Rght 294
Sensors (IMU, Gyros)
Vehicle
alfa
beta
Nz
Ny
Coul_Damp Bot(Veh) Left 3102 - Positions
Coul_Damp Top(Pay) Left 3103
Coul_Damp Bot(Veh) Rght 3101 -
Coul_Damp Top(Pay) Rght 294
Coul_Damp Bot(Veh) Left 3102 - Rates
Coul_Damp Top(Pay) Left 3103
Coul_Damp Bot(Veh) Rght 3101 -
Coul_Damp Top(Pay) Rght 294
Actuat to Vehicle
dy1
dy2
dy3
dy1_dd
dy2_dd
dy3_dd
dz1
dz2
dz3
dz1_dd
dz2_dd
dz3_dd
Vehicle to Sensors
phi
theta
psi
p-flex
q-flex
r-flex
Vehicle to Actuator (Eng Load-Torque)
TLY-1
TLY-2
TLY-3
TLZ-1
TLZ-2
TLZ-3

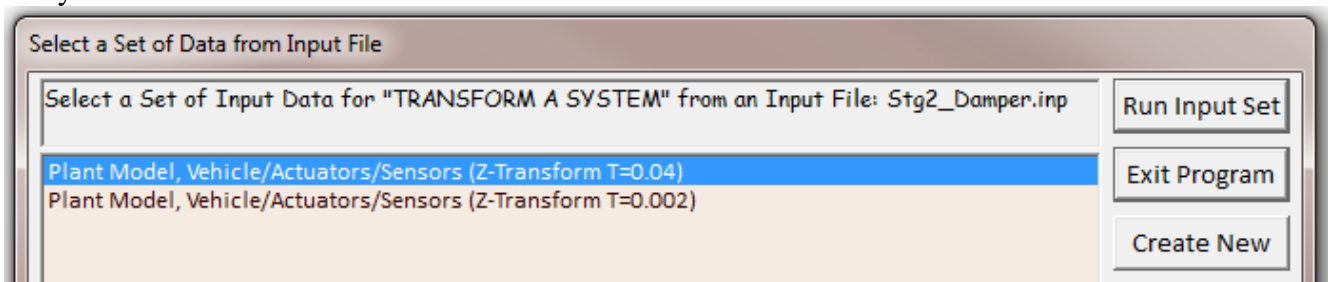
```

7 Discretization of the Plant Model

The continuous state-space plant model must also be transformed from the s-domain to the z-domain because it will be combined with the discrete flight control system using Simulink. The s to z transformation program will perform the transformation using a sampling period of 0.04 sec. From the Flixan main menu, go to “*Program Functions*”, “*Creating and Modifying Linear Systems*” and then “*Transformations from S to Z*”. From the filenames selection menu choose the same input data and systems files.



The s to z transformation data-set is already included in file “*Stg2-Damper.Inp*”. The set contains the title of the new transformed system, the title of the original system to be transformed, and the sampling period ($dT=0.04$). Use the following menu to select its title “*Plant Model, Vehicle/ Actuators/ Sensors (Z-Transform)*” and to perform the plant model transformation from s to z. The transformed discrete system will be saved in file “*Stg2-Damper.Qdr*” and its new title will be “*Plant Model, Vehicle/ Actuators/ Sensors (Z-Transform)*”. The discrete plant is also exported as an m-function in the Matlab subdirectory “*Payload Damper\Matan*”. Its title is “*Plant-Flxz40ms.m*” and it will be used in Simulink analysis models.

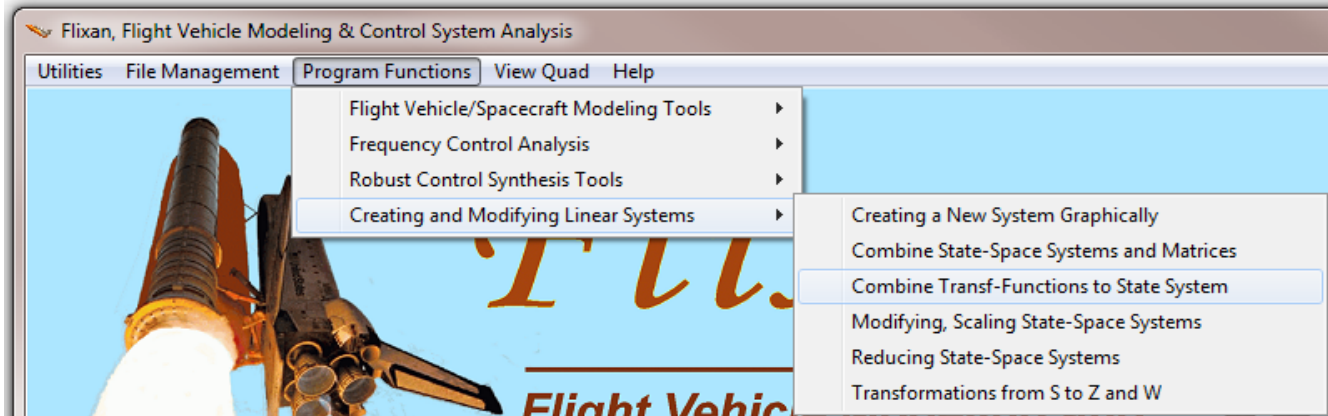


Plant Model S to Z transformation set in file “*Stg2_Damper.Inp*”.

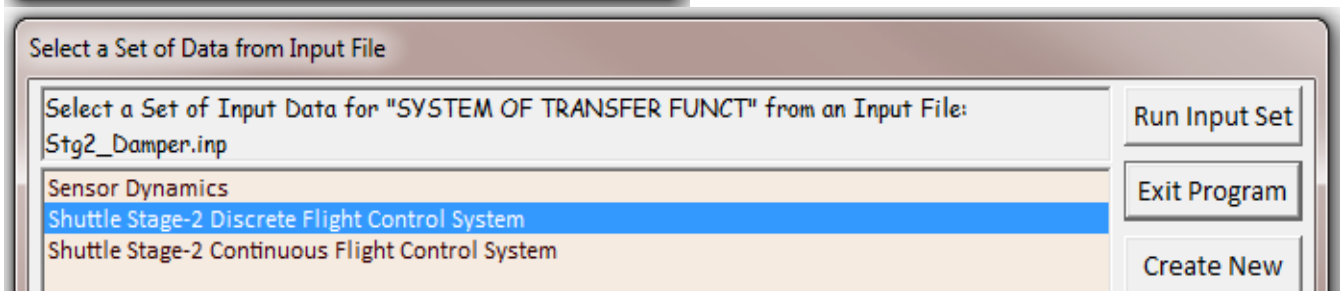
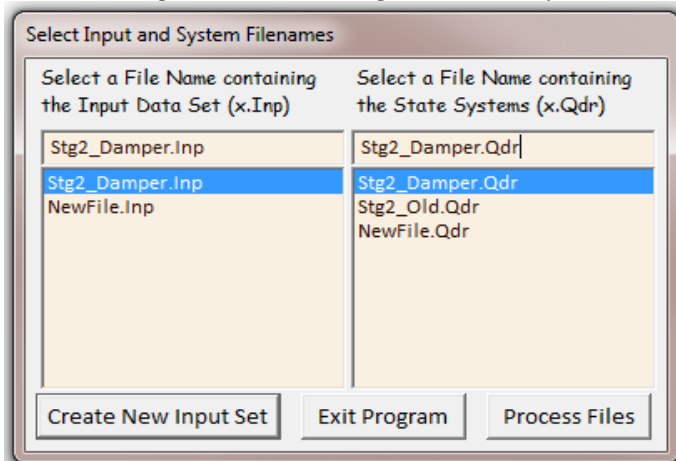
```
TRANSFORM A SYSTEM (S-Z-W) ..... (Titles of the New and Old Systems)
Plant Model, Vehicle/Actuators/Sensors (Z-Transform T=0.04)
Plant Model, Vehicle/Actuators/Sensors
! Transforms the Continuous Plant Model to Discrete Plant Model
! Using a 40 msec Sampling Period
From S-plane to Z-plane using the Z-Transform, dT= 0.04
```

8 The Flight Control System

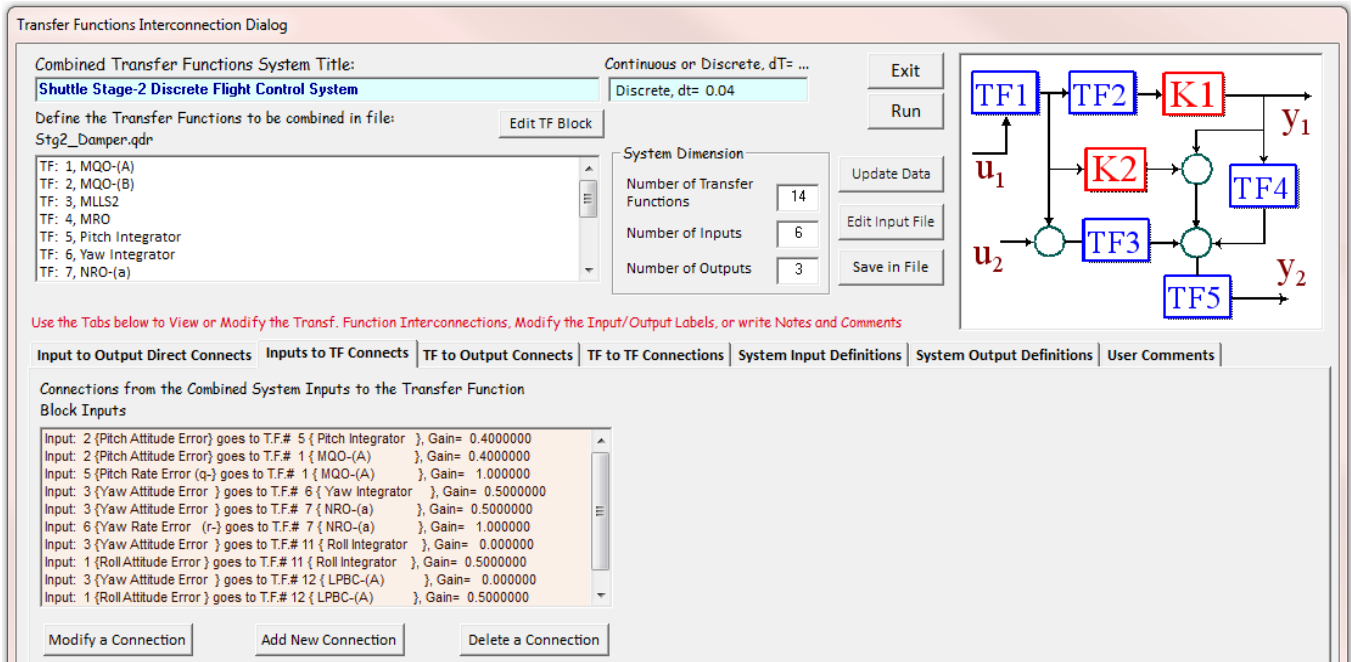
Figure 6 shows block diagrams of the pitch and lateral Space Shuttle flight control system during second stage. They are defined in transfer function blocks in the z-domain using a sampling period of 40 msec. The transfer function interconnections data-set title is “*Shuttle Stage-2 Discrete Flight Control System*” and it is saved in file “*Stg2_Damper.Inp*”. The transfer functions combination program is used to combine the TF blocks and to convert it to discrete state-space system. From the Flixan main menu choose “*Program Functions*”, “*Creating and Modifying Linear Systems*”, and “*Combine Transfer Functions to State-Space*”.



From the filenames selection menu choose the same input and systems filenames. The following menu shows the transfer function interconnection sets which are in file “*Stg2_Damper.Inp*”. Select the title “*Shuttle Stage-2 Discrete Flight Control System*” and click on “*Run Input Set*” to process the data.



The following dialog shows the control system transfer function interconnections. Click on “Run” button and the program will convert it to a discrete state-space system and it will save it in file “Stg2_Damper.Qdr” using the same title: “Shuttle Stage-2 Discrete Flight Control System”.



The discrete controller was converted to Matlab format and saved in the analysis folder “Matan” as an m-file function “controller_z.m”. The 6 FCS inputs are: roll, pitch, yaw attitude errors (attitude command minus attitude measurement), and roll, pitch, yaw rate gyro measurements. The three FCS outputs are the roll, pitch, and yaw demands, (DP_{TVC} , DQ_{TVC} , DR_{TVC}) that go to the TVC. A continuous flight control subsystem using the equivalent s-transfer function blocks was also created because the closed-loop coulomb damper simulations require a sampling rate faster than 40 msec. The title of the continuous transfer function subsystem is “Shuttle Stage-2 Continuous Flight Control System”. The transfer function interconnection data is also in file “Stg2_Damper.Inp”. The transfer functions combination program was also used to combine the transfer function blocks together and to create the continuous controller subsystem. It was also exported into Matlab as an m-function “controller_s.m”.

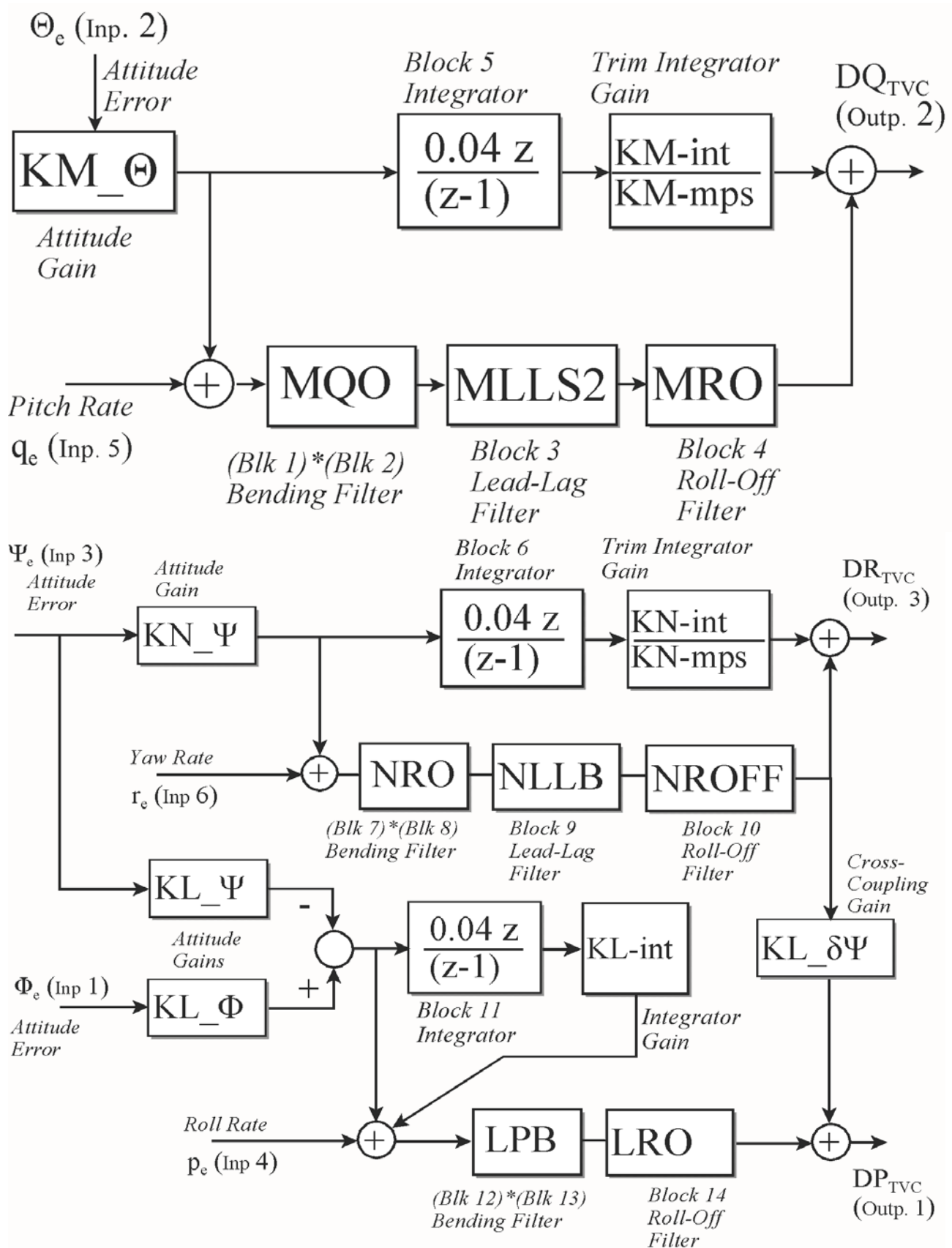


Figure 6 Pitch and Lateral Flight Control System during Stage-2

Discrete Flight Control System transfer-functions interconnection set for the Shuttle Second Stage located in file "Stg2_Damper.Inp".

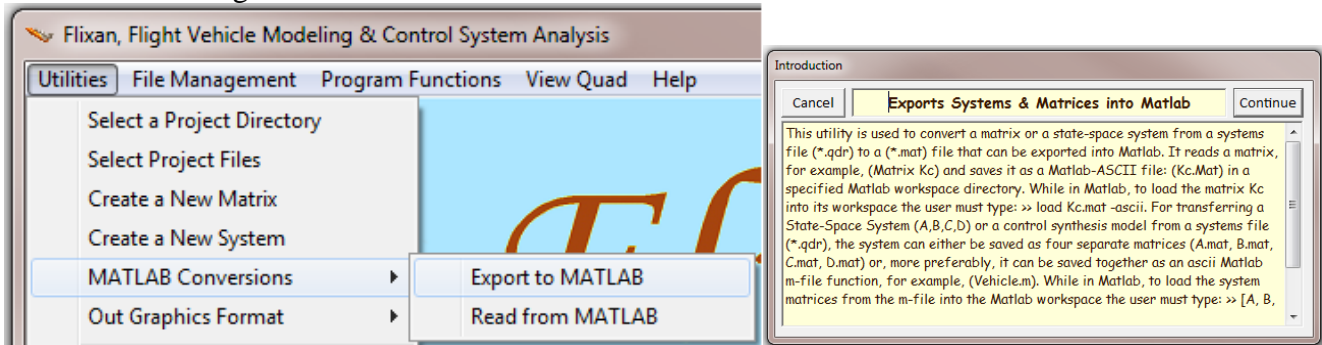
```

SYSTEM OF TRANSFER FUNCTIONS ...
Shuttle Stage-2 Discrete Flight Control System
! The Following System is a Pitch and Lateral Combined flight
! control system of the Space Shuttle during Second Stage of Ascent
Discrete, dt= 0.04
TF. Block # 1 MQO-(A)                                Order of Numer, Denom= 2 2
Numer .3481644   -.4381397   .3003516
Denom 1.00000   -1.3926868   .6030635
TF. Block # 2 MQO-(B)                                Order of Numer, Denom= 2 2
Numer .5192794   -.7480449   .4735804
Denom 1.00000   -1.3330898   .5779056
TF. Block # 3 MLLS2                                  Order of Numer, Denom= 2 2
Numer 1.138602   -1.5772626   .5841927
Denom 1.00000   -1.5772626   .7227952
TF. Block # 4 MRO                                    Order of Numer, Denom= 2 2
Numer .1503906   -.03515626  .0097656
Denom 1.00000   -1.5           .625
TF. Block # 5 Pitch Integrator                       Order of Numer, Denom= 1 1
Numer .04        0.00000
Denom 1.00000   -1.00000
TF. Block # 6 Yaw Integrator                         Order of Numer, Denom= 1 1
Numer .04        0.00000
Denom 1.00000   -1.00000
TF. Block # 7 NRO-(a)                               Order of Numer, Denom= 2 2
Numer .25        -.3387097   .2177419
Denom 1.00000   -1.548387   .6774194
TF. Block # 8 NRO-(b)                               Order of Numer, Denom= 2 2
Numer .574359    -.6153846   .4512821
Denom 1.00000   -1.076923   .4871795
TF. Block # 9 NLLB                                   Order of Numer, Denom= 2 2
Numer 1.124138   -1.255172   .3793103
Denom 1.00000   -1.255172   .5034483
TF. Block # 10 NROFF                                Order of Numer, Denom= 2 2
Numer .3397436   -.115385    .1858974
Denom 1.00000   -1.076923   .4871795
TF. Block # 11 Roll Integrator                      Order of Numer, Denom= 1 1
Numer .04        0.00000
Denom 1.00000   -1.00000
TF. Block # 12 LPBC-(A)                             Order of Numer, Denom= 2 2
Numer .5477522   -.6419696   .3149338
Denom 1.00000   -1.183954   .4046702
TF. Block # 13 LPBC-(B)                             Order of Numer, Denom= 2 2
Numer .4923835   -.5179801   .3897718
Denom 1.00000   -1.434638   .7988138
TF. Block # 14 LRO                                  Order of Numer, Denom= 2 2
Numer .3573574   .1501501   .0330330
Denom 1.00000   -.8108108   .3513513
-----
Block #, from Input #, Gain
5 2 0.4 the-error (KM_theta)
1 2 0.4 the-error (KM_theta)
1 5 1.0 q-error
6 3 0.5 psi-error (KN_psi)
7 3 0.5 (KN_psi)
7 6 1.0 yaw rate (r.gyro)
11 3 -0.0 psi_error (KL_psi)
11 1 0.5 phi-error (KL_phi)
12 3 -0.0 psi_error (KL_psi)
12 1 0.5 phi-error (KL_phi)
12 4 1.0 p_orb
.....
Block #, from Block #, Gain
2 1 1.0 MQO (1 & 2)
3 2 1.0 MLLS2
4 3 1.0 MRO
8 7 1.0 NRO (1 & 2)
9 8 1.0 NLLB
10 9 1.0 NROFF
12 11 0.075 LPBC (1) * kl_int
13 12 1.0 LPBC (2)
14 13 1.0 LRO
.....
Output #, from Block #, Gain
1 10 1.6 P-TVC KL_delpsi
1 14 1.0
2 5 0.106 Q-TVC KM_int/KM_mps
2 4 1.00000
3 6 0.075 R-TVC KN_int/KN_mps=0.075
3 10 1.00000
.....
Definitions of Inputs = 6
Roll Attitude Error (phi-err)
Pitch Attitude Error (theta-err)
Yaw Attitude Error (psi-err)
Roll Rate Error (p-err)
Pitch Rate Error (q-err)
Yaw Rate Error (r-err)
.....
Definitions of Outputs = 3
Roll FCS (DP-TVC)
Pitch FCS (DQ-TVC)
Yaw FCS (DR-TVC)
-----

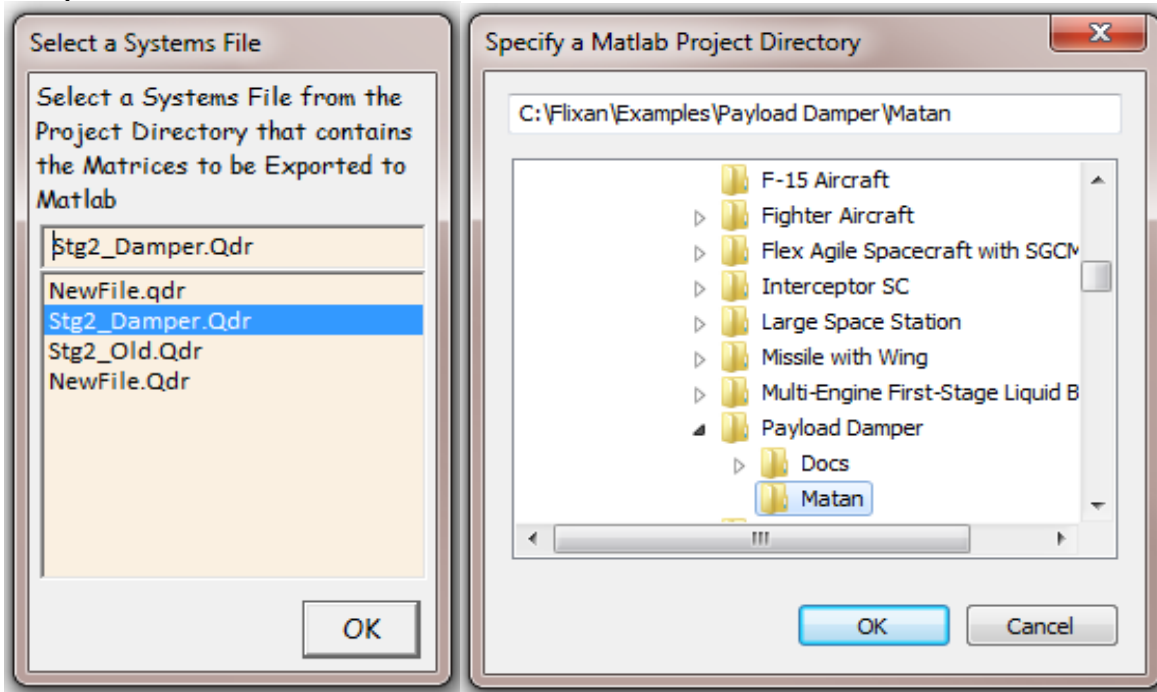
```

9 Exporting the State-Space systems to Matlab

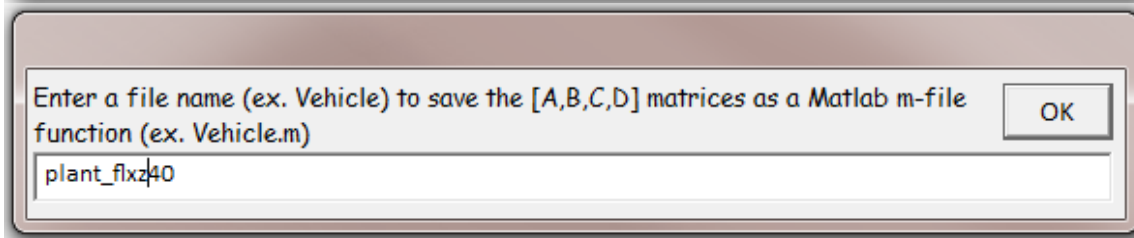
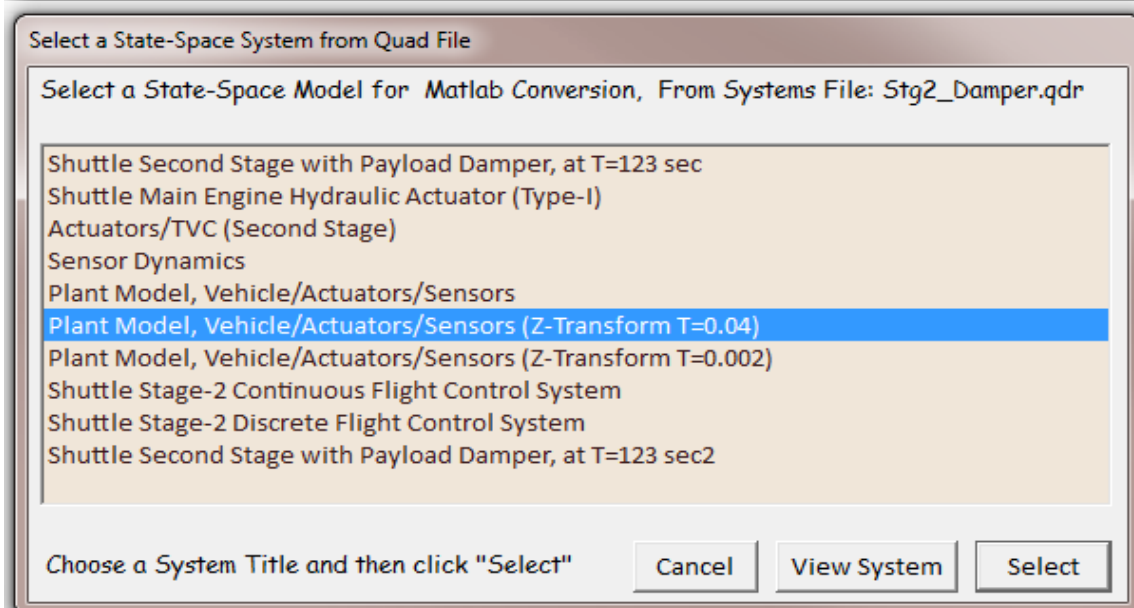
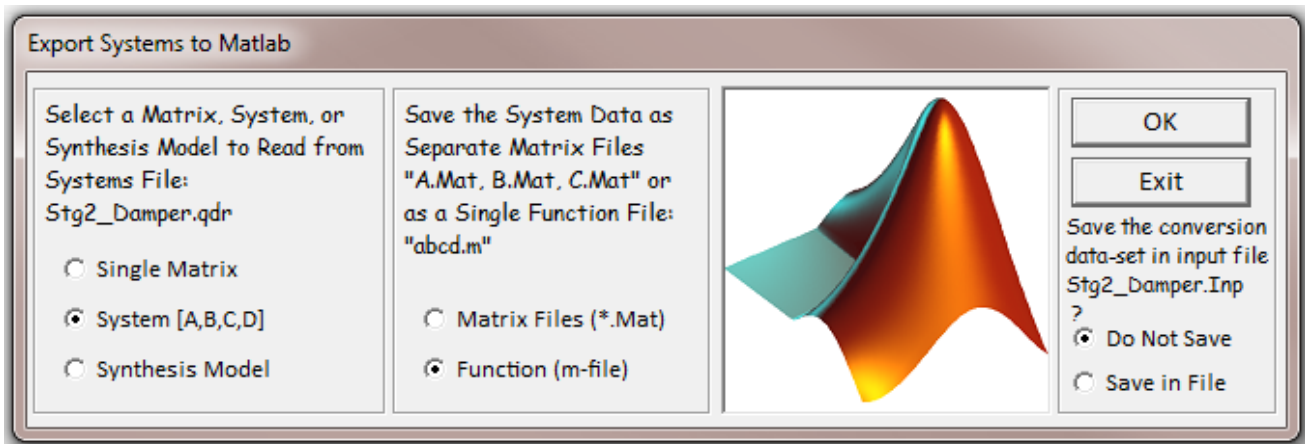
The creation of the plant and the controller systems is now complete and they are ready to be transferred to the Matlab folder “\Flixan\Examples\Payload Damper\Matan” where the frequency response analysis and simulations will be performed using Matlab and Simulink. Both, continuous and discrete versions will be transferred. A total of four systems will be converted using the “Export to Matlab” utility from file “Stg2_Damper.Qdr” and will be saved in the Matlab analysis subdirectory. To run the Matlab export utility you must first start the Flixan program and select the directory where the Flixan files are located, “\Flixan\Examples\Payload Damper”. From the Flixan main menu go to “Utilities”, then “Matlab Conversions” and click on “Export to Matlab”. The following is an introduction dialog and click “Continue”.



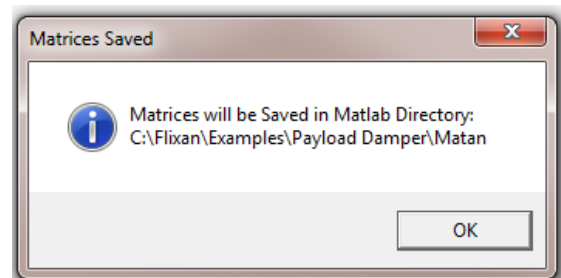
Select the file “Stg2_Damper.Qdr” that contains the system that you want to convert to Matlab format. The export utility also wants to know the Matlab project folder where you want to save the converted system file as a function m-file. Use the following menu to select the folder “\Examples\ Payload Damper\ Matan”.



Use the following menu to define the format of the output Matlab system “System (A,B,C,D)” and as a “function m-file”. From the systems selection menu select the title of the system to be converted. In this case select “Plant Model, Vehicle/ Actuators/ Sensors (Z-Transformed)” and click “Select”.



Enter also the name of the m-file that will contain the system function “*plant_flxz40*” (without the .m). The discrete plant model will be saved in the Matlab analysis folder as an m-file function “*plant_flxz40.m*”. Repeat the same process to export the continuous plant system “*Plant Model, Vehicle/ Actuators/ Sensors*” to the same Matlab subdirectory as an m-function named “*plant_flxcont.m*”. Repeat the process to export the continuous flight control system “*Shuttle Stage-2 Continuous Flight Control System*” to the Matlab folder as an m-function “*controller_s.m*”. Repeat also for the discrete flight control system “*Shuttle Stage-2 Discrete Flight Control System*” using a filename “*controller_z.m*”.



10 Linear System Stability Analysis

The analysis begins by checking the system stability in Matlab using an open-loop Simulink model “*Open_Loop_z.mdl*”, shown in Figure 7. The purpose is to demonstrate the structural mode instability problem using classical frequency domain stability analysis and the need for introducing the mechanical dampers. The model consists of the discrete plant subsystem “*Plant Model, Vehicle/ Actuators/ Sensors (Z-Transformed)*”, shown in Figure 8, which is combined with the discrete flight control system “*Shuttle Stage-2 Discrete Flight Control System*” in open-loop interconnection with the loop opened at the flight control system output. The two systems are discretized at 40 msec. It will be used to generate Bode and Nichols plots and to analyze the flex mode stability one loop at a time. The analysis is performed in subdirectory “*\Examples\Payload Damper\Matan*” where the two discrete systems were previously saved. Figure 7 is currently configured for pitch axis analysis with the loop opened at the output of the pitch flight control system, while the roll and yaw loops are closed. Stability in the other two axes is analyzed by opening and closing the appropriate loops, one loop at a time. The m-file “*run_fcs.m*” is used to load the two discrete subsystems “*plant_flxz40.m*” and “*controller_z.m*” in Matlab, combine them together via the Simulink model “*Open-Loop-z.Mdl*” and to calculate the frequency response across the opened loop. The model can be modified by opening and closing the appropriate loops in order to check stability in the other two directions.

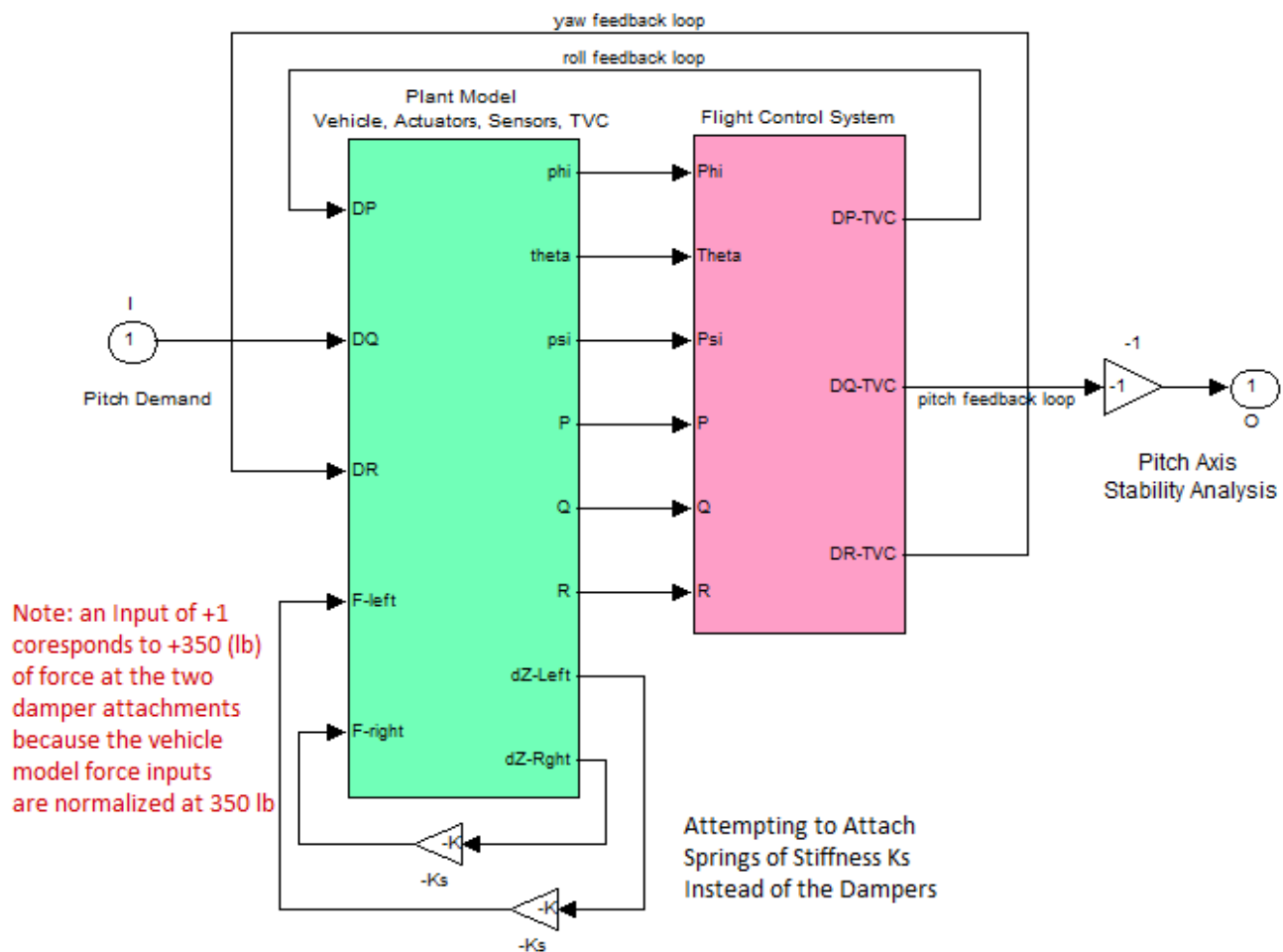


Figure 7 Open-Loop Stability Analysis model “*Open_Loop_z.mdl*” Consisting of the Plant and the Flight Control Systems. The loop is opened at the Pitch TVC input.

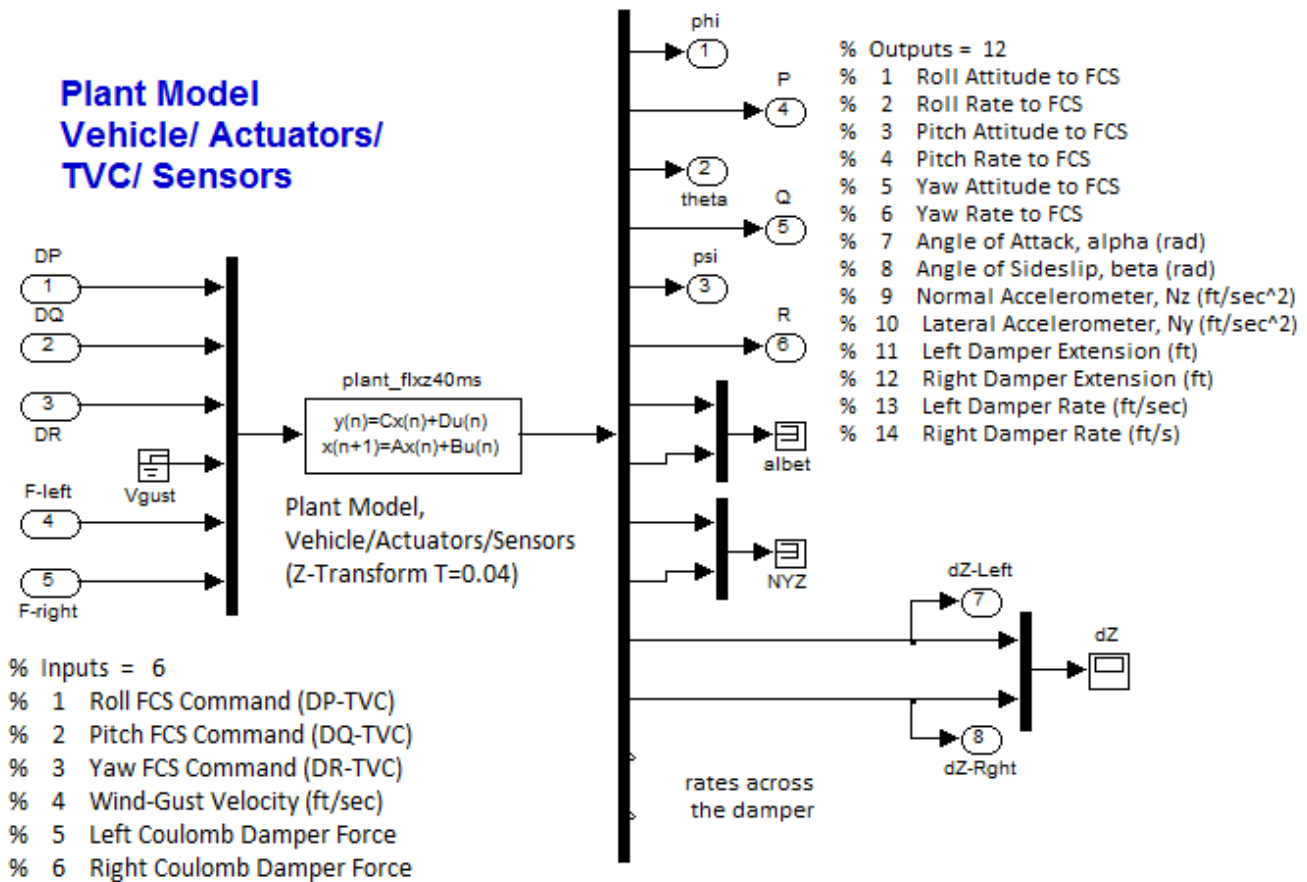


Figure 8 Discrete plant model including damper forces for inputs and output extensions and rates of the structure across the two dampers

As already mentioned the flex vehicle model was created with the structure across the dampers unclamped so the relative motion at the two ends of the dampers is not constrained. We will analyze the system stability in two cases: (a) when the structure at the ends of the dampers is unconstrained, and (b) when the two ends are clamped by stiff mechanical struts in place of the Coulomb dampers. For this reason two mechanical feedback loops are included in Figure 7 with gains K_s representing the stiffness of the fastening bars. The stiffness gain K_s produces a force across each strut proportional to the relative motion across it. The purpose of this exercise is to analyze the effects of varying the clamping stiffness K_s without introducing damping in the relative motion.

So let us begin by calculating the Bode and Nichols plots of the open-loop system with the struts removed, $K_s=0$. Figure 9 (a, b, c) shows the Bode and Nichols stability analysis plots for the pitch, roll, and yaw axes. The pitch analysis results show that there is structural mode instability at 9.1 (r/s) and another mode close to instability at 9.72 (r/s). Reduced flex mode margin is also observed in the roll and yaw directions at the 15.8 (r/s) mode. The vehicle has sufficient rigid-body stability margin and the propellant modes are phase-stable.

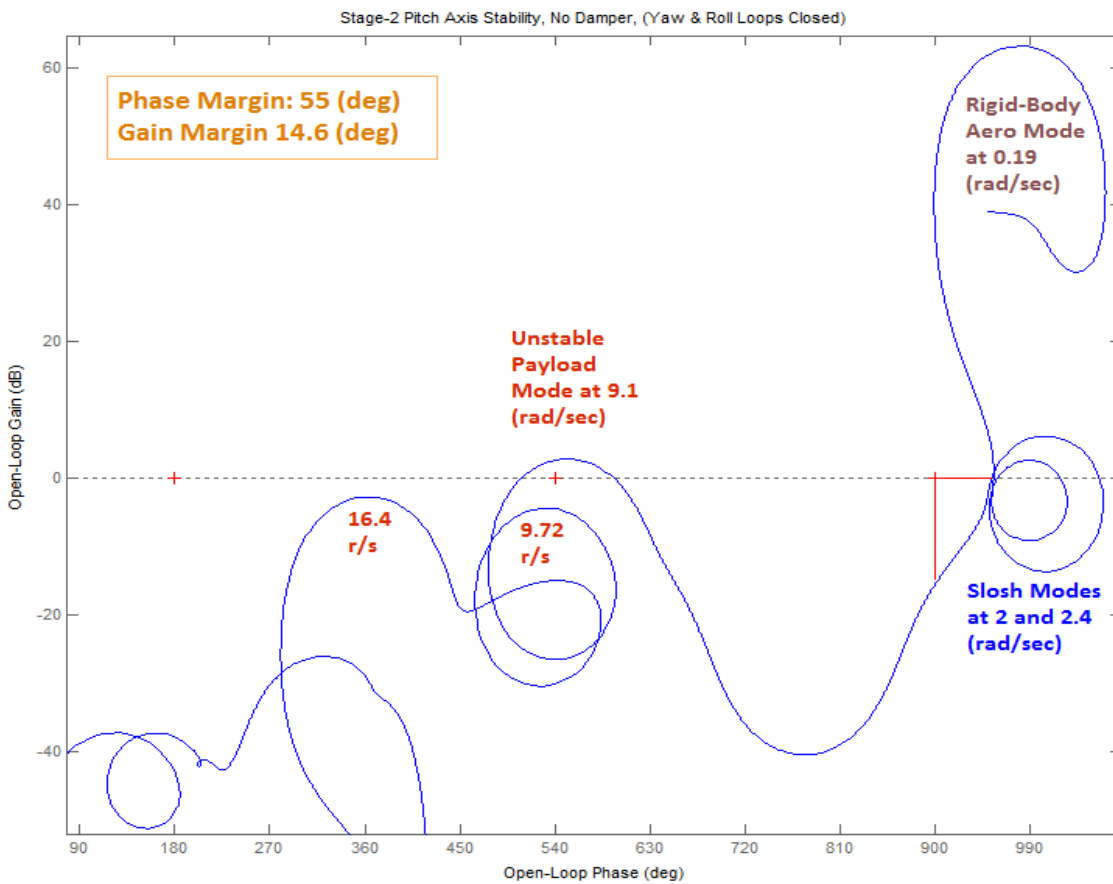
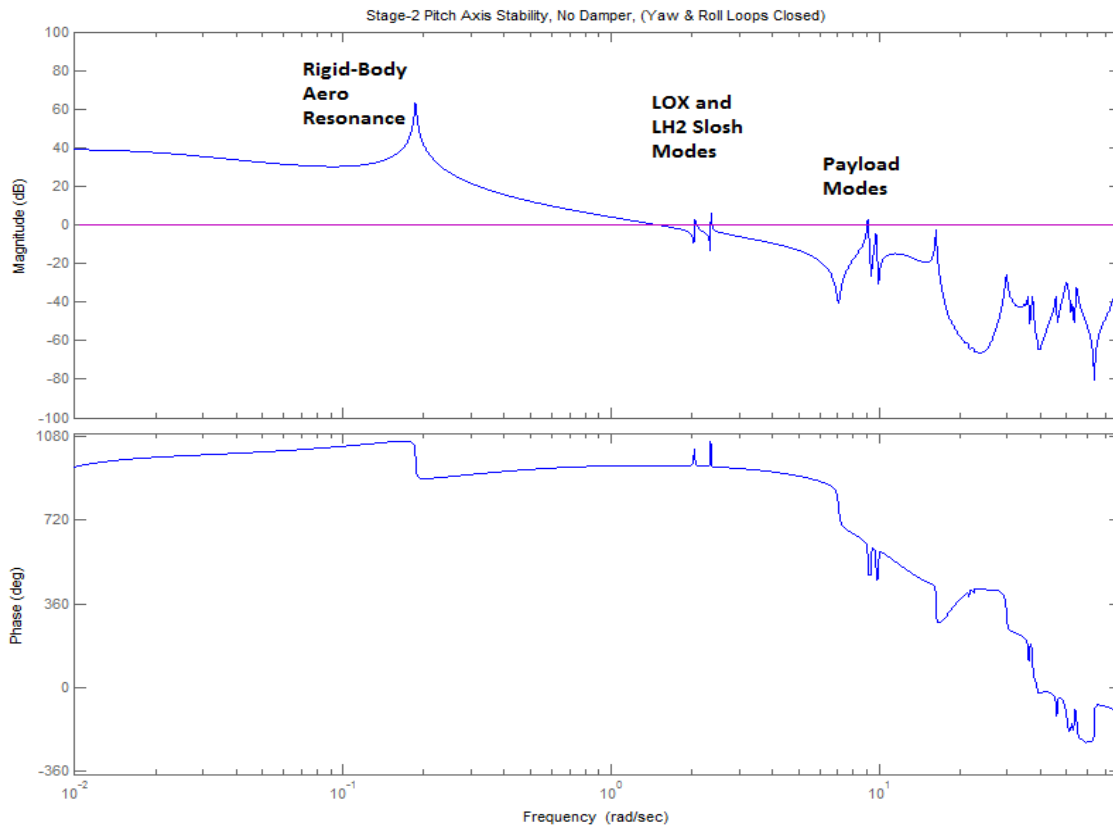


Figure 9a Bode and Nichols plots for the opened Pitch axis (roll and yaw are closed)

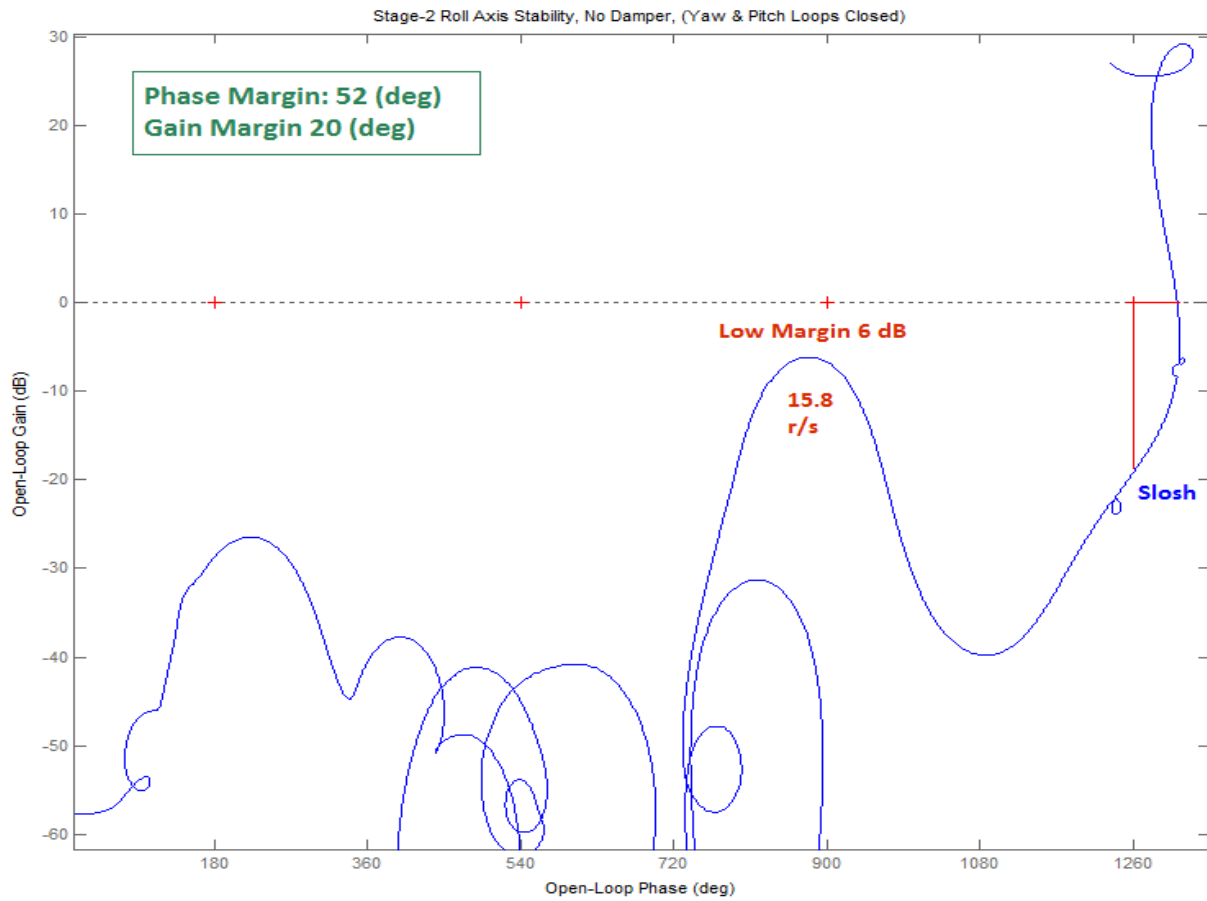
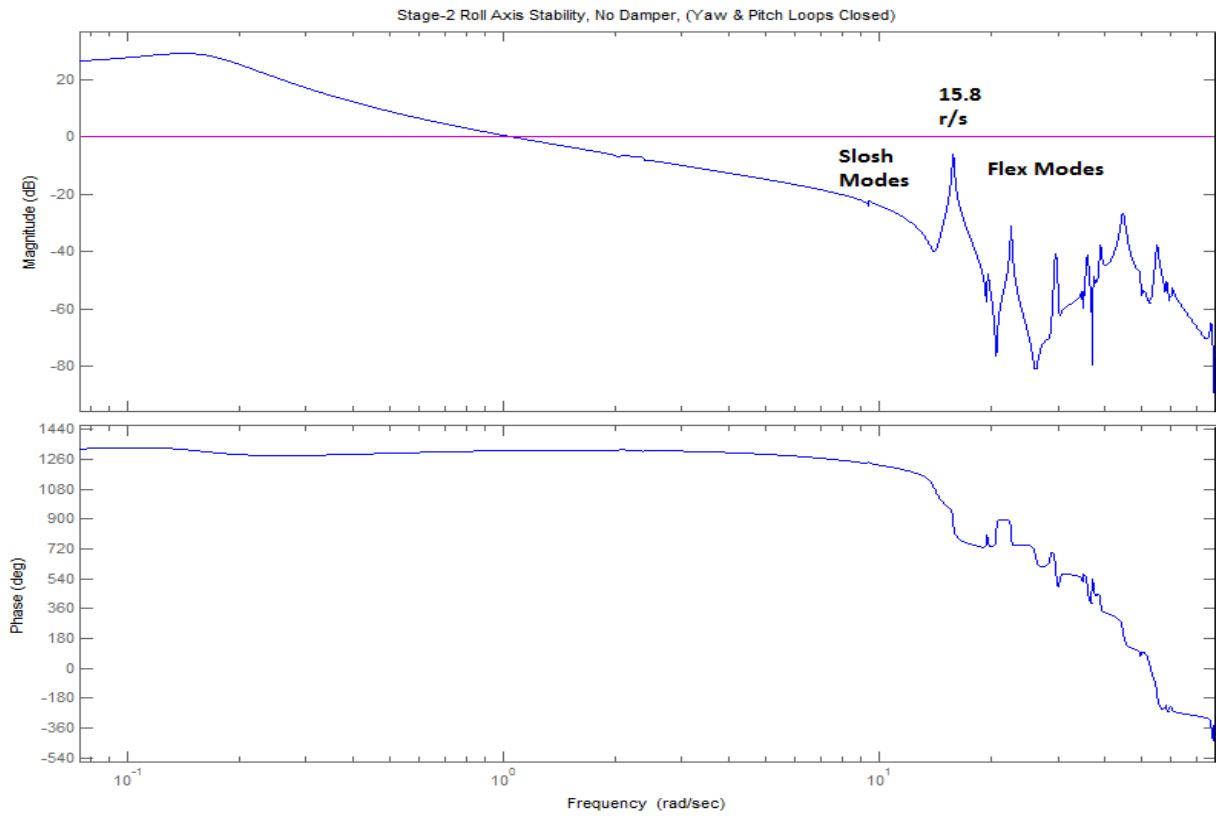


Figure 9b Bode and Nichols plots for the Roll axis (pitch and yaw are closed)

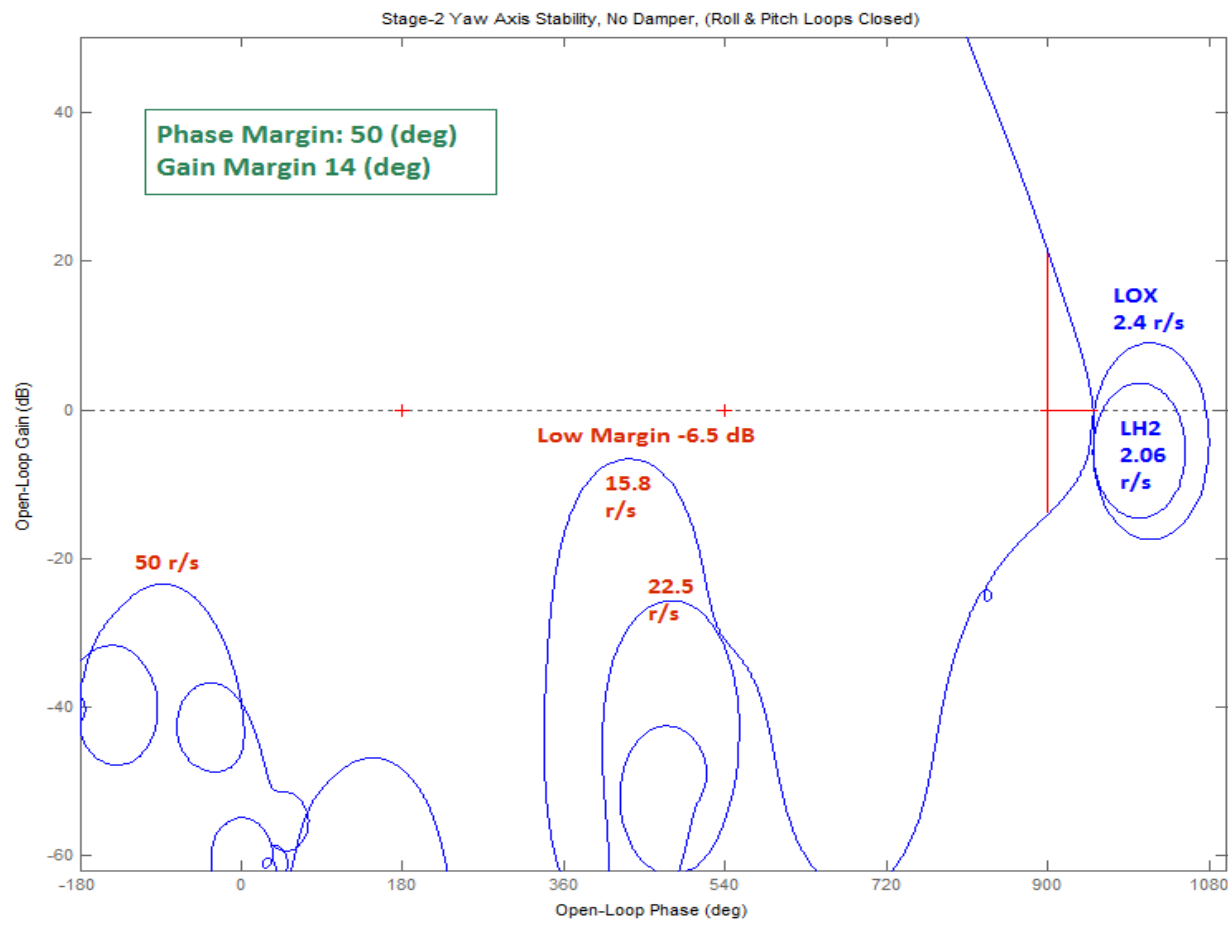
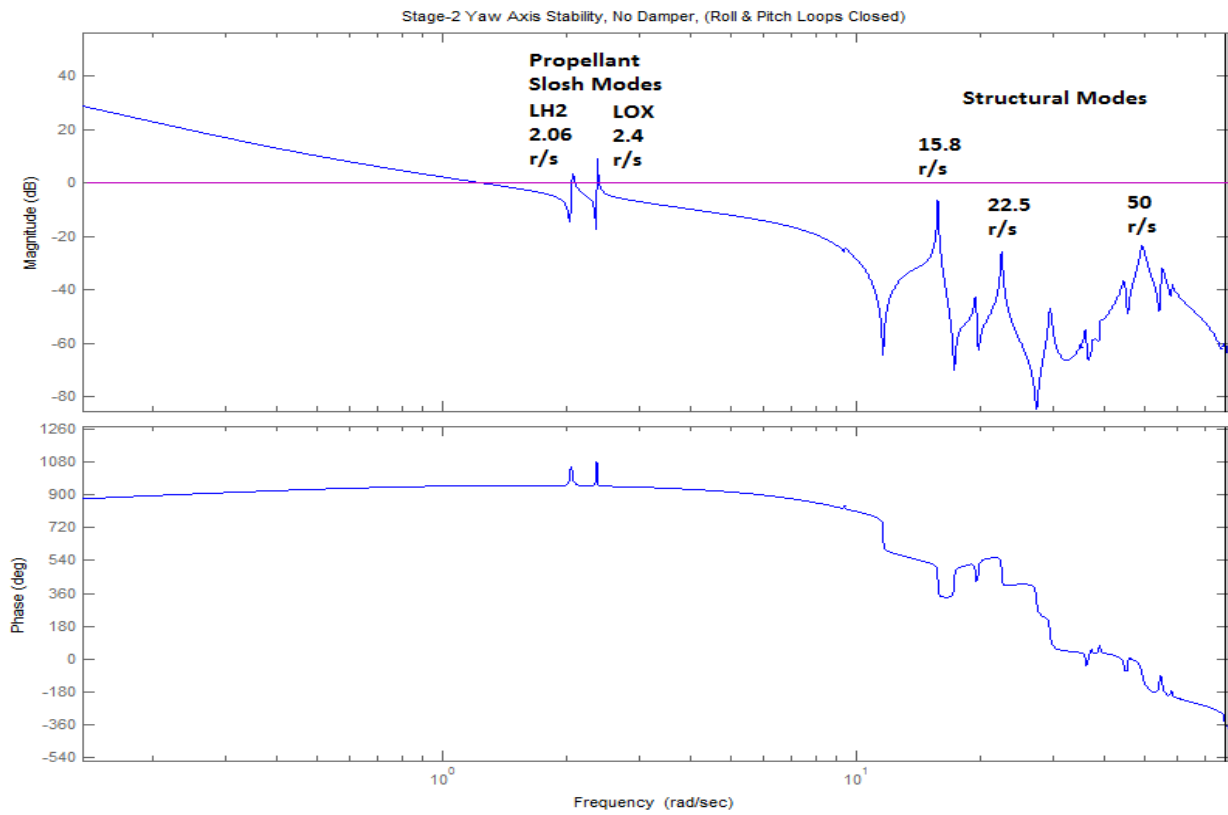


Figure 9c Bode and Nichols plots for the opened Yaw axis (roll and pitch are closed)

The following stability analysis plots demonstrate that introducing the spring stiffnesses K_s to clamp the ends between the vehicle and the payload attachments in order to stiffen the structure, not only it does not provide any modal attenuation but it aggravates the flex mode instability even further. This is more noticeable in pitch where two modes now encircle the critical point, but also in roll and yaw where the 15.9 (r/s) mode is near instability. The reason is because stiffening the connection between the vehicle and payload does not reduce the overall vehicle flexibility and the sensitivity of the rate gyros to flexing. Instead of springs we need to introduce an energy dissipating device such as the Coulomb Damper that is capable of attenuating the structural motion between the vehicle and payload.

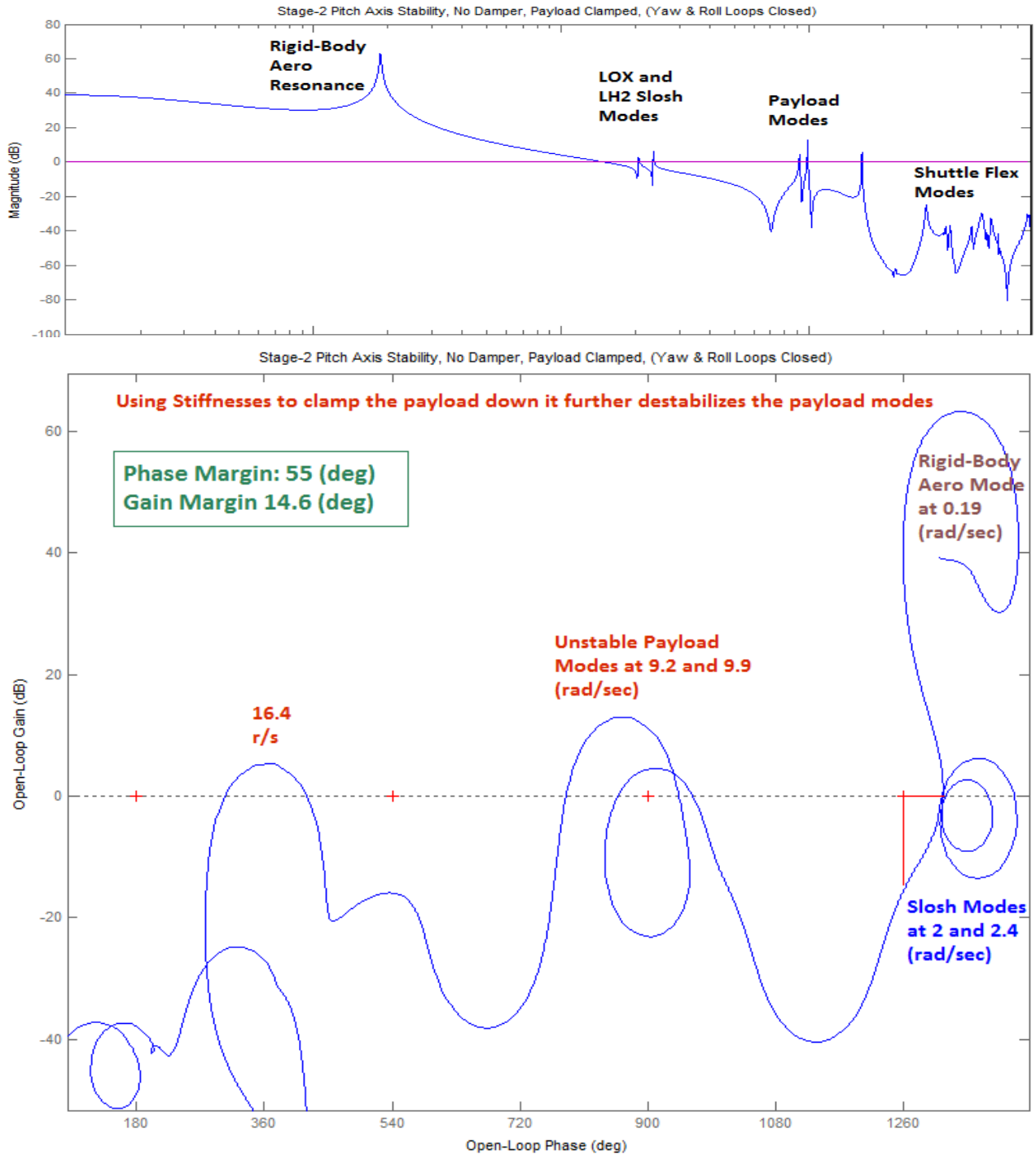
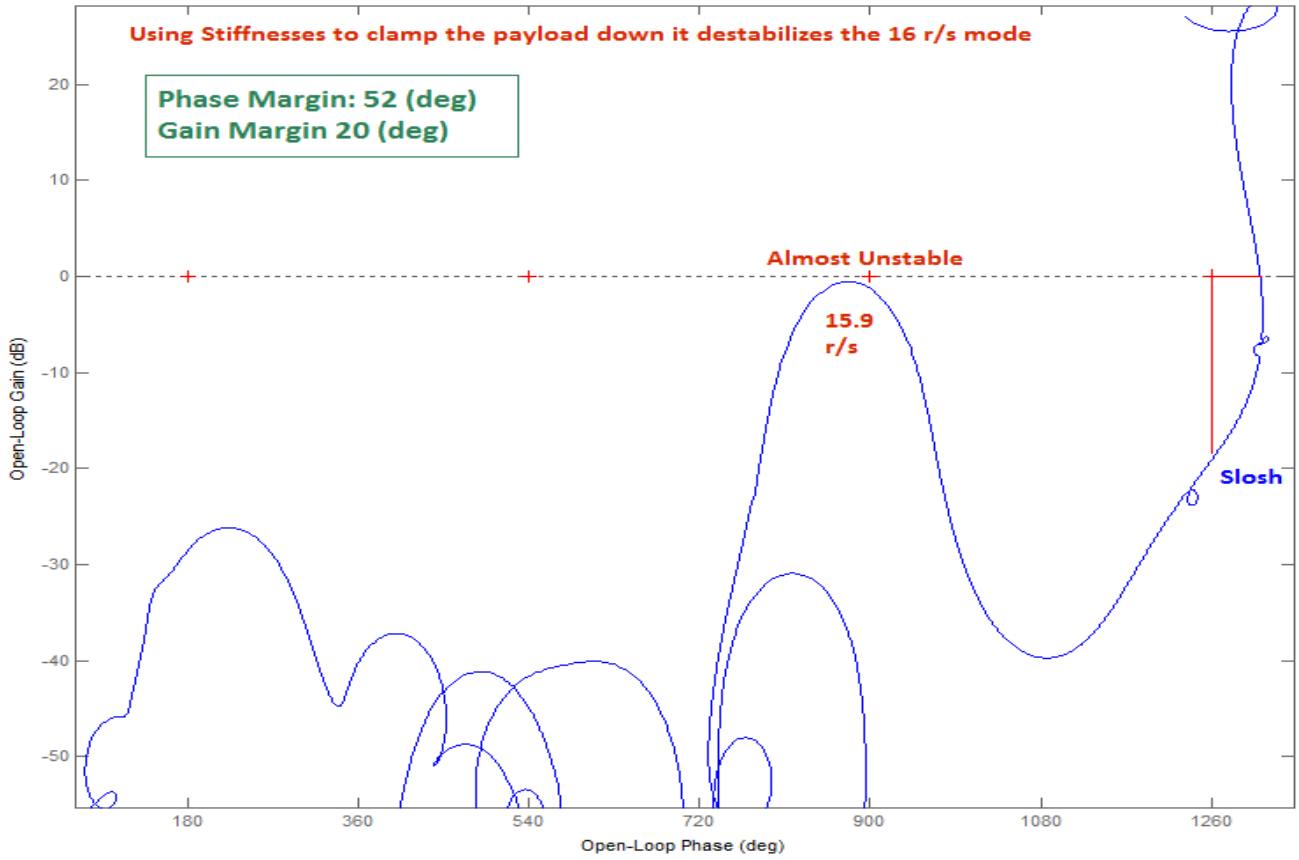
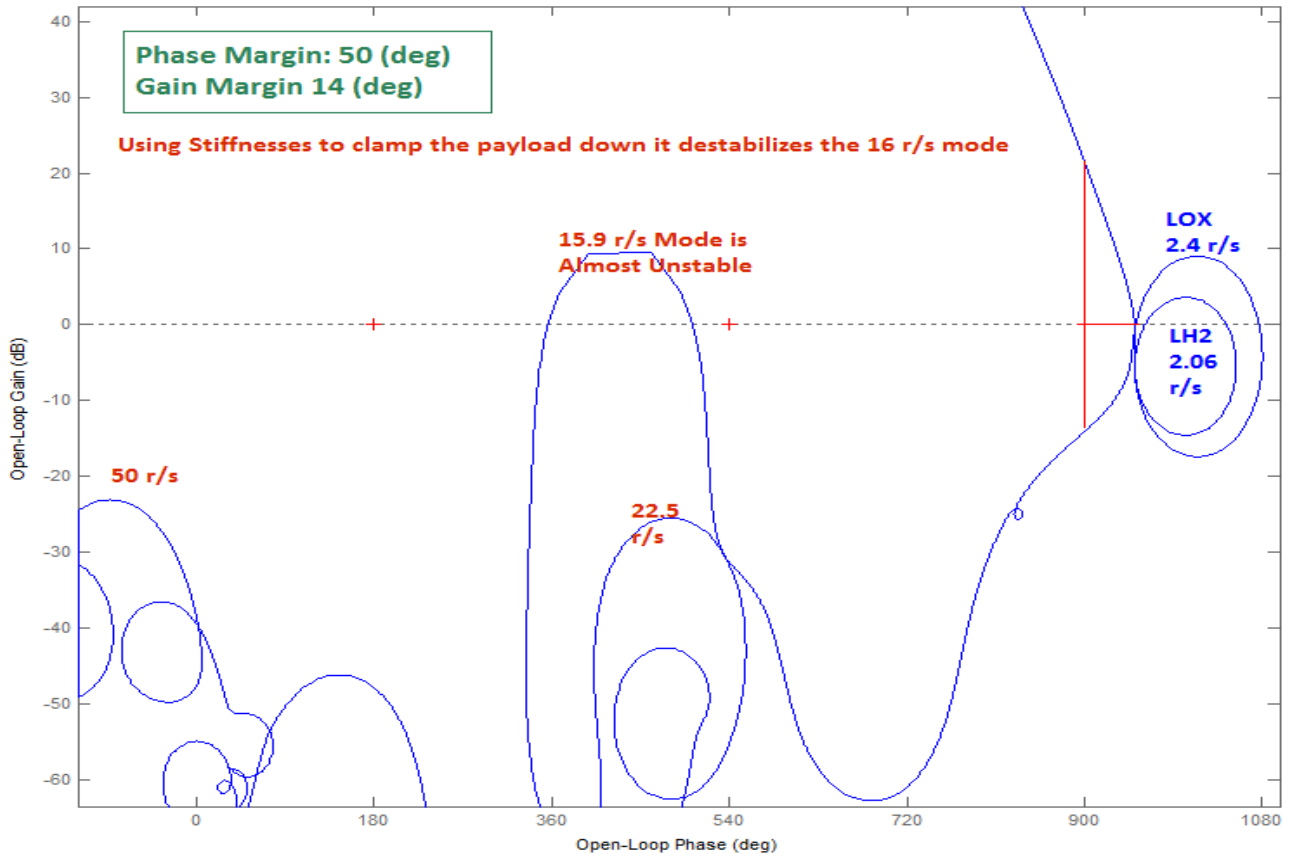


Figure 10 Including springs instead of the Coulomb dampers it further aggravates the flex instability.

Stage-2 Roll Axis Stability, No Damper, Payload Clamped, (Yaw & Pitch Loops Closed)



Stage-2 Yaw Axis Stability, No Damper, Clamped Payload, (Roll & Pitch Loops Closed)



11 The Coulomb Damper

The coulomb damper is a non-linear energy dissipating device shown in Figure 10. Its operation is similar to an automotive shock absorber. The difference is that energy is dissipated by sliding friction rather than viscous friction. One end of the device is attached to the payload and the other side is attached to the Shuttle cargo bay floor. Sliding friction is generated from a cylindrical shaped brake shoe that is forced in axial direction against the wall of a metal cylinder by means of wedges. The sliding friction force is adjusted by pre-setting the compression forces against the wedges. The damping does not take place until the breakout (stiction) force is exceeded. The coulomb damper is also characterized by its spring-compliance and the free-play.

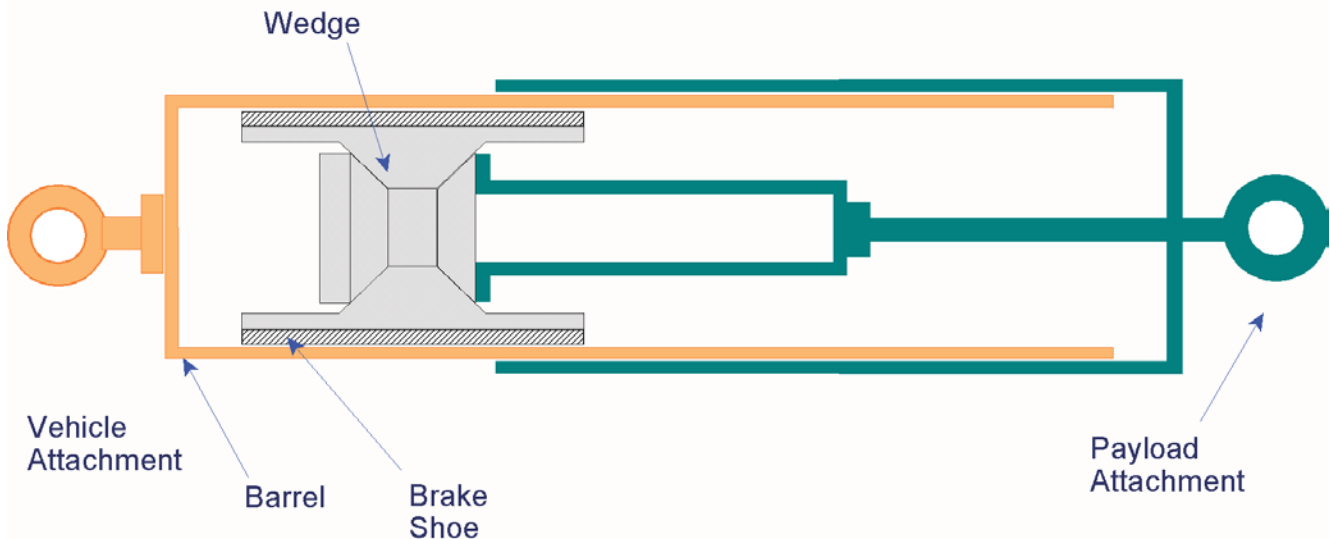


Figure 10 Non-Linear Coulomb Damper

The non-linear behavior of the coulomb damper is illustrated in Figure 11 that plots force versus displacement. Let us suppose that one end of the coulomb damper is attached to a fixed point and it is initially positioned at point O. The point O is an arbitrary reference from where we measure relative displacements. Assume that one end of the damper is pulled from one side. It will extend by a small amount S (the dead-band distance from O to A) without generating a reaction force. From point A to point B it behaves like a mechanical spring of stiffness K_D generating a restraining force proportional to the amount of extension, as long as the force does not exceed the maximum breakout force F_{max} . By extending it further past point B the device will overcome stiction, it will brake loose and begin sliding while dissipating energy through friction. The output force, however, that opposes the motion will not exceed F_{max} .

Let us suppose now that the device is extended all the way to point C while it is exerting max force and we begin reducing the pulling force. The spring compliance K_D will take effect and as the force is reduced the extension will retract back slightly to point D where the force drops to zero. At point D you begin pushing it in the opposite direction, it will begin sliding backwards, but you will not experience any opposing (negative) force until you pass the dead-band ($2S$), which is the distance from point D to point E. At point E you will begin experiencing the stiffness again and the force will increase in the opposite direction until you reach the breakaway force in the opposite direction at point F. At point F the device brakes loose and the negative force saturates at $-F_{max}$, and it starts sliding again in the negative direction while dissipating energy through friction. At some point G you begin to gradually reduce the negative force to zero and the device retracts slightly back to point H due to

stiffness K_D . At point H you can repeat the positive force cycle again after passing through the dead-band ($2S$) between points H and I, and overcoming the stiffness K_D between points I and J.

To summarize, three operating regions exist in the Coulomb Damper. At very low amplitudes from an arbitrary reference point O where the input does not exceed the dead-band $\pm S$, and the output force is zero. At intermediate amplitudes where the input exceeds the dead band but it does not exceed the breakout point the device operates in the compliance region. No damping takes place there but only a cyclic storage and release of energy due to K_D . The motion is symmetrical about the center of the dead-zone. At high amplitudes the breakout force is exceeded, the device is sliding while energy is dissipated, and it provides passive damping.

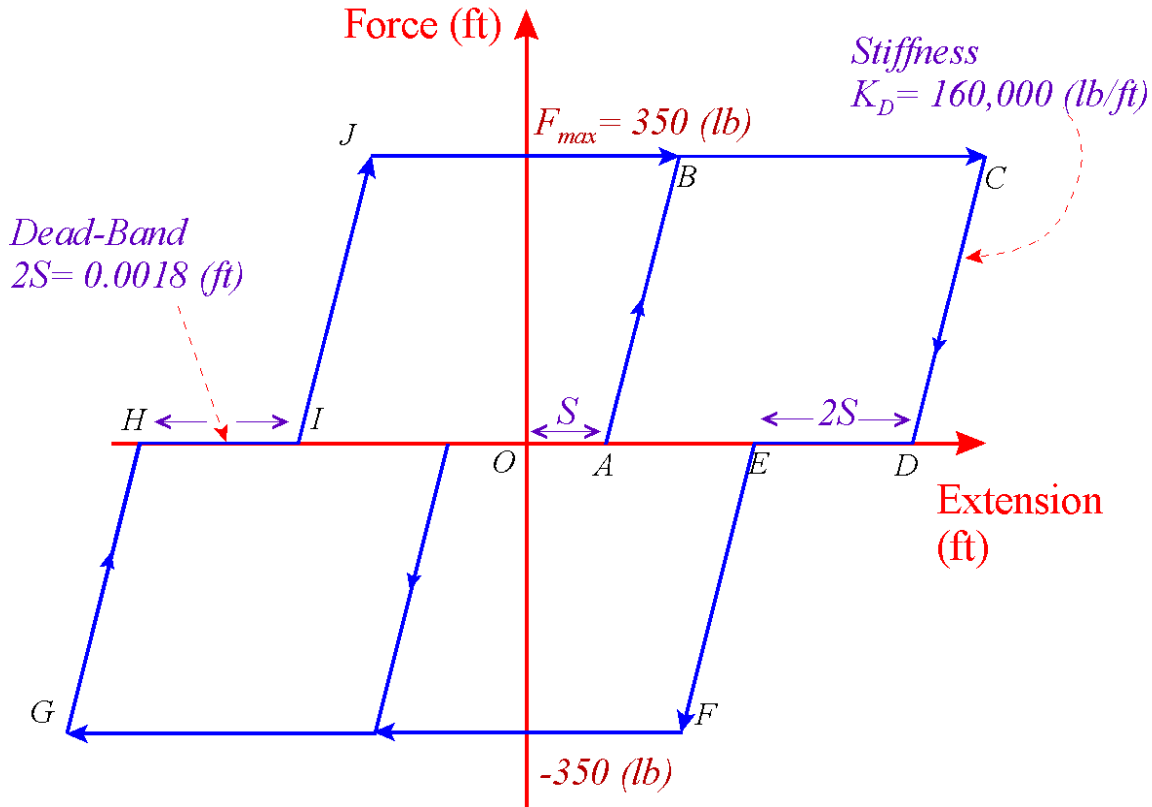


Figure 11 Force versus Displacement Characteristics of the Coulomb Damper

As it is already described the flexible payload and its cradle are supported by two coulomb dampers. The front end of the cradle is rigidly attached to the Shuttle cargo bay. The rear end of the cradle is attached to the vehicle cargo bay by the coulomb dampers. The bottom end of each damper is attached to the vehicle and the top ends are attached to the mounting structure that holds the payload. Structural nodes and mode shapes for the four attachment points are available in the flex model. They are used for calculating relative displacements across the dampers as a function of damper force.

12 The Describing Function Method for Analyzing Non-Linearities

The describing function is a frequency domain analysis method that is used for determining the existence of limit cycles in non-linear SISO systems. It also determines the amplitude and frequency of the limit-cycle. When the input to a non-linear element is sinusoidal, the output is periodic with the same period as the input, but it is not sinusoidal. It contains higher harmonic frequencies in addition to the fundamental component. The describing function $N(e)$ of a non-linearity is the equivalent “gain” of the non-linearity at the first harmonic (ω) in response to an input sinusoid $e \sin(\omega t)$. It is calculated as a function of the amplitude (e) which is the feedback error signal. In other words, the describing function of a non-linearity is defined to be the complex ratio of the fundamental harmonic component of the output divided by the input of the non-linearity.

In the conventional linear control systems analysis using Nyquist plots, the system exhibits a limit cycle (critically stable) when the locus of $G(j\omega)$ passes through the critical point $(-1, j0)$. In the describing function analysis, the critical point $(-1, j0)$ is replaced by the entire $-1/N(e)$ locus, where $N(e)$ is the DF locus function of amplitude e . The $-1/N(e)$ locus is plotted on the same Nyquist or Nichols chart as the plant locus $G(j\omega)$, and from the relative location of the two loci we can determine graphically the stability of the closed-loop system. When there are no intersections it implies that the system is either stable or unstable depending on the encirclements of the locus similar to the -1 point in linear analysis. When there are intersections between the $G(j\omega)$ and the $N(e)$ loci, from the intersection points we can approximately determine the frequency and the amplitude of possible limit cycles. The frequency is determined from the $G(j\omega)$ locus, and the amplitude from the $-1/N(e)$ locus.

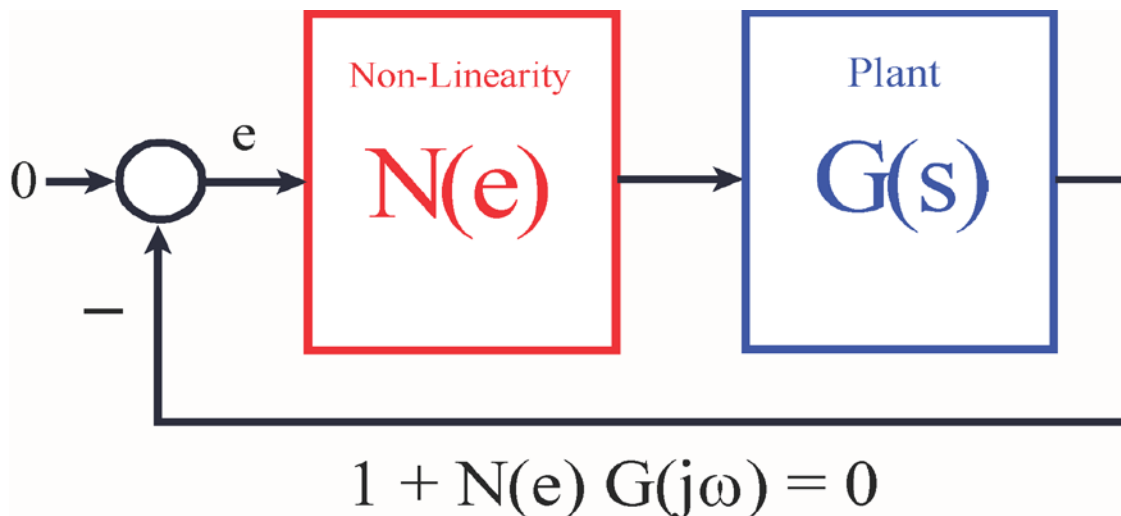


Figure 11 Feedback System with an input Non-Linearity and the characteristic polynomial

The describing function analysis is not an exact method because it is assumed that only the fundamental frequency component of the system output is significant. This assumption is often acceptable because the harmonics in the output of the non-linearity are usually of smaller amplitude than the fundamental, and in addition, the higher frequency harmonics are also filtered by the actuator and the control system that usually includes low pass filters. Therefore, it is often valid to ignore the effects of the high frequency harmonics in the DF analysis.

A disadvantage of the DF frequency domain method is that the non-linearity must be lumped as a single input, single output block, connected with the SISO plant model as in Figure (11). Therefore, we cannot analyze the three axes coupled system in the MIMO sense with two independently operating

non-linear dampers. The block diagram in DF analysis must be configured with the two dampers combined as a single non-linearity block $N(e)$. In the DF analysis the loop is not opened at the control system output. The flight control system loop remains closed, but the loop is opened across the damper because we are interested in the stability across that loop. This is a purely mechanical loop within a continuous system. Since the damper motion is mainly in the z direction we can decouple the plant system into two single-loop systems connected to a single non-linearity that can be analyzed separately.

- A pitch system $G_s(s)$ that captures the symmetric flexibility of the combined structure where both dampers operate symmetrically and in phase with each other as a result of a symmetric excitation and affecting only the symmetric structural modes, and
- An anti-symmetric $G_a(s)$ system that captures the structure's anti-symmetric (rolling) motion, where the two dampers are operating in the opposite phase with each other in response to anti-symmetric structural flexibility and affecting only the anti-symmetric structural modes.

In either case the input to the plant is the damper force and the output is damper extension. The non-linearity is not included in the linear plant $G(s)$, but it will appear in the $1/N(e)$ locus. The DF analysis result is the amplitude and frequency of the limit-cycle which is obtained graphically by the intersections of the two loci. Figure 12 shows a Simulink model “*Open_Loop_DF.mdl*” that is used to generate the locus $G_s(j\omega)$ for the DF analysis. The loop is opened across the damper. The input is damper force which is the same for both dampers since they operate in phase and the output is their average displacement. A short delay is included to be consistent with the simulation model.

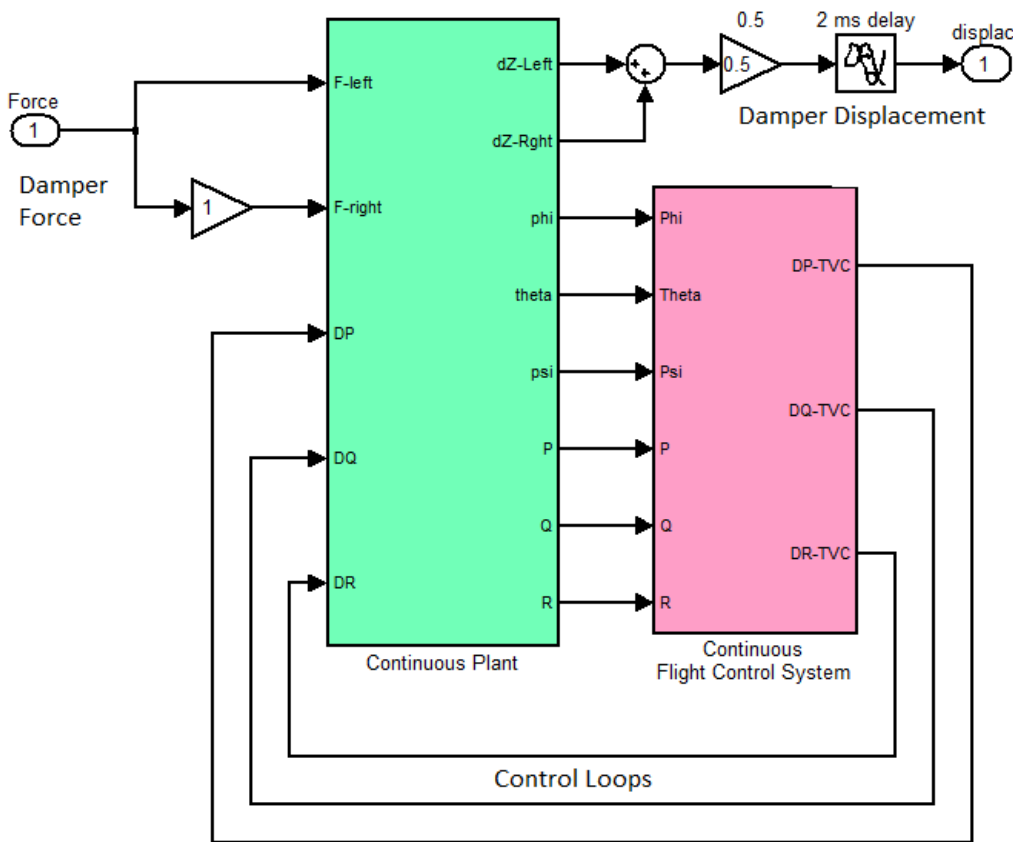


Figure 12 Simulink model “*Open_Loop_DF.Mdl*” used for calculating the frequency response $G(j\omega)$ across the absent damper.

In the case of the symmetric plant $G_s(s)$ the input applies equal forces at the two dampers to excite the symmetric modes (an input of 1 unit corresponds to 350 lb). The output is an average left and right damper extension in (feet). In the anti-symmetric case $G_a(s)$ we apply a positive force on the left damper and change the sign of the gain to -1 on the right damper to apply an equal and opposite force on the other side. This excites the anti-symmetric structure. We must also change one of the signs in the summing junction at the output and the output becomes $0.5*(\text{left} - \text{right})$ representing the average anti-symmetric extension in (feet).

We use continuous systems for both the plant and the controller to avoid the additional 40 msec delay that would have appeared in the frequency domain analysis if we had used the discrete plant and controller systems. The loop across the damper is a mechanical and continuous loop and it does not cause delays due to sampling and the zero-order-hold. If we had used discrete systems, the additional 40 msec phase delay would have affected the limit-cycle prediction results. The continuous plant system title is “*Plant Model, Vehicle/Actuators/Sensors*” and the controller is “*Shuttle Stage-2 Continuous Flight Control System*”, and they were exported to the Matlab directory from file “*Stg2_Damper.Qdr*” as m-functions “*plant_flxcont.m*” and “*controller_s.m*”. A Matlab script “*run_df.m*” is used to perform the Describing Function analysis using a Nichols plot.

13 Calculating the Describing Function of the Coulomb Damper

The next step is to calculate the Describing Function of the Coulomb Damper non-linearity for the first harmonic. The DF magnitude and phase can be obtained analytically using the usual DF calculation method by integrating the response of the non-linearity to a sinusoid function, between 0 and 2π . The Describing Function $N(E)$ for the Coulomb Damper in phasor form as a function of amplitude (E) is obtained analytically from the following equations. Where: K_D is the damper stiffness in (lb/ft), F_D is the damper breakout force (lb), S is the dead-band (ft), and E is the amplitude of the sinusoidal input displacement (feet).

$$N(E) = a(E) + jb(E) = M(E) \angle \phi(E)$$

$$M(E) = \sqrt{a(E)^2 + b(E)^2} \quad \phi(E) = \tan^{-1} \frac{b(E)}{a(E)}$$

$$b(E) = \frac{K_D}{\pi} \left[(1 + \sin \theta_A)^2 + (\sin \theta_B - \sin \theta_C)^2 \right] - \frac{2F_D}{\pi E} (\sin \theta_A + \sin \theta_C)$$

$$a(E) = \frac{K_D}{\pi} \left[\theta_A + \theta_C - \theta_B + \frac{\pi}{2} - 2 \cos \theta_A - \frac{\sin 2\theta_A}{2} - \frac{\sin 2\theta_B}{2} - \frac{\sin 2\theta_C}{2} + 2 \sin \theta_B \cos \theta_C \right]$$

$$+ \frac{2F_D}{\pi E} (\cos \theta_A + \cos \theta_C)$$

$$\text{where: } d = \frac{F_D}{K_D}; \quad \theta_A = \sin^{-1} \left(\frac{d}{E} - 1 \right); \quad \theta_B = \sin^{-1} \left(\frac{d + 2S}{E} - 1 \right); \quad \theta_C = \sin^{-1} \left(\frac{2d + 2S}{E} - 1 \right)$$

We also have a Matlab program “*DF_Calculate.M*” that uses a simulation model “*DescFun_Sim.Mdl*” to perform the integration (from 0 to 2π) and to calculate the DF. The model is shown in Figure 13 and it uses the following damper parameters.

- Dead-band amplitude $S=0.0009$ (feet),
- Maximum breakout force $F_D= 350$ (lb). The normalized value is 1.
- Maximum amplitude before breakout is 0.0031 (feet).

- Stiffness $K_D = 160,000$ (lb/ft). The normalized value is 457.

The program calculates the DF at different input amplitudes (E) and plots it. Figures (13 a & b) show the DF magnitude versus input displacement, and also the phase versus input displacement characteristics of the damper. The device behaves like a memory-less non-linearity, imaginary part only with no phase response, up to the breakout point. The peak amplification occurs at the breakout point, 0.0031 (ft). After the breakout point the phase drops and causes energy dissipation. The DF is not frequency dependent. The DF calculations are saved in file “dfdata.mat” and used later by another Matlab program “run_df.m” which calculates the $G(j\omega)$ and overlays the DF inverse $-1/N(e)$ on a Nichols plot.

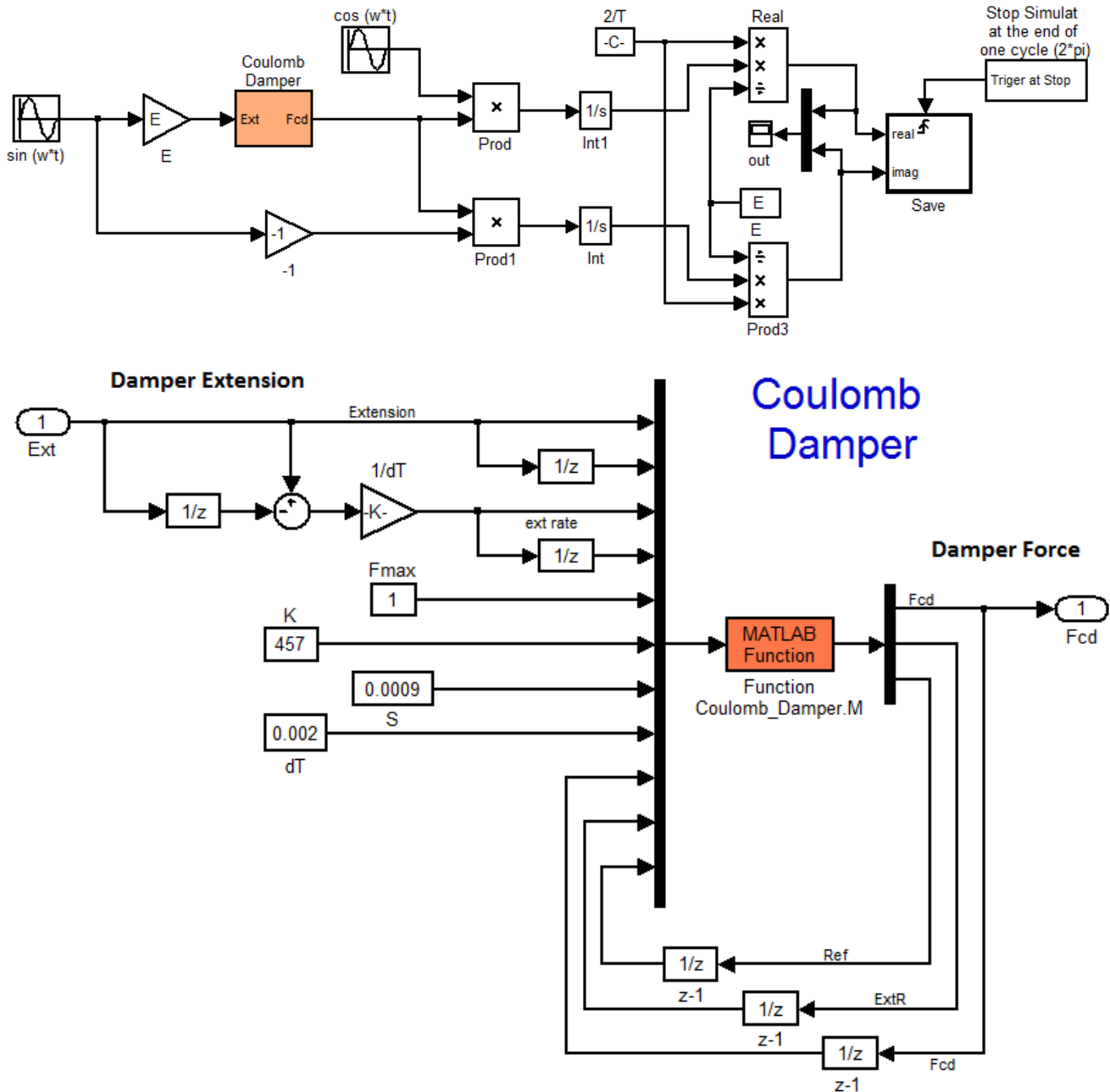


Figure 13 Simulink Model “DescFun_Sim.Mdl” for Calculating the DF of the Coulomb Damper

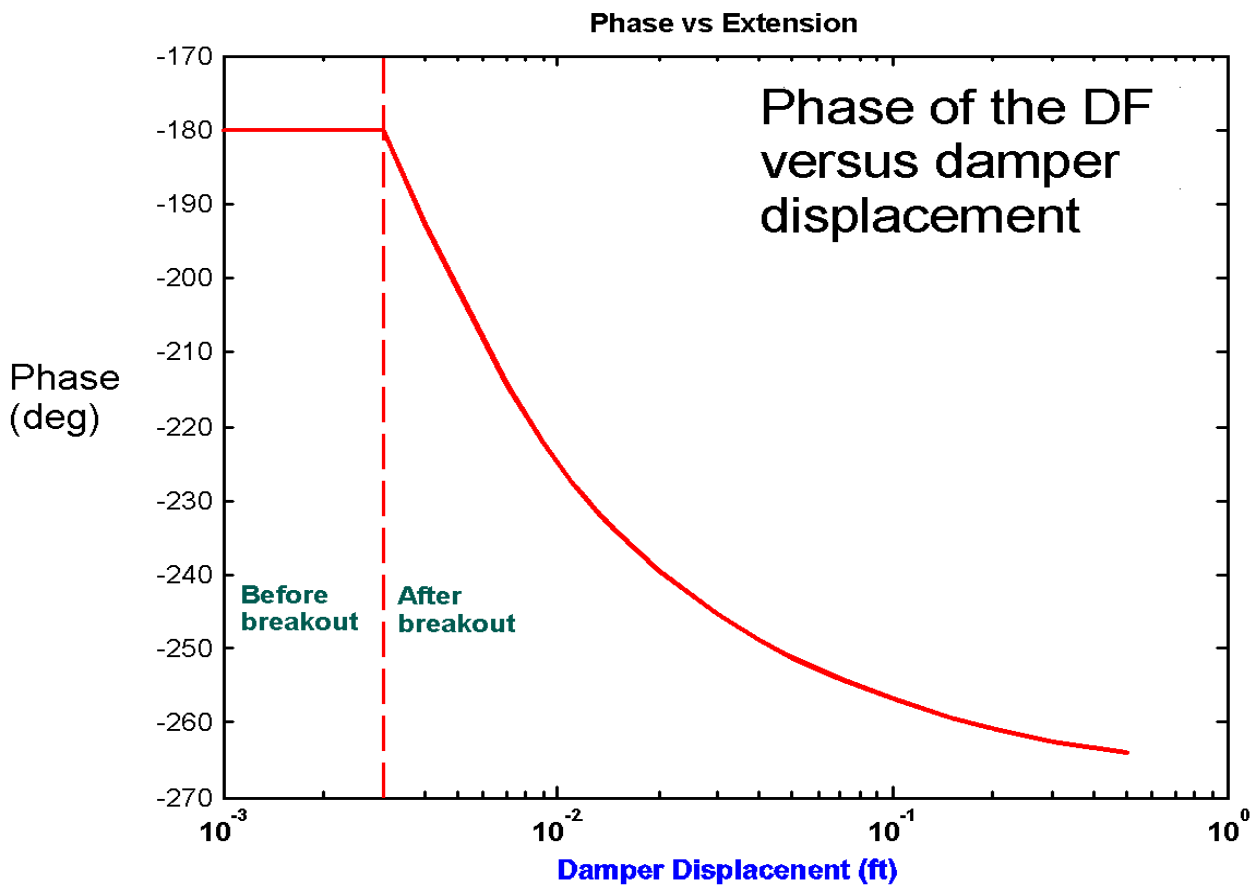
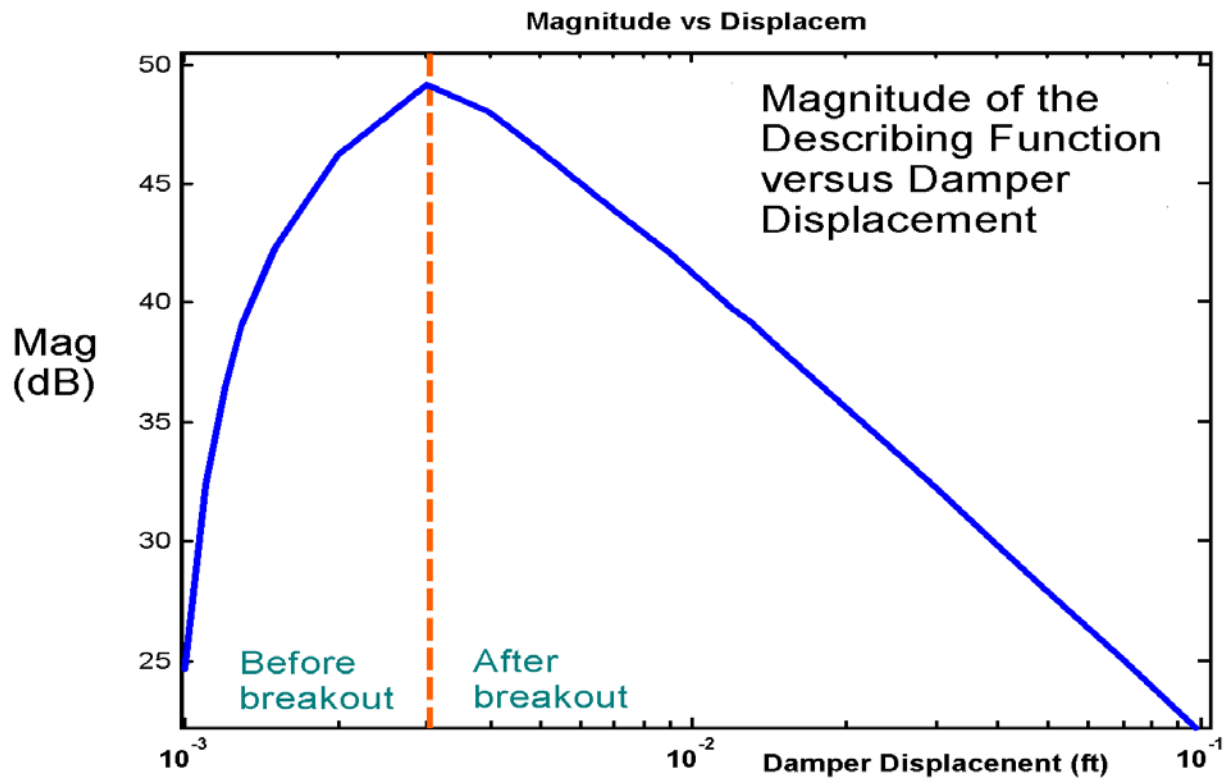


Figure 13 Magnitude and Phase of the Coulomb Damper DF as a function of displacement (E)


```

function out=Coulomb_Damper(Ext,Ext1,Dext,Dext1, Fmax,K,S,dT, Fcdi,Extri,Refi)
% SIMULATES COULOMB DAMPER DYNAMICS.
% EXT, EXT1= PRESENT AND PAST VALUE OF RELATIVE DISPLACEMENT ACROSS THE DAMPER
% DEXT,DEXT1=PRESENT AND PAST VALUES OF RELATIVE RATE ACROSS THE DAMPER
% REF= LOCATION OF REFERENCE POINT ( OUTPUT ONLY )
% FCD= Output COULOMB DAMPER FORCE
% DT = TIME STEP
% -----
XI= S + Fmax/K;

%.. CHECK FOR FREEPLAY/COMPLIANCE REGION, Below Braking point (no damping)
if (abs(Fcdi)>=Fmax && Dext*Extri<0)
    TAU=dT*Dext1/(Dext1-Dext); %.. FIND TIME OF CORNER
    Ref=Ext1 + Dext1*TAU/2 + XI*sign(Dext); %.. FIND POSITION OF NEW REFERENCE
else; Ref=Refi; %.. Same Reference point as before
end

Extr=Ext-Refi; %.. RELATIVE EXTENSION from Reference

if (abs(Extr) >= XI); Fcd= Fmax*sign(Extr); %.. FORCE= MAX_FORCE SIGN OF REL EXT
elseif (abs(Extr) < S); Fcd= 0; %.. < FREEPLAY, FORCE=0

%.. IF REL_EXT< FREEPLAY/COMPLIANCE
else
    Fcd= K*(Extr-S*sign(Extr)); %.. Force due to Compliance
end
out=[Fcd;Extr;Ref];

```

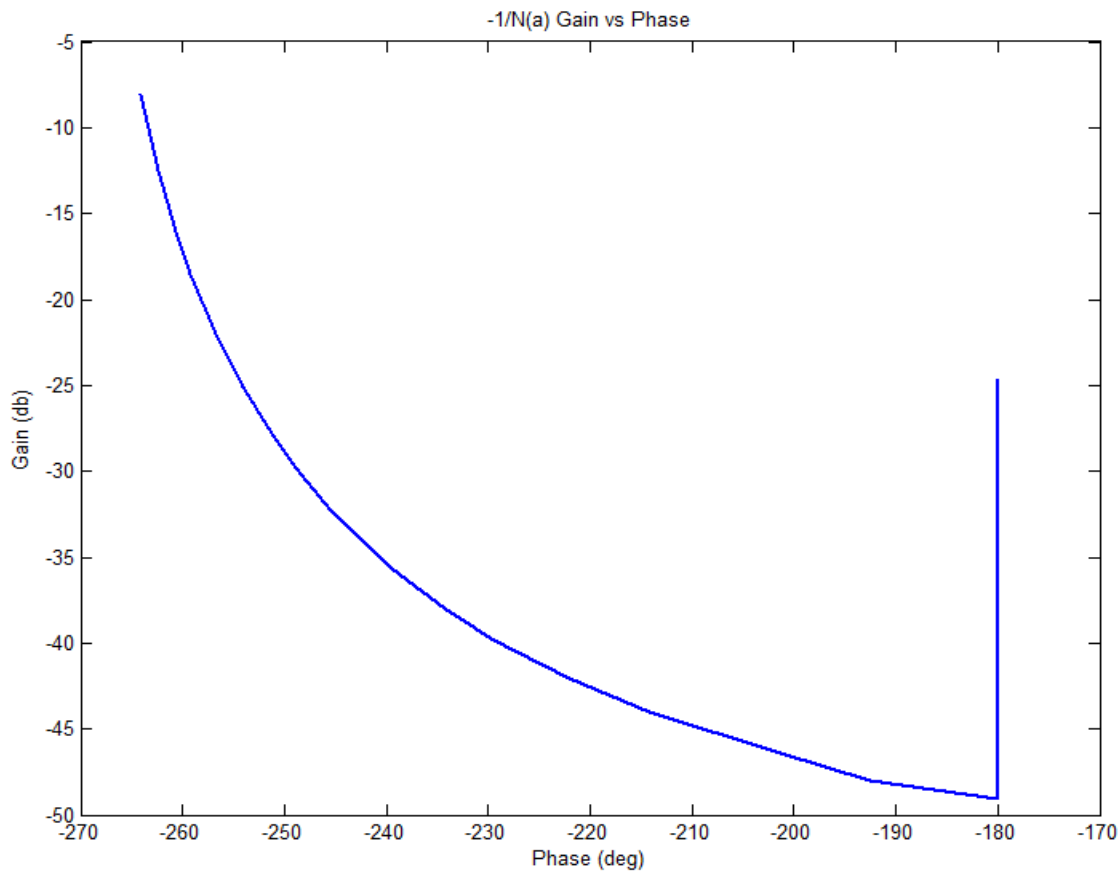


Figure 14 Gain versus Phase of the Inverse DF locus $-1/N(e)$ to be co-plotted with $G(j\omega)$

14 Analyzing the Describing Function Results

The Matlab script file “*run_df.m*” shown below calculates the open-loop frequency response of the plant $G(s)$ across the damper connections. It loads the continuous plant and the continuous controller and it uses the Simulink model “*Open_Loop_DF.Mdl*” to calculate the plant frequency response. The plant and controller systems are combined together as shown in Figure 12 and the controller loop is closed. A delay is included in the continuous controller output to simulate the 40 msec controller transport lag. The m-file calculates the $G(j\omega)$ locus which varies as a function of frequency (ω) and plots it on a Nichols chart. It also overlays the $-1/N(e)$ locus on the same Nichols plot. $N(e)$ is not frequency dependent but varies only as a function of sinusoidal damper extension amplitude (e). The intersections of the loci determine the limit-cycles size and frequency. Not all intersections are convergent. Some intersections do not sustain oscillations and are referred to as divergent. The methodology regarding limit-cycle convergence is based on the Nyquist stability theorem and it will not be discussed here.

```

% Program calculates the frequency response G(jw) of the plant across
% the non-linearity and overlays the -1/N(e) locus
% The intersections determine the existence of limit-cycles
global Phdf Mdf
d2r=pi/180; r2d=180/pi;
[Av1, Bv1, Cv1, Dv1]= plant_flxcont;           % Continuous Plant
[Acs, Bcs, Ccs, Dcs]= controller_s;           % Continuous Stage-2 Controller

label='Nichols Anti-Symmetric Frequ Response Across the Damper for Describ Function Analysis'
[As,Bs,Cs,Ds]= linmod('Open_Loop_DF');         % Cont. Frequ Response Model
sys=ss(As,Bs,Cs,Ds);                           % Perform Linearization
%[As,Bs,Cs,Ds]= dlinmod('Open_Loop_DF',0.002); % Disc. Frequ Response Model
%[n,n]=size(As); E=eye(n);
%sys=dss(As,Bs,Cs,Ds,E,0.002);                 % Perform Linearization

lfr=40000; ph2=zeros(1,lfr); mg2=ph2; w=logspace(-2,2.8,lfr); % and Frequ domain analysis
[mg,ph]= Nichols(sys,w);
for i=1:lfr                                     % Create locus of G(jw)
    ph2(i)=ph(1,1,i);
    mg2(i)=20*log10(mg(1,1,i));
end
load dfdata                                     % Load the DF data with the -1/N(a) locus
Phdf2=Phdf+2*360;                               % create another 1/N(e) locus 360 deg away
Phdf1=Phdf+1*360;                               % create another 1/N(e) locus 360 deg away

% Overlay loci
figure(1); plot(ph2,mg2, Phdf2,Mdf, Phdf1,Mdf,'LineWidth',1.5); title(label)
figure(2); Nichols(sys,w); title(label)

```

Figure 15 Matlab file “*run_df.m*”

Figure 15 shows the overlay of the two loci. The Nichols plot of the symmetric system $G_s(j\omega)$ is co-plotted with the inverse of the damper DF which is $-1/N(a)$. In the symmetric system the damper forces are applied in phase and they excite the pitch flexibility. The $-1/N(a)$ locus is shown twice because it repeats every 360° similar to the (+) point in the classical Nichols charts. The intersections indicate that according to the Nyquist criteria there is a convergent limit cycle at 10.5 (rad/sec) indicating that the system will maintain a damper oscillation at 10.5 (rad/sec) at an amplitude of 0.004 (ft). There is

also a convergent limit-cycle at a lower amplitude of 0.0013 (feet) which is at 9.78 (rad/sec) frequency. This intersection point is in the vertical $\pm 180^\circ$ section of the $1/N(a)$ describing function locus which corresponds to the device operating in the spring/ dead-zone region before breakout. The amplitude (zero to peak) of the Coulomb damper oscillation is obtained from the magnitude of the locus at the intersection and from the DF plot in Figure 13. There is also a divergent (green) intersection point between the two convergent limit-cycles. The loci are almost touching at a higher frequency which indicates the possibility of a limit cycle at 24 (rad/sec). However, it is of low amplitude and its existence is questionable.

The intersection at 9.1 (rad/sec), (shown in green) corresponds to a large damper displacement 0.4 (ft). However, this is not a convergent limit-cycle according to the convergence criteria and it will not sustain an oscillation at that frequency. The DF analysis results indicate that when the system is excited with a disturbance causing the dampers to extend to an amplitude (e_d) where: $0.004 > e_d > 0.4$ (feet), the damper oscillations will decay and the limit-cycles will converge towards an amplitude of 0.004 (ft) and a frequency of 10.5 rad/sec. When the disturbance excites the coulomb dampers to amplitudes greater than 0.4 (ft) the oscillations will grow to an instability.

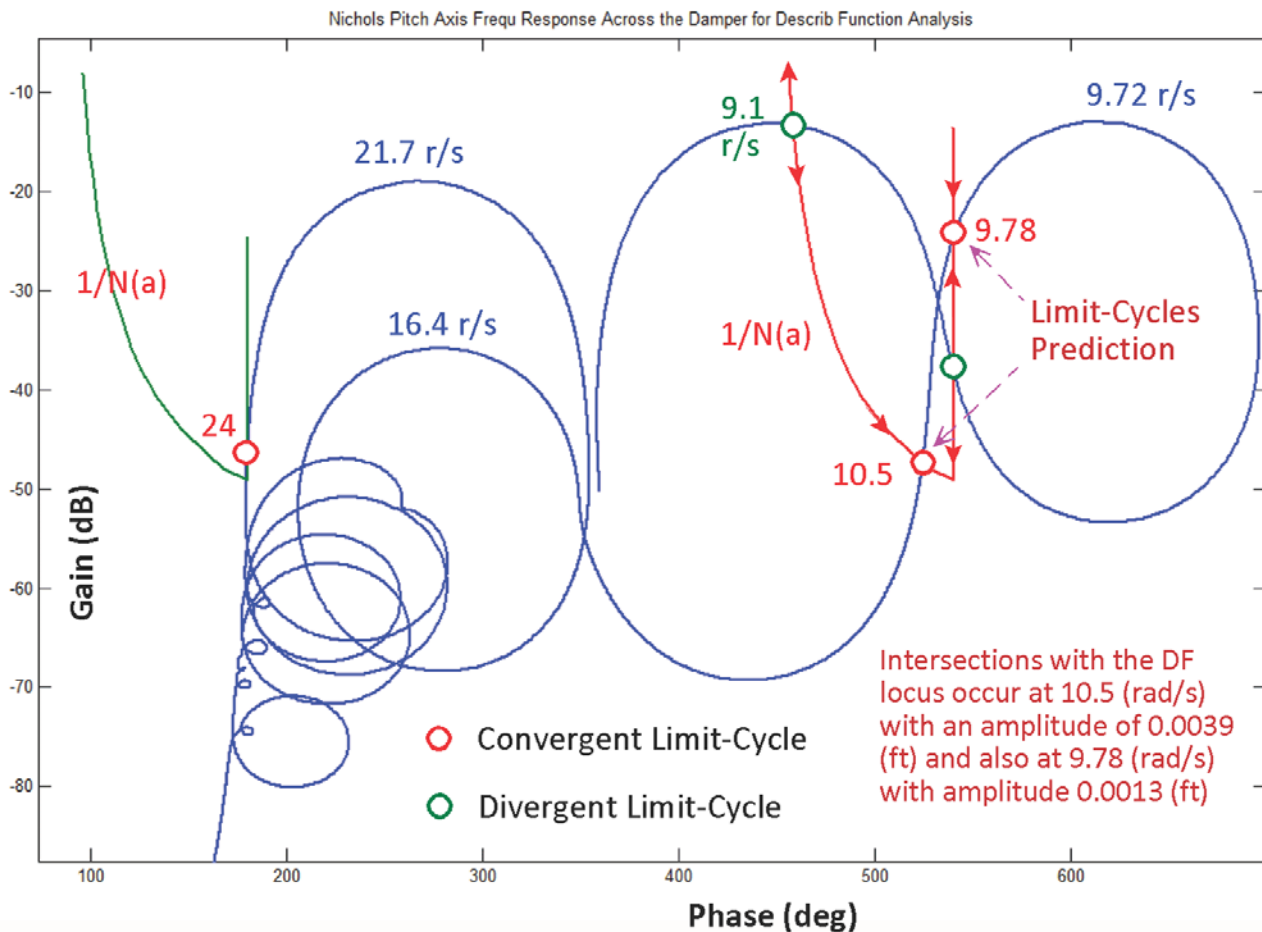


Figure 15 Describing Function Analysis of the Symmetric System $G_s(s)$, 3 Limit-Cycles are determined by the intersections with the $-1/N(a)$ locus

A similar analysis is performed in the anti-symmetric direction using the anti-symmetric system $G_a(j\omega)$, where the two damper forces are driven 180° out of phase exciting the roll flexibility. The Simulink model “*Open_Loop_DF.Mdl*” was modified by changing the right damper force sign to negative, and also the output is changed to measure the average anti-symmetric extension (left-right)/2. The Nichols plot of the anti-symmetric plant is shown in Figure 16. The intersections indicate that there is a convergent limit cycle at 61.3 (rad/sec) which is at an amplitude of 0.0033 (ft), slightly above the breakout point. There is also almost an intersection with the 15.8 mode where the closest point is at 16.2 (rad/sec). An intersection at this point would create an asymmetric limit-cycle at the two dampers at 0.003 (feet) amplitude. This is consistent with the roll/yaw linear analysis which indicates a low margin at the 15.8 (rad/sec) anti-symmetric mode.

To conclude the frequency domain DF analysis, the results indicates that the system with the two Coulomb dampers has the potential of limit-cycling at some acceptable low amplitudes. This is assuming that the disturbance forces on the dampers that occur in the cargo bay during flight are small enough not to excite damper displacements that would exceed 0.4 (feet). This amount of excitation would induce an enormous structural mode divergence that might lead to structural failure. We must therefore use non-linear simulations to examine possible disturbances that could excite the system into this type of divergent state.

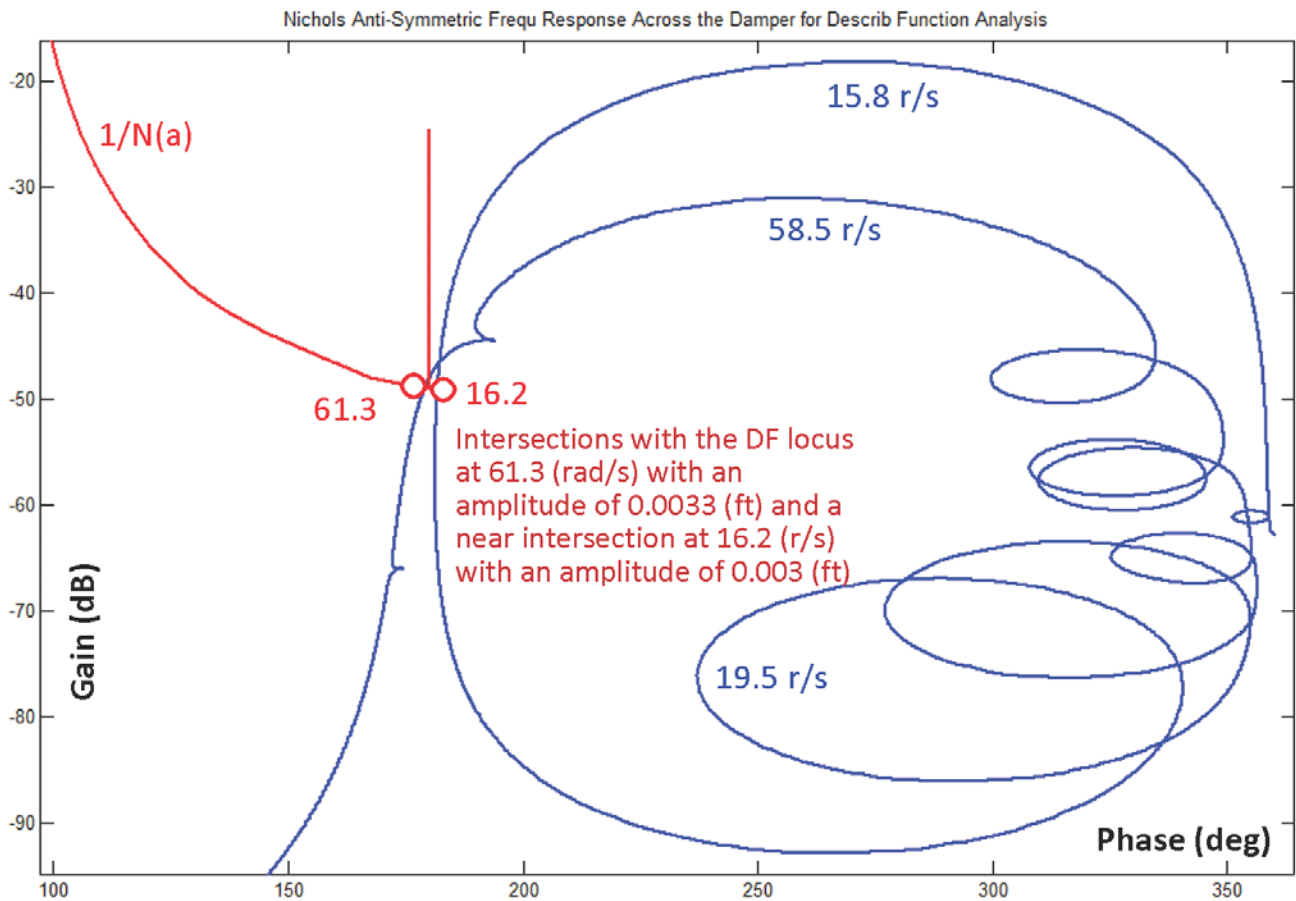


Figure 16 Describing Function Analysis of the Anti-Symmetric System $G_a(s)$

15 Time Domain Simulations

In this section are presenting simulation models that will be used to support our frequency domain analysis results. Our first step is to validate the linear analysis instability problem of the unclamped structure without the dampers. In Figure 9a we showed that the pitch flight control system has an unstable flexible mode when the dampers are not connected and that the frequency of instability is 9.08 (rad/sec). We will also show that attaching springs in place of the dampers does not fix the instability problem. The next step is to attach the coulomb dampers at two places between the vehicle and the payload and to demonstrate that they provide a significant amount of vibration attenuation by dissipating energy. We will also demonstrate the existence of various limit-cycles by applying different types of excitations and causing the system to converge at different limit-cycle frequencies and amplitudes as it was predicted by the frequency domain DF analysis. We will also show the response of the flight control system to attitude step commands.

15.1 Step Response of the Discrete Closed-Loop System without Damper

The discrete closed-loop simulation model is shown in Figure 17. It uses the discretized plant model sampled at 40 msec, “*Plant Model, Vehicle/Actuators/Sensors (Z-Transform $T=0.04$)*” and the discrete flight control system “*Shuttle Stage-2 Discrete Flight Control System*” from file “*Stg2_Damper.qdr*”. The two systems were converted to Matlab functions “*plant_flx40ms.m*”, and “*controller_z.m*” in Section 9, and embedded in the Simulink model “*Closed_Loop_Sim_z40.mdl*” that performs the simulation. The discrete plant and the flight control commands are shown in detail below.

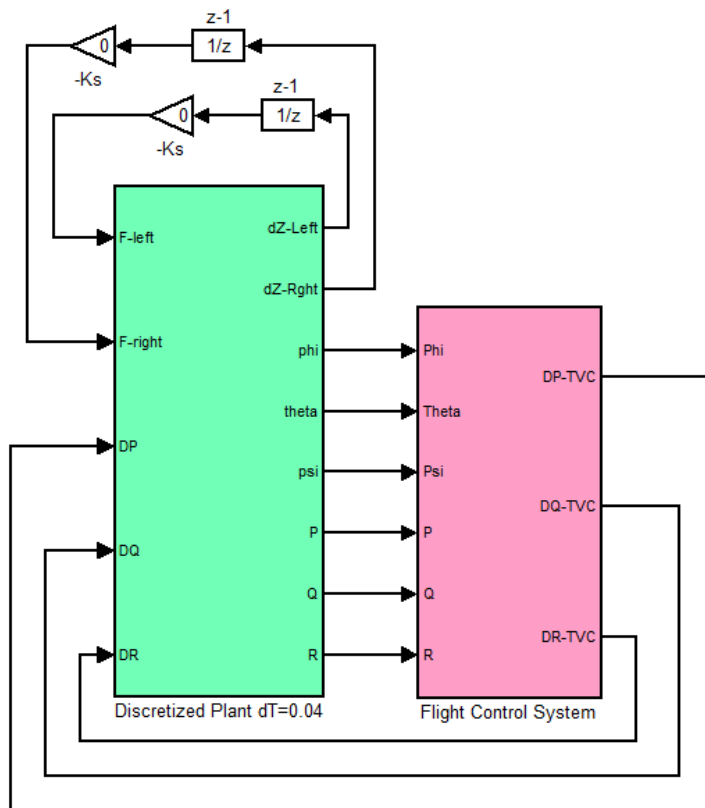


Figure 17a Discrete Closed-Loop Simulation Model “Closed_Loop_z40.Mdl” without Dampers

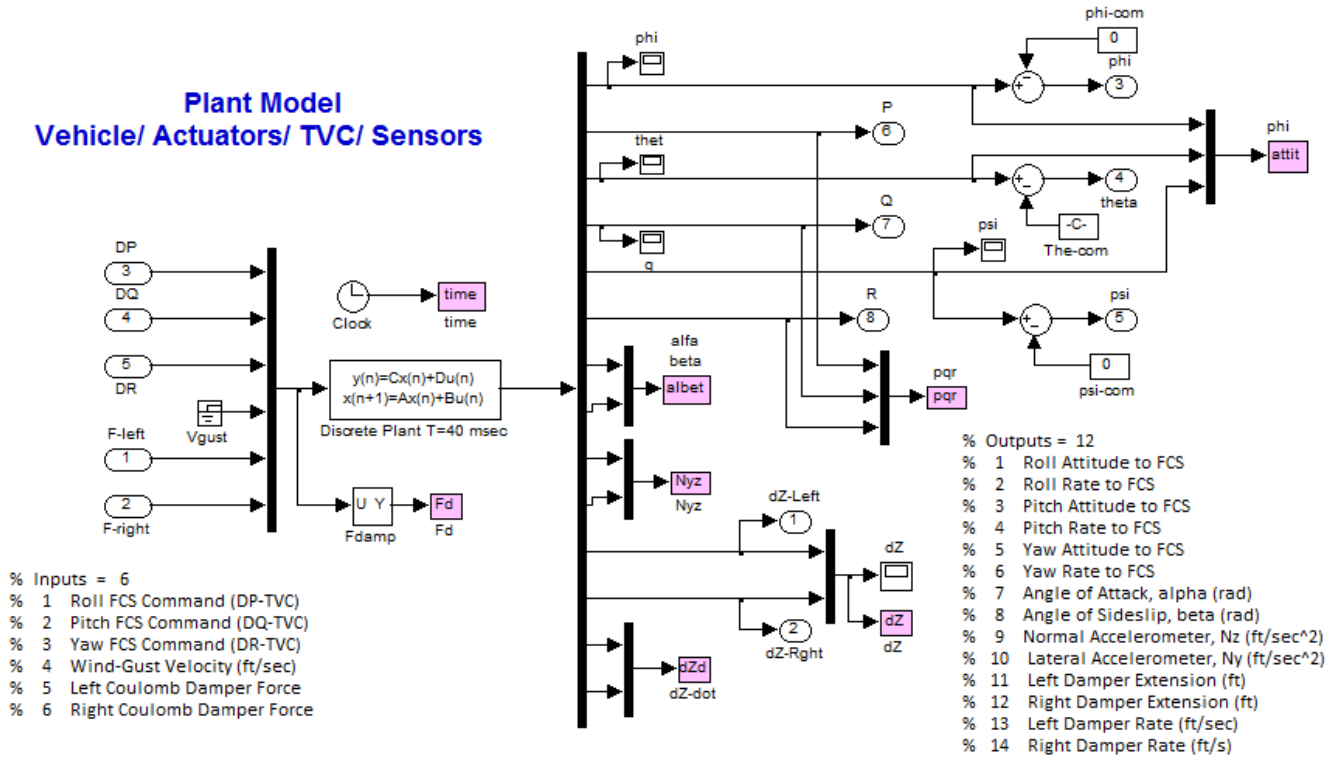


Figure 17b The discretized subsystem “Plant Model, Vehicle/Actuators/Sensors (Z-Transform T=0.04)” with attitude commands

The attachment struts that constrain the relative motion of the payload are not attached in this model because it represents the case where the payload is cantilevered, and allowing the 9.08 rad/sec payload mode to oscillate freely. The two mechanical feedback loops provide the capability to attach springs in place of dampers but in this case the stiffnesses are set to zero.

A pitch attitude command of 1 (deg) is applied at the theta-command input to excite the pitch motion. The system response is shown in Figure 16. The pitch attitude responds to the 1 deg command but it begins to oscillate and eventually it diverges. The unstable oscillation is at 9.08 (rad/sec) as it was predicted by the encirclement of the (+) point in the pitch stability analysis Nichols plot. Including negative values in the two feedback gains to represent the spring stiffnesses K_s of the mechanical fasteners does not improve stability. In fact it becomes worse and it drives additional modes to divergence.

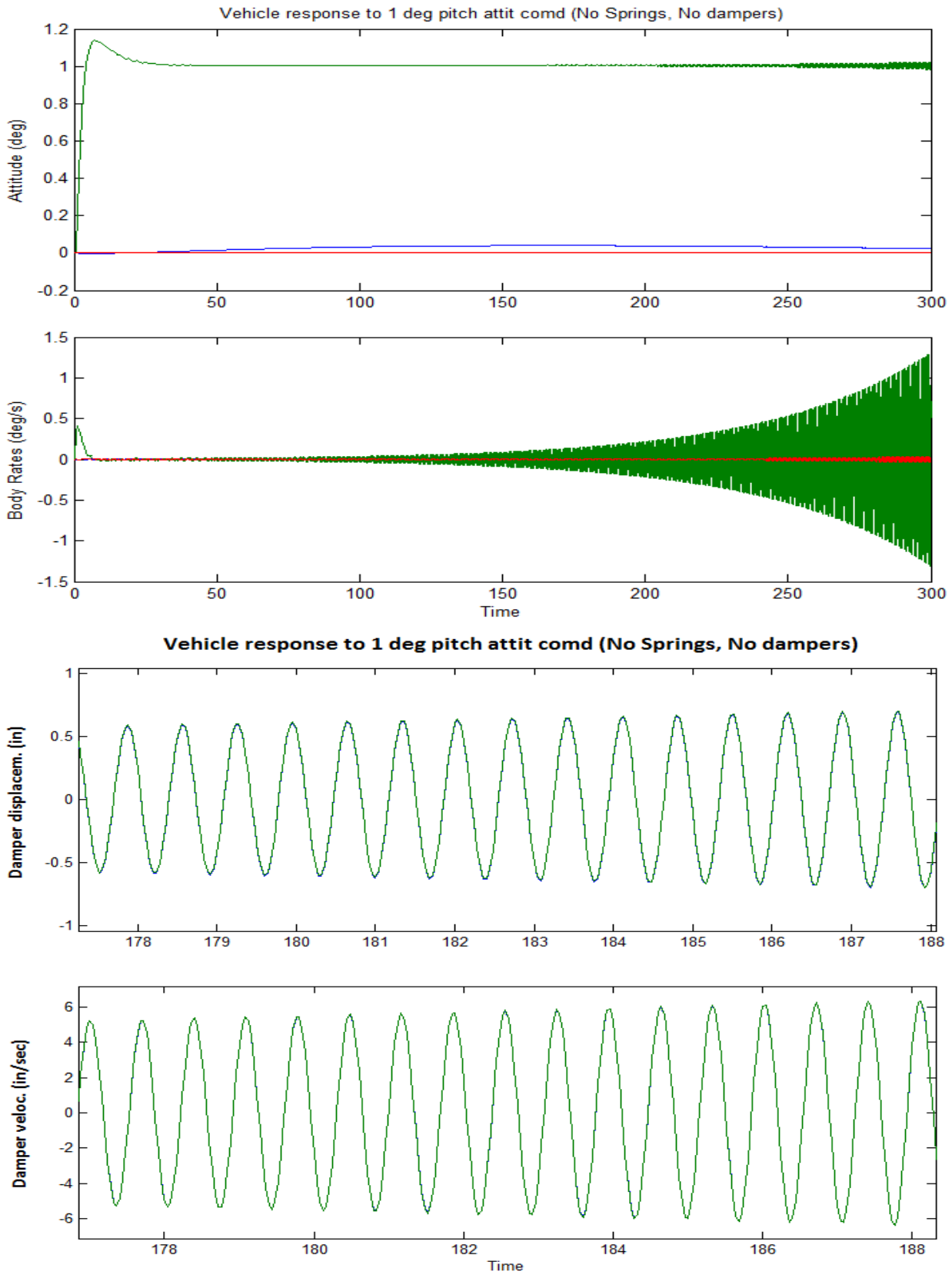


Figure 18 System without dampers diverges at the pitch payload mode frequency 9.08 (rad/sec)

16.2 Closed-Loop System Response with the Coulomb Dampers Connected

The next step is to include the two non-linear Coulomb dampers in the simulation. However, we can't use the discrete simulation model of Figure 17 which operates at 25 Hz sampling rate. It may be ideal for flight control analysis but it is too slow for the damper loop. The mechanical feedback loops that generate the damper forces as a function of the damper displacements and velocities are too slow at 40 msec sampling and it would affect the limit-cycle results. For this reason a continuous Simulink model "Closed_Loop_Sim_s.mdl", shown in Fig. 19, was created to simulate the Coulomb damper closure. It uses continuous state-space systems for both the plant and the controller. The plant model is the system "Plant Model, Vehicle/Actuators/Sensors" and the continuous flight control system is "Shuttle Stage-2 Continuous Flight Control System". They were created in file "Stg2_Damper.Qdr" and were converted to Matlab as described in Section 9. They are embedded in the Simulink model "Closed_Loop_Sim_s.mdl", which performs the simulation at a fixed 2 msec rate.

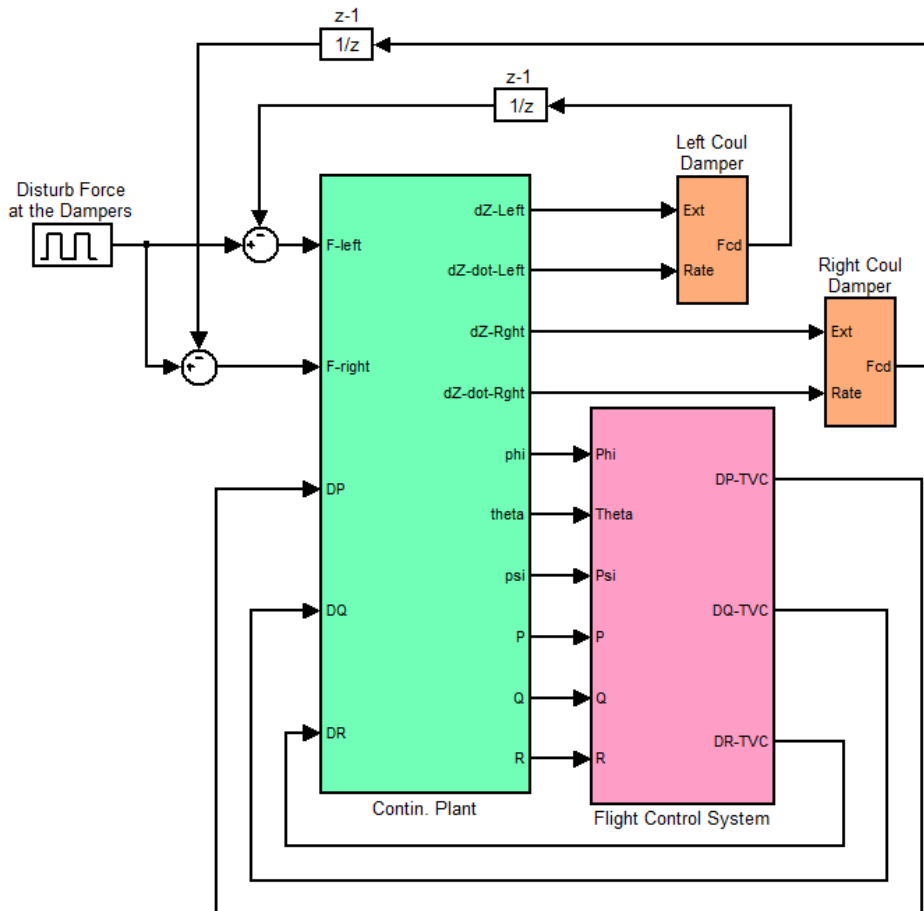


Figure 19 Fast Closed-Loop Simulation Model "Closed_Loop_Sim_s.Mdl" with Coulomb Dampers

The two dampers are included in separate blocks. The inputs to each damper block are damper displacement and rate. The output from each damper is the reaction force which is fed back at the damper attachments as already described in Figures (3 & 5). The coulomb damper block is shown in Figure 20. It uses a Matlab function "Coulomb_Damper.m" which calculates the damper force as a function of its displacement and rate. The simulation model receives also attitude commands in roll, pitch, and yaw. A 40 msec delay was included at the output of the continuous control system to simulate the transport delay.

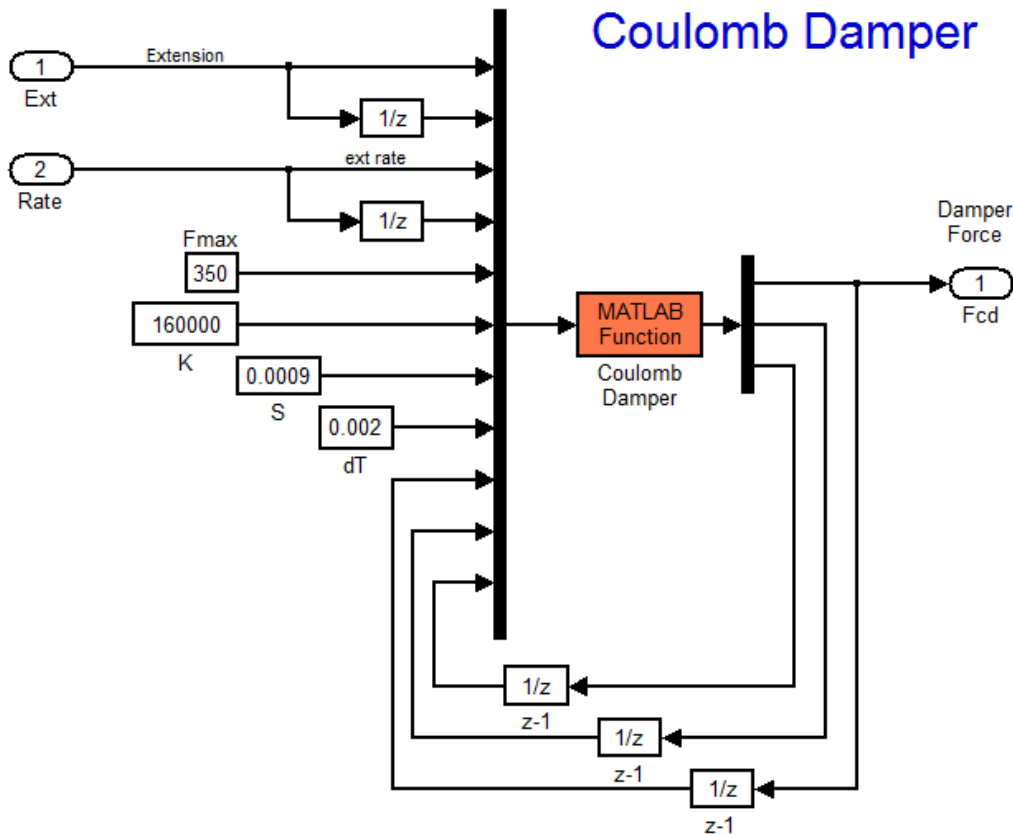


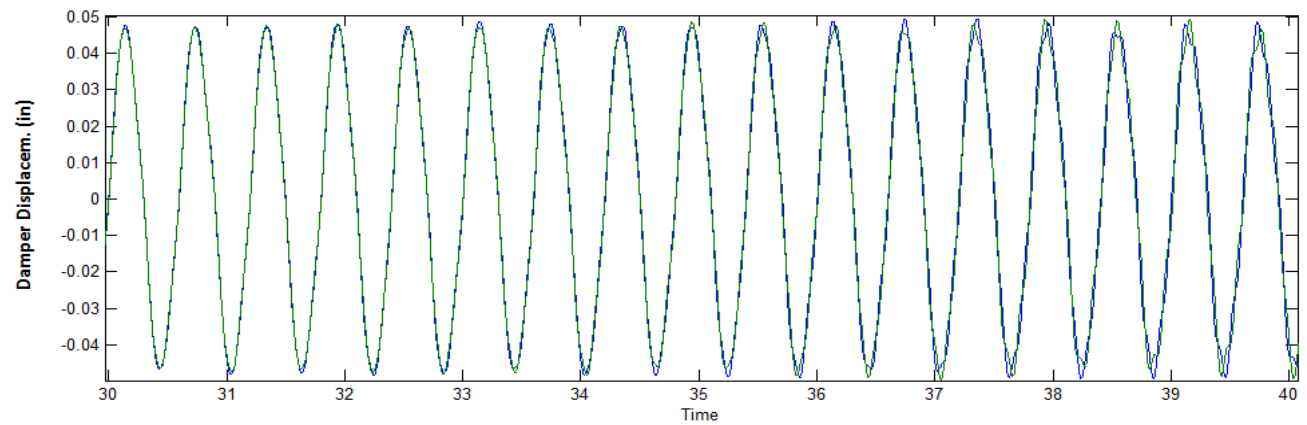
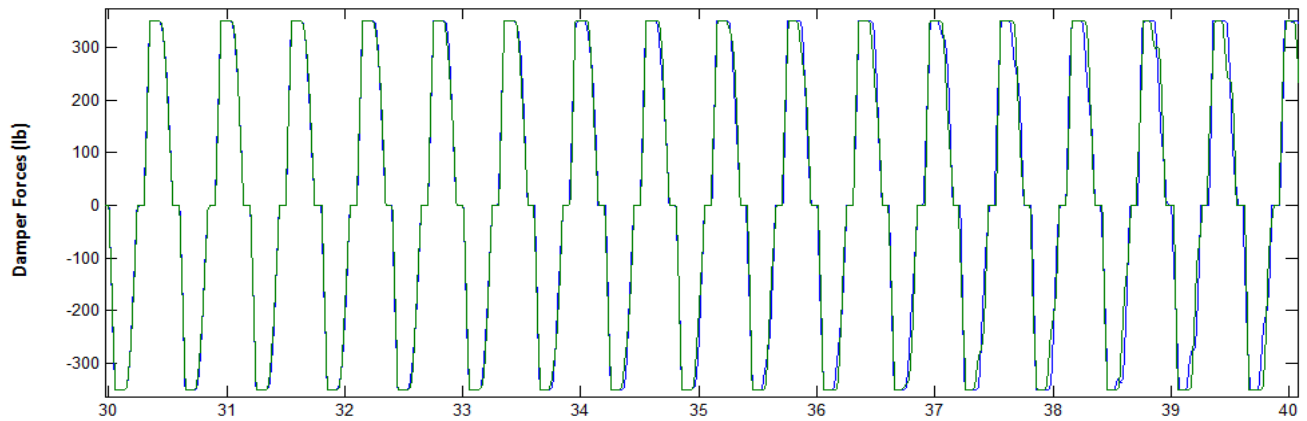
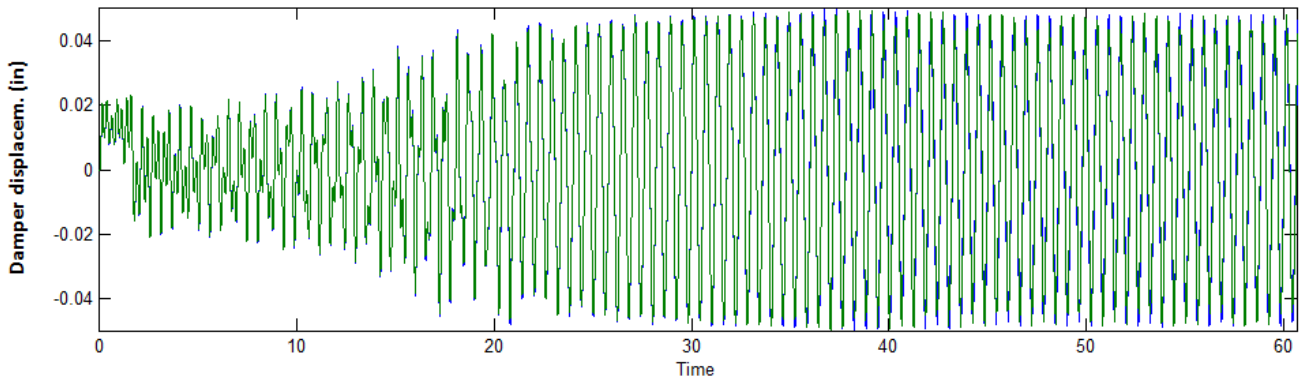
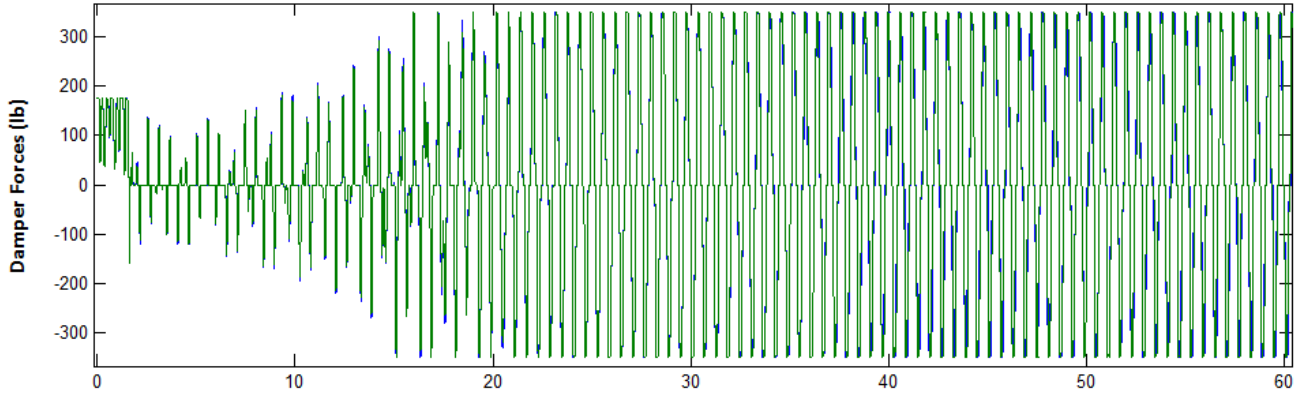
Figure 20 Non-Linear Coulomb Damper Block generates the reaction force as a function of displacement.

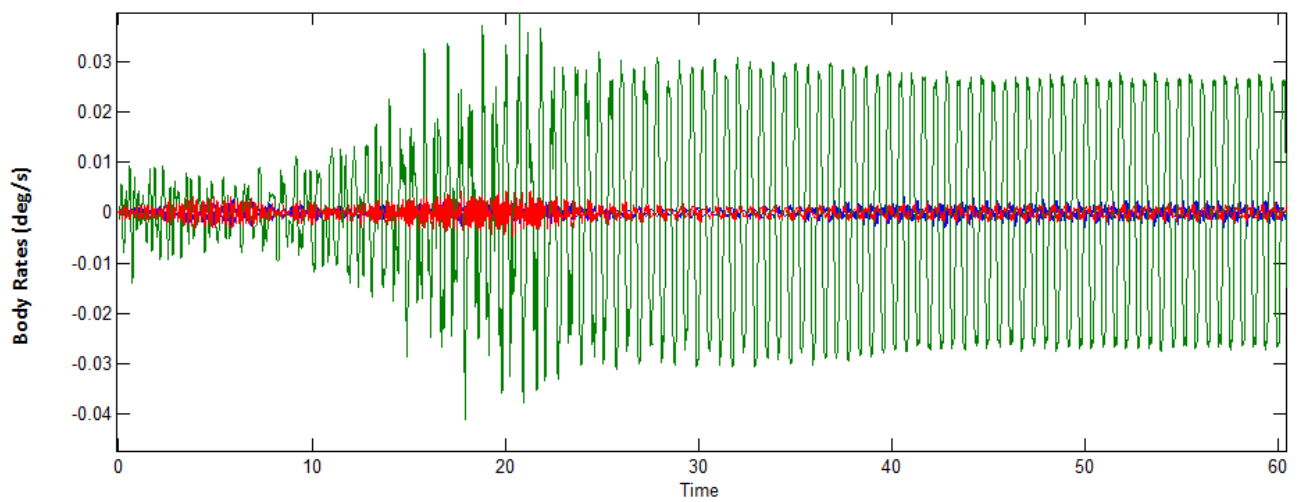
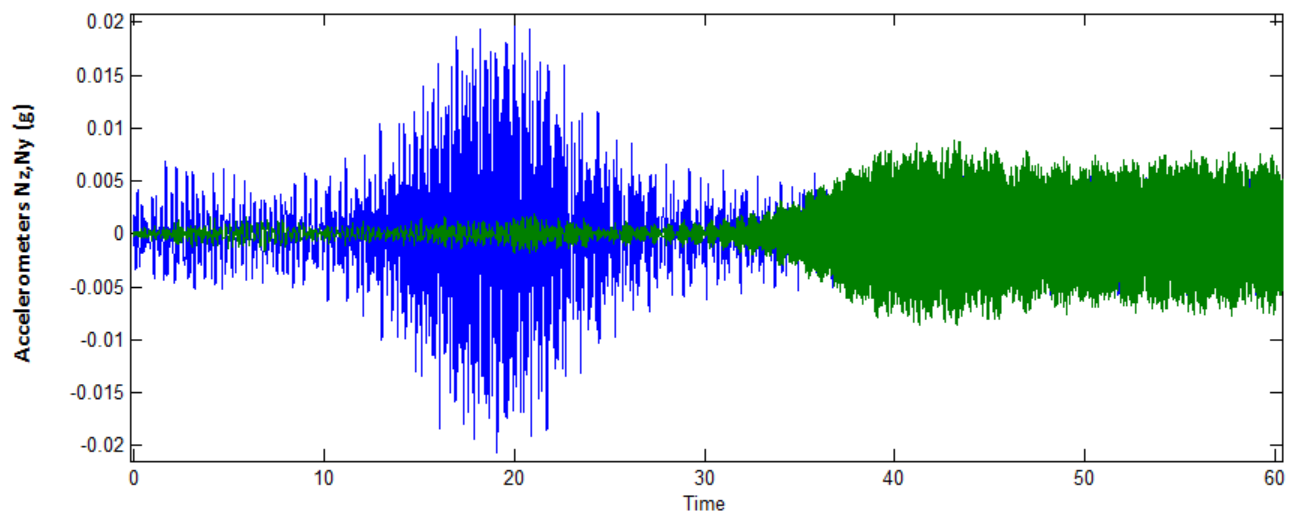
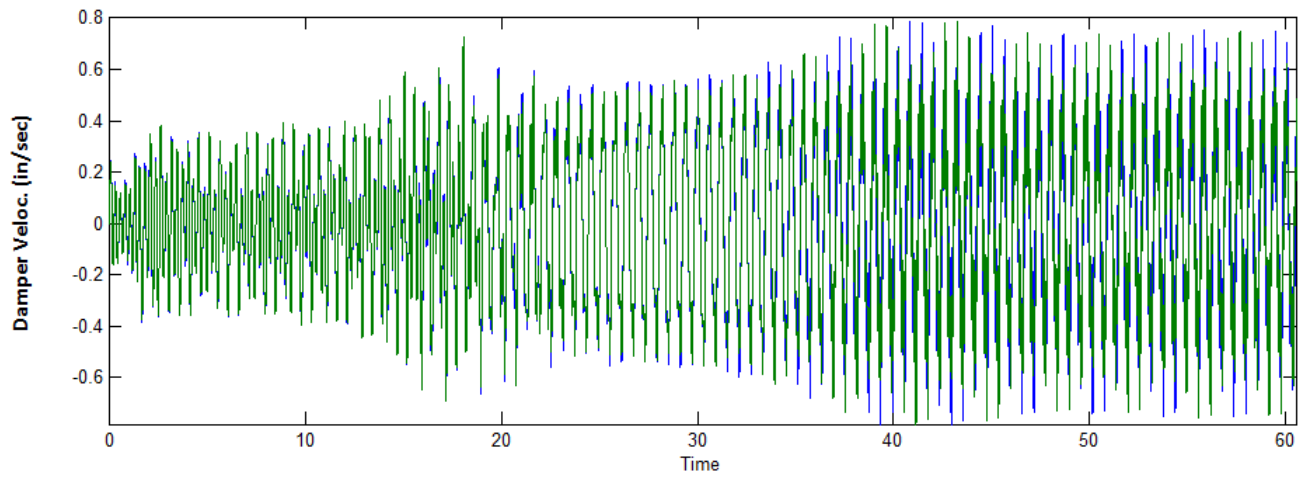
The purpose of the simulation is to excite sustained oscillations and to validate the limit-cycle frequencies and amplitudes that were predicted by the DF analysis. The structure is excited internally in the cargo bay by 2 impulse disturbance forces applied at the two dampers. The input forces can be applied either symmetrically, thus exciting both dampers in phase with each other and hence the pitch flexibility, or anti-symmetrically, exciting the dampers in opposite directions and therefore the roll flexibility. The disturbance impulses are applied on both sides of the damper attachments in opposite directions to excite only the flexibility without generating any rigid body vehicle motion. By varying the level and the direction of the disturbance excitation we can bias the system to converge at different limit-cycles and to confirm our frequency domain predictions.

Case-1, Exciting the 10.47 (rad/sec), 0.004 (ft) amplitude limit-cycle

This is the most dominant limit-cycle resonance in the symmetric Gs(s) direction because the closed-loop system has a tendency to oscillate at that frequency. In the following simulation we excite the model “Closed_Loop_Sim_s.mdl” with a symmetric impulse force of 175 (lb) on both dampers. The system converges to a limit-cycle of amplitude 0.0039 (ft) or 0.0475 (inches) and a frequency of 10.47 (rad/sec) which is very close to the limit cycle predicted by the pitch DF analysis. The output forces saturate at 350 (lb) indicating that the dampers exceeded their breakout force. The symmetric limit-cycle excites also the vehicle accelerometers and pitch rate (green). The roll and yaw excitations (blue & red) are small.

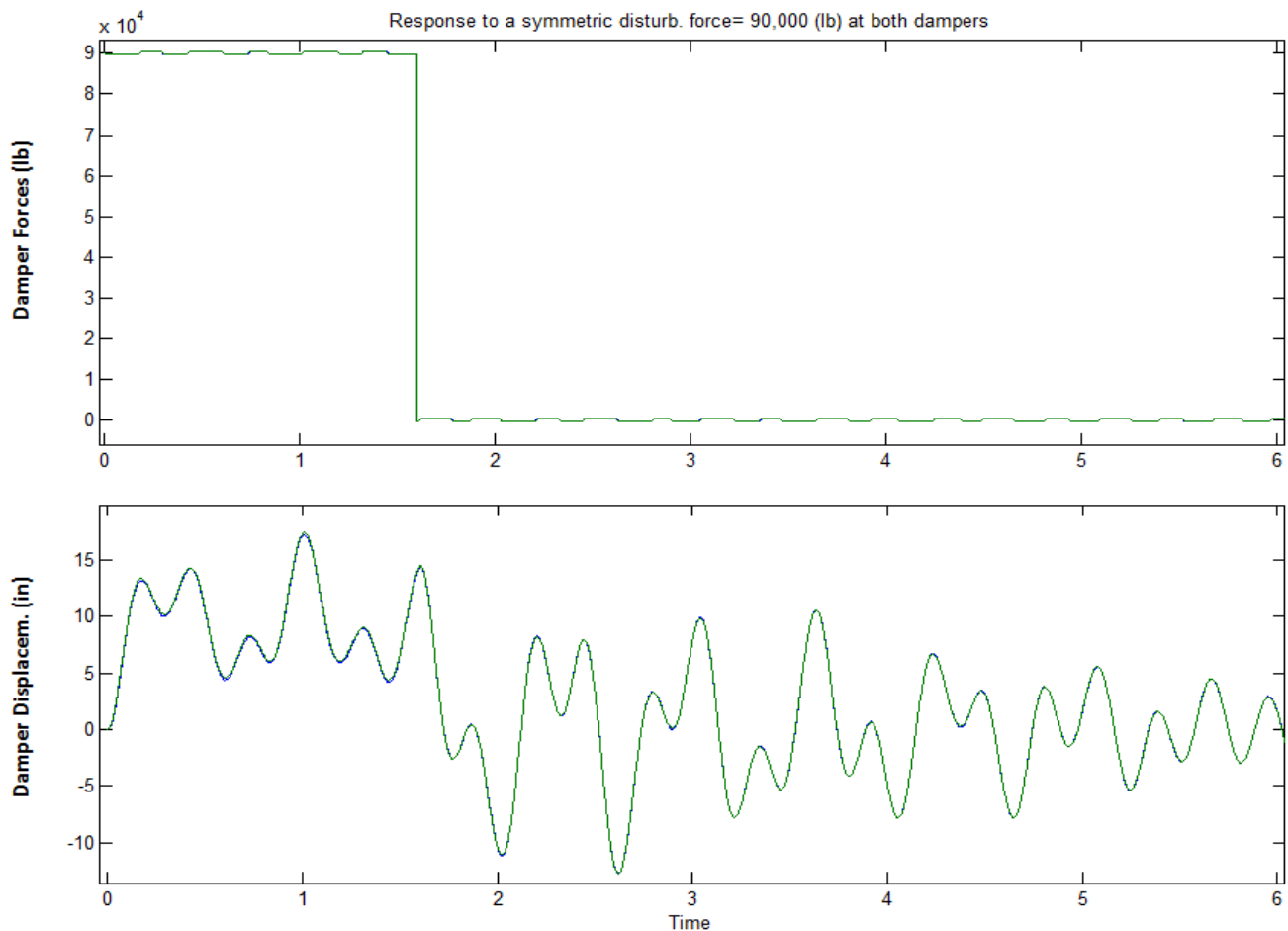
Response to a symmetric disturb. force= 175 (lb) at dampers

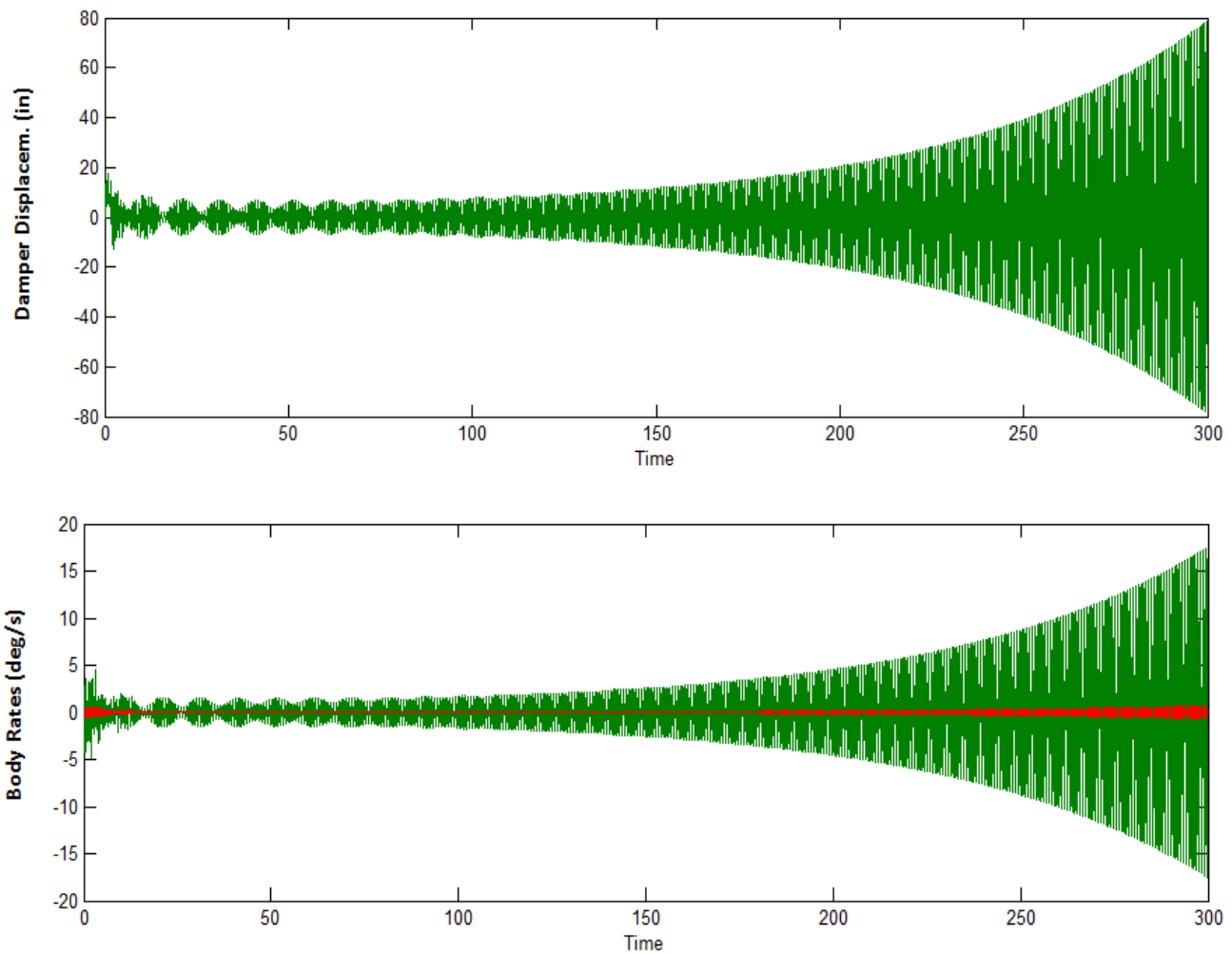




Case-2, Show that the pitch system can diverge when the excitation is very big

In the pitch axis DF analysis in Fig. 15 we predicted that the intersection of the loci at the frequency of 9.1 (r/s) in the $G_s(j\omega)$ locus is not a convergent limit-cycle and the arrows on the locus are therefore pointing away from the intersection. This point corresponds to an amplitude of 0.4 (ft) in the $1/N(a)$ locus. It means that if the initial disturbance causes damper displacement smaller than 0.4 (ft) the oscillations will converge toward the 10.48 (rad/sec) limit-cycle which is convergent, as already demonstrated in the previous simulation. If, on the other hand, the displacements begin at an amplitude greater than 0.4 (feet), the oscillation will diverge towards instability. In order to excite such a big initial displacement in the simulation we must apply a huge disturbance force at the dampers. In the example below we apply a symmetric impulse force of 90,000 (lb) which causes about a foot displacement on both dampers. The results show that the divergence continues to grow without reaching saturation as it was predicted in the describing function analysis. This excitation, however, is not realizable under normal circumstances because there is no force of such magnitude available in the cargo bay to excite this type of a divergence. It physically means that the gain in oscillatory energy due to the instability of the structural mode exceeds the amount of energy that can be dissipated by the Coulomb dampers.

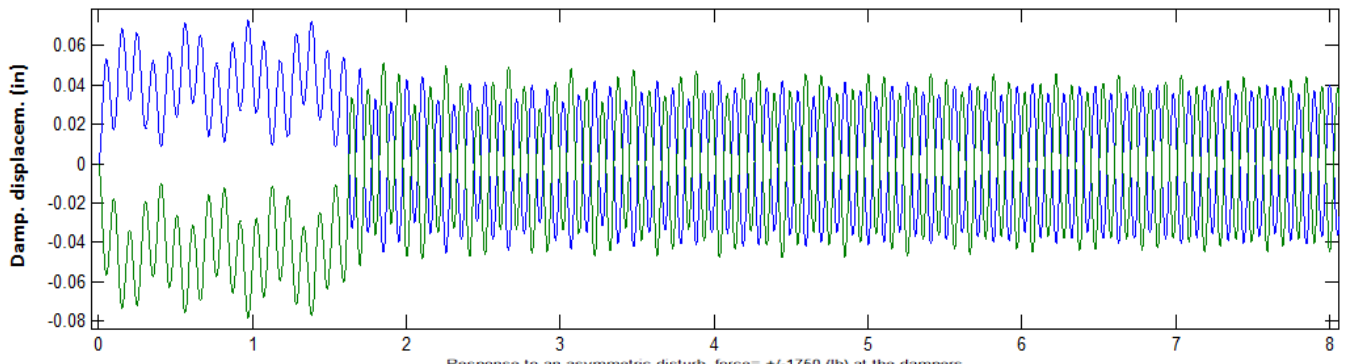
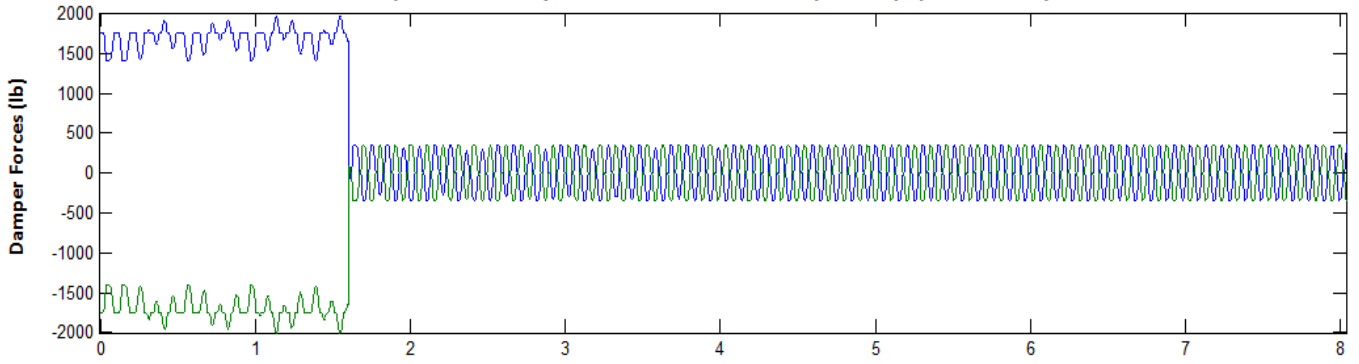




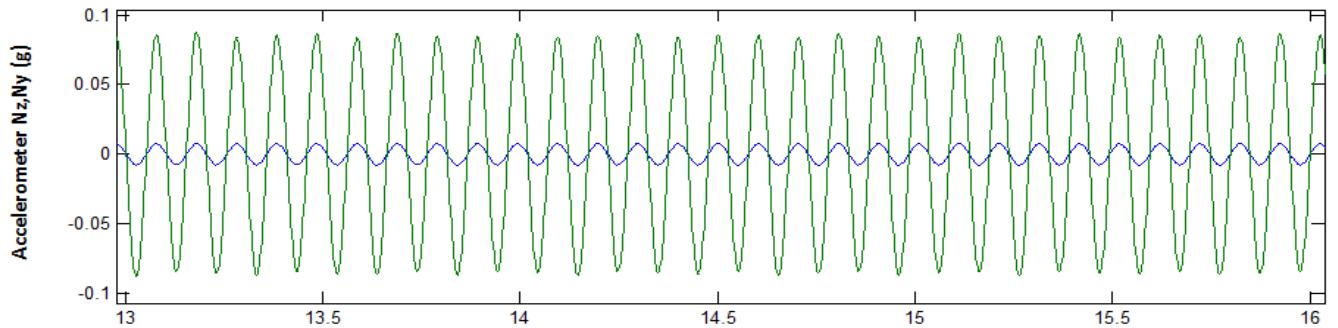
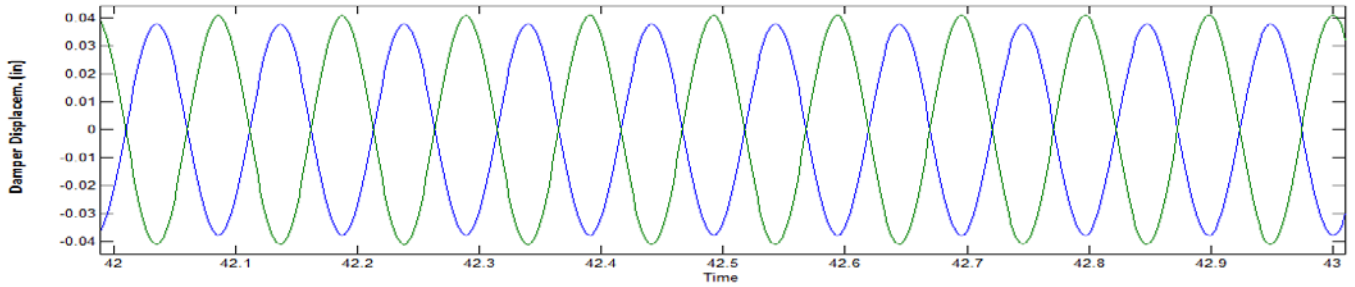
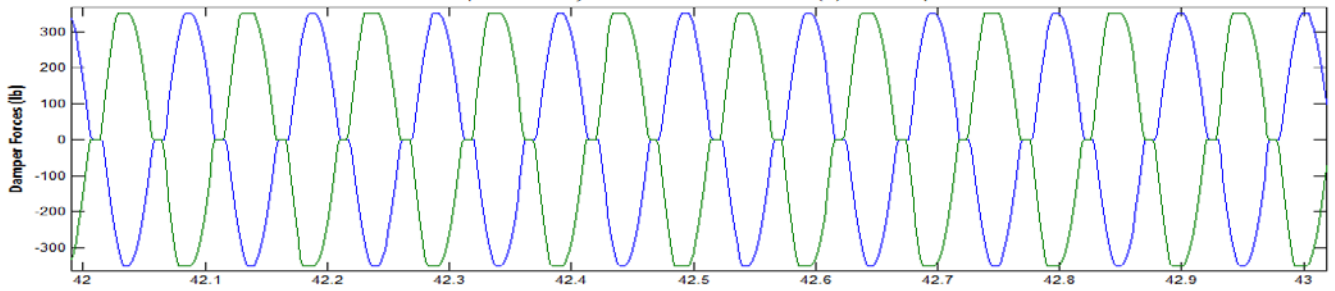
Case-3, Exciting Anti-Symmetric Limit-Cycles at 61.5 and 16 (rad/sec)

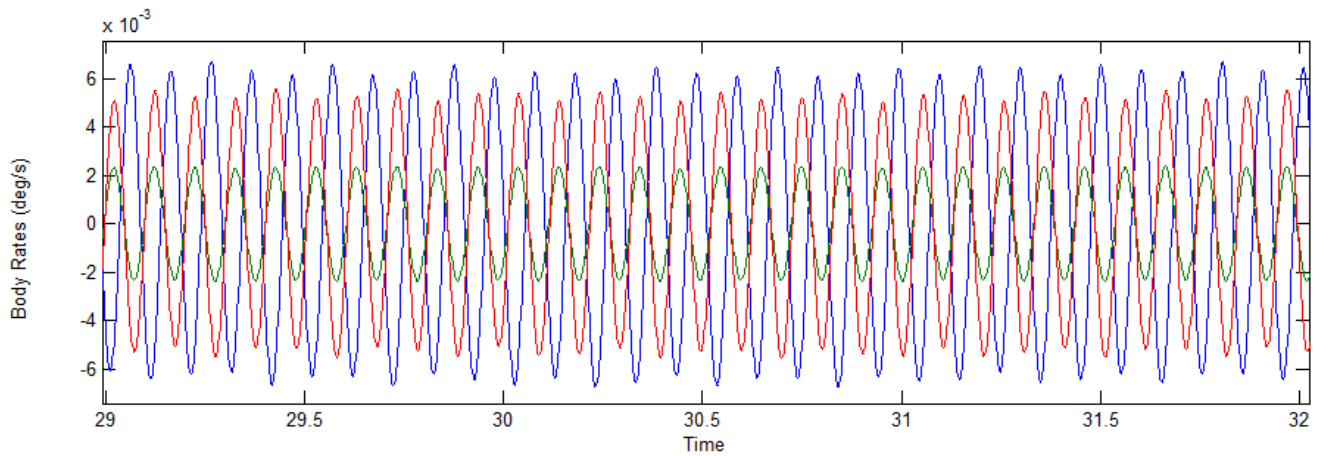
We will now demonstrate the existence of the anti-symmetric limit cycle that was predicted in the anti-symmetric Describing Function analysis, in Figure 16. From the intersection of the loci in the Nichols chart we had predicted the presence of a convergent limit-cycle at a frequency 61.5 (rad/sec) and at an amplitude of 0.0033 (ft). The system has a natural tendency to converge at the dominant pitch limit-cycle. In order to properly excite it towards converging in an anti-symmetric limit cycle we must apply equal and opposite disturbance forces at the two dampers. In the case below we apply a positive impulse of 1750 (lb) on the left damper, and an equal and opposite -1750 (lb) impulse on the right damper. This excites an anti-symmetric motion at the two dampers, as shown. The blue curves show the left damper force and displacements and the green curves correspond to the right damper. After an initial transient the displacements converge to an amplitude of 0.0034 (ft), or 0.04 (inch), and a frequency of 61.5 (rad/sec), as it was predicted in the DF analysis. The damper forces reach the 350 (lb) force breakaway indicating that energy is dissipated through friction. The left and right displacements and force oscillations are 180° out of phase, an indicator of an asymmetric limit-cycle. The limit-cycling also affects the roll and yaw vehicle rates, blue and red respectively, but it also couples into pitch (green). The acceleration is mainly in the lateral (N_y) direction with a small contribution in N_z .

Response to an asymmetric disturb. force= +/-1750 (lb) at the dampers



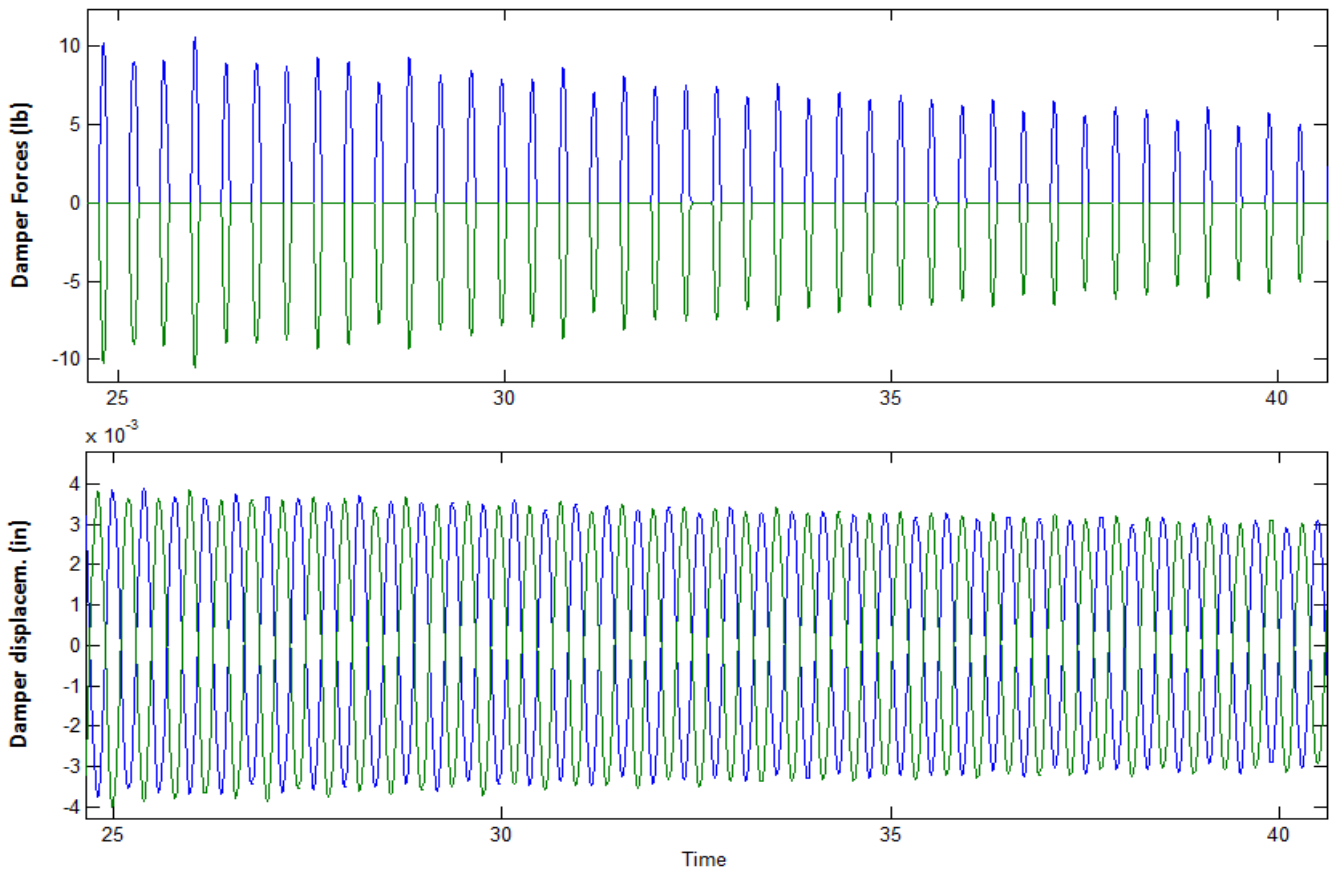
Response to an asymmetric disturb. force= +/-1750 (lb) at the dampers





Notice that when the asymmetric input excitation is smaller, for example ± 900 (lb), this will not excite the 61.5 (rad/sec) limit-cycle. It will excite, however, an oscillation at 16 (rad/sec). According to Figure 16 this point is almost, but it does not exactly qualify to be a limit-cycle, because $Ga(j\omega)$ gets near, but it does not really intersect the locus at 16 (rad/sec). Furthermore, since it does not intersect the locus in the curved energy dissipating region we should expect the damper activity to remain within the dead-zone and stiffness regions and never reach the ± 350 (lb) force breakaway region. The oscillations in this case are not sustained like in a genuine limit-cycle but they are very lightly damped, as shown below.

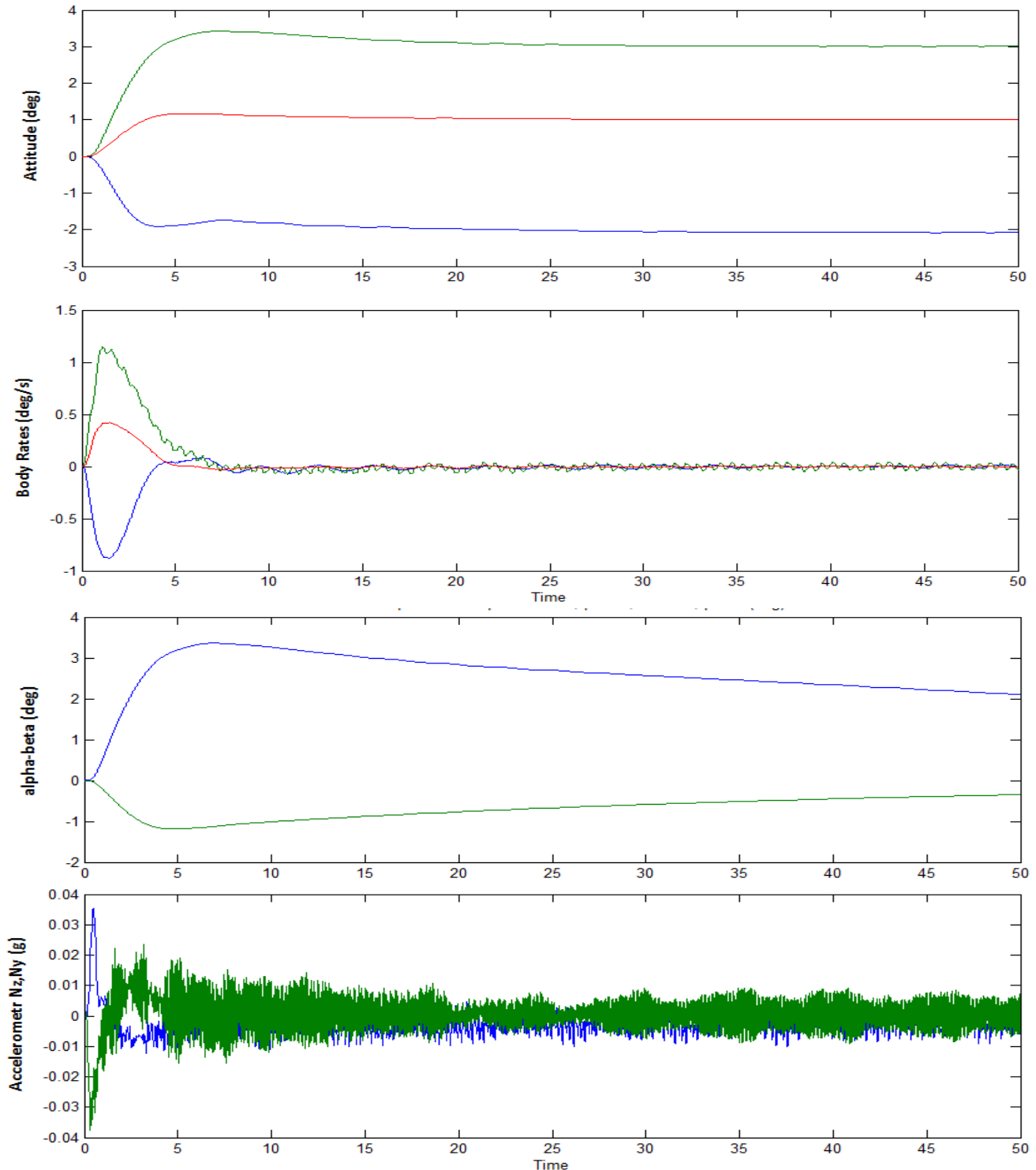
Response to an asymmetric disturb. force= +/- 900 (lb) at the dampers



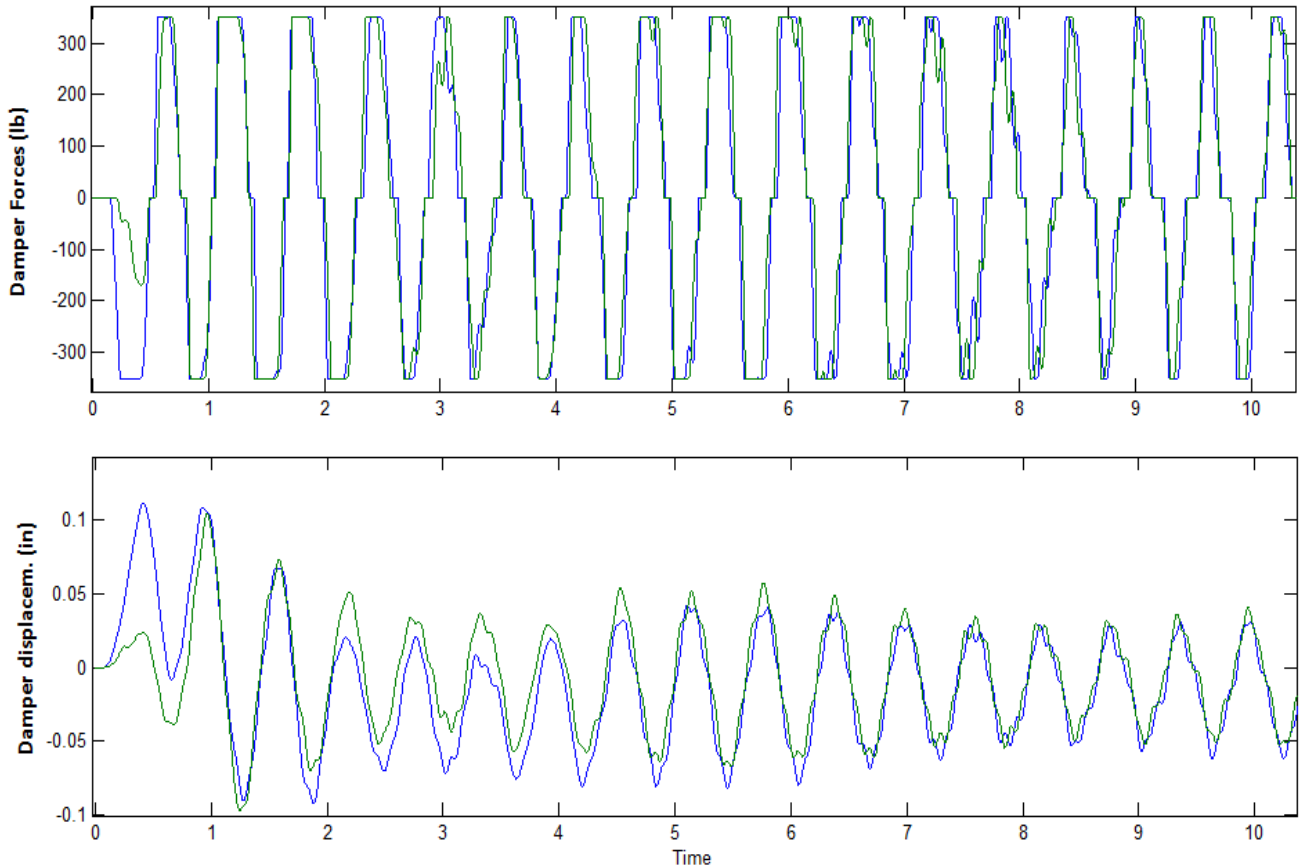
Case-4, Vehicle Response to Step Attitude Commands

We finally simulate the flight control system response to step attitude commands from guidance. The system is simultaneously commanded to an attitude change of -2 deg in roll, 1 deg in yaw, and 3 degrees in pitch. The responses are shown below with the attitude converging to the commanded values. The system also converges to one of the predicted pitch limit-cycles, at frequency 10.48 (rad/sec) and 0.004 (feet) amplitude.

Vehicle response to step attit cmd, phi=-2, theta=3, psi=1 (deg)



Vehicle response to step attit cmd, phi=-2, theta=3, psi=1 (deg)



16 Summary

To summarize this payload vibration analysis we shall attempt to explain the meaning of this stable and divergent limit-cycle situation using simple logic. When the payload flexibility excitation through vehicle motion and external forces is reasonably small the dampers are capable of attenuating the payload modal instability by dissipating energy through static friction. As a result the system converges to some reasonably small and sustained limit-cycles depending on the magnitude and direction of the excitation.

However, when the external excitation is extremely large, causing payload displacements at the dampers to exceed 0.4 feet, the mechanical energy that is dissipated through friction is trivial in comparison with the energy stored in the structural mode. This structural energy is growing due to the mode instability. When this happens, the payload structural mode is no longer restrained by the friction forces from the dampers and it diverges to unacceptably high amplitudes. Realistically speaking, a force of 90,000 (lb) of magnitude across the dampers cannot occur in the cargo bay of a launch vehicle unless an explosion takes place. The two coulomb dampers are, therefore, capable and safe to attenuate the payload vibrations during flight to sufficiently low amplitudes.